2008-08-13

Chemical-Biological Investigation of KCNQ1/KCNE K^+ Channel Complexes: A Dissertation

Trevor J. Morin
University of Massachusetts Medical School

A Chemical-Biological Investigation of KCNQ1/KCNE K^+ Channel Complexes

A Dissertation Presented

By

Trevor J. Morin

Submitted to the Faculty of the University of Massachusetts Graduate School of Biomedical Sciences, Worcester in partial fulfillment of the requirements for the degree of

Doctor of Philosophy

August, 13 2008

Biochemistry/Molecular Pharmacology

Signature page

The following approval page, bearing the signatures of the chairperson and all members of the student's committee, Thesis Advisor, and the Dean of the Graduate School of Biomedical Sciences, occupies the page as follows:

A Chemical-Biological Investigation of KCNQ1/KCNE K^+ Channel Complexes

A Dissertation Presented
By

Trevor J. Morin

The signatures of the Dissertation Defense Committee signifies completion and approval as to style and content of the Dissertation

William Kobertz, Ph D, Thesis Advisor

C. Robert Matthews, Ph D, Member of Committee

Ann Rittenhouse, Ph D, Member of Committee

Stephen Miller, Ph D, Member of Committee

Christopher Miller, Ph. D., Outside Member of Committee

The signature of the Chair of the Committee signifies that the written dissertation meets the requirements of the Dissertation Committee

Kendall Knight, Ph D, Chair of Committee

The signature of the Dean of the Graduate School of Biomedical Sciences signifies that the student has met all graduation requirements of the school.

Anthony Carruthers, Ph. D.
Dean of the Graduate School of Biomedical Science
Biochemistry/Molecular Pharmacology
August, 13 2008

Dedication

I dedicate this thesis work to my parents Dr. David P. Morin, M.D. and Ellen L. Morin, R.N.. They have provided unconditional love and support during difficult times and times of joy.

Acknowledgements

I am most grateful to my thesis advisor, Bill Kobertz. His encouragement and support while conducting my thesis research was instrumental to its completion. I admire his depth of knowledge in two different scientific disciplines, Chemistry and Biology, and his ability to use them synergistically. During my research career I will also strive to combine disciplines and relay the lessons that I've learned in the Kobertz Lab (and stories from "The Miller Lab").

I also thank my lab mates for support, technical discussions, advice and friendship. It has been a true pleasure working with all of them. Particularly, Jessica Rocheleau, Steven Gage, and Karen Mruk have been helpful in electrophysiology experiments and manuscript editing, Kshama Chandrashakar, Tuba Bas and Yuan Gao for biochemistry experiments, Karen Mruk and Zhengmao Hua for chemistry experiments, and Virla Berrios for construct development. I also thank Nick Rhind for critical manuscript evaluation.

I thank my committee members, Bob Matthews, Ann Rittenhouse, Stephen Miller and my committee chair Ken Knight, who I consider a colleague and friend. Their suggestions and thoughtful considerations have been greatly appreciated and aided in thesis completion. I would also like to acknowledge Chris Miller for agreeing to act as my outside committee member.

Most of all I thank my family for standing by me during times of stress and despair. I owe them for what I have now. The final acknowledgement is to my wife, Tomoko, she is an amazing and talented scientist and my perfect substrate.

Abstract

KCNE β-subunits modulate KCNQ1 (Q1) voltage-gate K^+ channels providing the current diversity required for Q1 channels to function in a wide variety of cell types and tissues. In the present thesis, the stoichiometry of KCNE1 (E1) β-subunits in functioning Q1 channels is investigated, along with the formation of heteromeric channel complexes, complexes containing 2 different KCNE β-subunits. The chemical approaches used to answer these questions were then expanded to generate a novel labeling reagent.

To determine the stoichiometry of the Q1/E1 complex, I devised an iterative subunit counting approach that relies on a chemically releasable K^+ channel blocking reagent. The extracellularly applied reagent irreversibly blocks charybdotoxin (CTX) sensitive Q1 channels by chemically modifying E1 peptides that contain an N-terminal cysteine residue. Chemical release of the inhibitor and subsequent iterative applications of the reagent reported that Q1 channels partner with two KCNE β-subunits.

To determine whether heteromeric Q1-KCNE complexes form, I synthesized a similar, but non-cleavable, K^+ channel blocking reagent that detects specific KCNE peptides in functioning complexes by irreversible channel inhibition. Using this "KCNE sensor", heteromeric Q1/E1/E3, Q1/E1/E4 and Q1/E3/E4 complexes were shown to form, traffic to the cell surface and function. Using mathematical subtraction to visualize the irreversibly blocked current, the currents and gating kinetics of the different heteromeric complexes were revealed and a hierarchy of KCNE subunit modulation of Q1 channels was determined: E3>E1>>E4.

Building on this technology, a chemically releasable K^+ channel blocking reagent was created to specifically label KCNE β-subunits with biotin. The reagent delivers biotin to CTX sensitive Q1 channels and labeling occurs through free thiols provided by either cysteine residues or thiol modified sugars. This preliminary data demonstrates a novel strategy for labeling endogenous K^+ channels in native cells.

Table of Contents

List of Tables

List of Figures

List of Symbols and Abbreviations

α	Alpha
β	Beta
Ac_5ManNTGc	1,3,4,6-tetra-O-acetyl-2-acetylthioacetamido-2-deoxy-α-D-mannopyranose
$BM[PEO]_3$	Bismaleimide-3(polyethylene glycol)
CHO	Chinese hamster ovary
Clv	Cleavable linker
CTX	Charybdotoxin
CTX-Clv	Charybdotoxin cleavable-linker maleimide construct
CTX-Lclv-Biotin	Charybdotoxin cleavable-linker maleimide biotin construct
CTX-MTSET	Charybdotoxin 2-(trimethylammonium)ethyl]methane thiosulfonate bromide
Dts	dithiasuccinyl
E1, E3, E4, E5	KCNE1, KCNE3, KCNE4, KCNE5
ER	Endoplasmic reticulum
ESI	Electrospray ionization
FRET	Fluorescence energy transfer
HA	hemagglutinin-tagged
HRMS	High resonance mass spectrometry
HRP	Horse radish peroxidase
I_{Ks}	Slow cardiac potassium current
K^+	potassium
LPA	leupeptin, pepstatin and aprotinin
Mal-ES	maleimide ethylsulfonate
ManNAc	N-acetyl-D-mannosamine
MTSET	2-(trimethylammonium)ethyl]methane thiosulfonate bromide
N-linked	Asparagine linked
PMSF	phenylmethylsulfonyl fluoride
Q1	KCNQ1
Q1*	charybdotoxin sensitive KCNQ1 channel
Q1/E1	KCNQ1/KCNE1 complex
TCEP	Tris(2-carboxyethyl)phosphine
TEVC	Two-electrode-voltage-clamp
UTRs	Untranslated regions
VSD	Voltage sensing domain

Standard one or three letter code was used to abbreviate amino acids. Mutated residue abbreviated by position number. Chemical compounds or formulas are abbreviated with standard periodic chart abbreviations for elements.

Preface

References to publications that represent the work contained within the thesis:

Morin, T. M. and W. R. Kobertz (2007). "A Derivatized Scorpion Toxin Reveals the Functional Output of Heteromeric KCNQ1-KCNE K^+ Channel Complexes." ACS Chem. Biol. **2**(7): 469-473.

Morin, T. M. and W. R. Kobertz (2008). "Counting Membrane-Embedded KCNE β-subunits in Functioning K^+ Channel Complexes." Proc. Natl. Acad. Sci. USA **105**: 1478-1482.

Morin, T. M. and W. R. Kobertz (2008). "Tethering Chemistry and K^+ Channels." J. Biol. Chem. ***(in press)***.

Chemicals not directly generated by the author:

William Kobertz synthesized the cleavable linker (Clv) and generated figures 1-1 and 1-2. Zhengmao Hua synthesized the Biotin-maleimide linker (Clv-Biotin).

Figure not generated by author:

Figure I-1b was originally published by João H. Morais-Cabral, Yufeng Zhou and Roderick MacKinnon, Nature 414, 37-42(1 November 2001)

CHAPTER I: Introduction and Literature Survey

Introduction

Voltage-gated K^+ channels are multi-subunit integral membrane proteins that allow the passive diffusion of K^+ ions down their electrochemical gradient. Although the ultimate task of these channels, creating an aqueous hole in the membrane through which K^+ ions may pass, seems inconsequential, the physiological relevance is enormous; K^+ channels are responsible for governing neuronal excitability, maintaining cardiac rhythmicity, and establishing the resting potential and epithelial electrolyte homeostasis in a wide variety of tissues (Robbins, 2001; Bezanilla, 2006).

Voltage-gated K^+ channels contain three essential components, a discriminating selectivity filter (or pore) through which K^+, but not other ions pass, a voltage sensing domain (VSD), and an intracellular gate formed by intracellular C-terminal helices (the helix bundle crossing) that can impede or permit the flow of ions through the channel (figure I-1a) (Bezanilla, 2006). A change in the intracellular membrane potential causes movement in the VSD resulting in a conformational change within the protein allowing the intracellular gate to open and permit K^+ ions to flow down their concentration gradient near the rate of diffusion. The ability of these channels to selectively pass K^+ is due to the spacing and sequence (Glycine-Tyrosine-Glycine) of backbone carbonyl atoms in the pore region of the channel that energetically stabilize K^+ ions and exclude other ions of similar size and charge (figure I-1b). This means of K^+ ion selection was

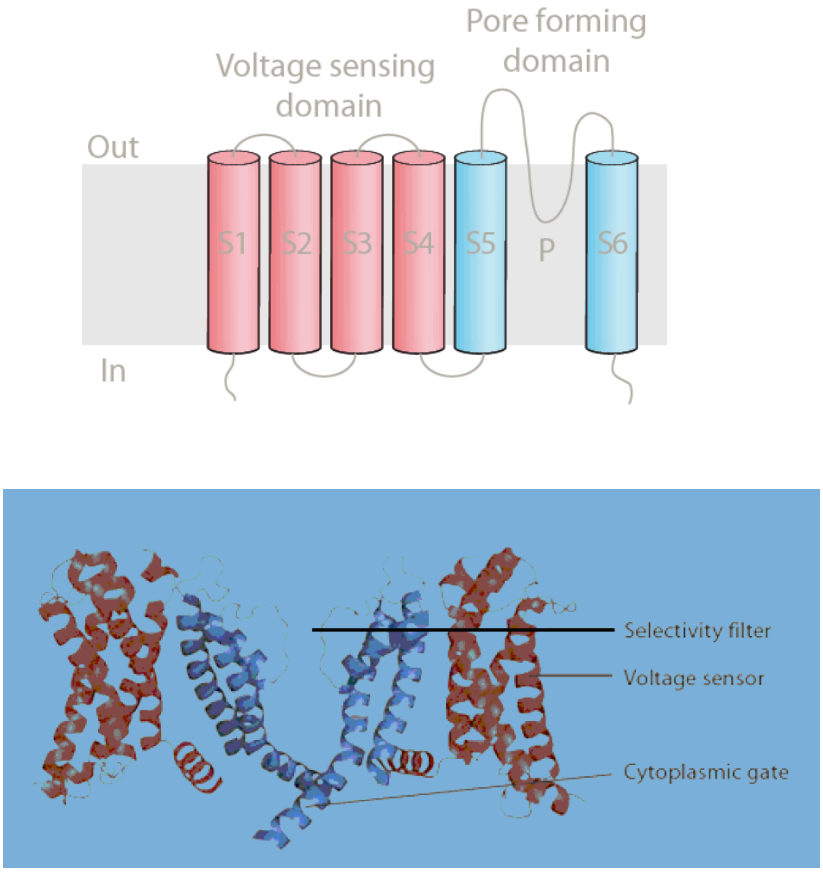

Figure I-1a. Topology diagram of a Kv channel (top) and High resolution structure of K^+ channel Kv2.1 paddle chimera channel (PDB: 2R9R) (bottom)

(top) The figure shows the voltage sensing domain S1-S4 (red), S4 contains arginine residues giving it a net positive charge. The pore forming domain S5-S6 (blue) contains the pore loop (P) and the GYG amino acid sequence is responsible for K^+ selectivity.

(bottom) For clarity, the front and back subunits have been removed. The figure shows the three essential components of a voltage-gate K^+ channel, voltage sensing domain (red), cytoplasmic gate (blue) and the selective pore, which is formed by 4 selectivity filters (gray loops) when subunits are assembled into tetramers.

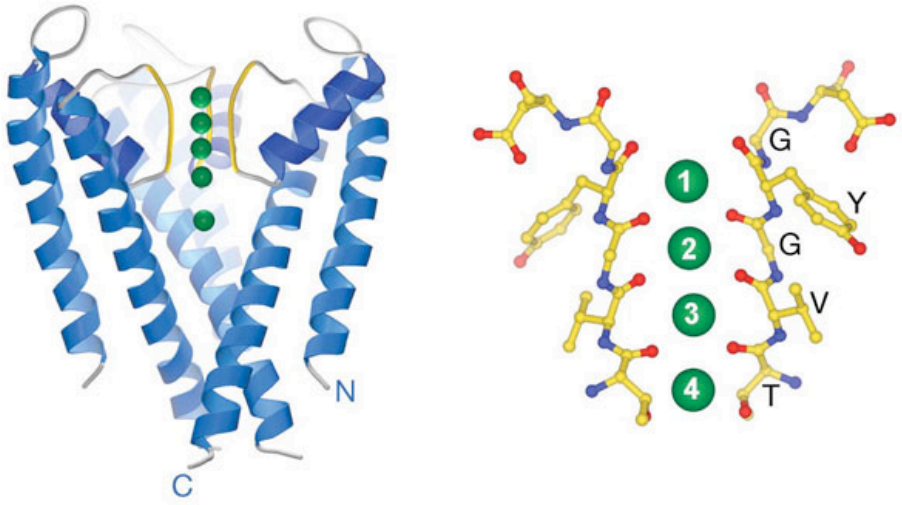

Figure I-1b. Possible locations of K+ ions in the selectivity filter and importance of GYG backbone spacing.

(left) Ribbon representation of the KcsA channel with the subunit closest to the viewer removed. Potassium ions (green spheres) bind at four locations in the selectivity filter (yellow) and in the water-filled cavity at the membrane centre (bottom ion).

(right) Close-up view of the selectivity filter in ball-and-stick representation, with the front and back subunits removed. The four K+ ions are numbered to indicate the location of binding sites in the filter; position 1 is closest to the extracellular solution and position 4 is closest to the cavity. Key amino acids forming the selectivity filter are shown. Pictures were originally published by João H. Morais-Cabral, Yufeng Zhou and Roderick MacKinnon, Nature 414, 37-42(1 November 2001)

visualized after the first voltage-gated K^+ channel was crystallized (Doyle et al., 1998; Cordero-Morales, 2006). More recent bacterial and mammalian K^+ channel crystal structures have assisted in the difficult task of assigning the exact position of the integral membrane segments and how their movements translate into opening and closing the channel (Doyle et al., 1998; Long et al., 2005a). High resolution crystal structures of voltage-gated mammalian K^+ channels and molecular dynamic simulations reveal channel closing may occur through a ratcheting mechanism with the S4-S5 linker pushing down on the helix bundle crossing closing the intracellular gate. Still hotly debated is the precise trajectory and displacement of the S4 segment in these voltage-gated channels during opening and closing conformational changes (Long et al., 2005a).

Diversifying K^+ channel architecture is the existence of accessory (orβ) subunits that partner with the ion conducting (or α) subunits. Although it's clear these β-subunits have a tremendous influence over channel function and modulation, very basic questions about them remain. This thesis sought to answer two structural questions surrounding KCNQ1 (Q1) K^+ channels: 1) What is the stoichiometry of KCNE β-subunits in a functioning Q1/KCNE channel complex, and 2) can two different KCNE β-subunits partner with and modulate a functioning Q1 K^+ channel? The approach used to answer these questions was then expanded to specifically modify K^+ channel α and β-subunits with biotin, creating a novel labeling method that will facilitate future investigations and characterization of K^+ channel α/β subunit complexes in native tissues.

KCNQ1 K^+ Channels

Tetrameric assembly of KCNQ1 (Q1) proteins creates voltage-gated K^+ selective ion channels found in many tissues throughout the human body, including cardiac, digestive, reproductive, and circulatory. As such, these channels are involved in a number of diverse functions, some of the best studied are their role in maintaining cardiac rhythmicity through repolarization of cardiac myocytes (Barhanin et al., 1996; Sanguinetti et al., 1996), auditory transduction by maintaining K^+/water homeostasis in the inner ear (Pusch et al., 1998), and proper digestion by establishing the resting membrane potential in colonic crypt cells (Schroeder et al., 2000).

Each Q1 monomer consists of 6 transmembrane spanning segments termed S1-S6, with S1-S4 creating the VSD, while S5-S6 form the pore domain and K^+ selective filter upon tetrameric assembly (figure I-1a). Upon a change in intracellular membrane potential relative to the extracellular potential from negative to more positive, the VSD undergoes a transition from its resting to active state, largely due to the electronic repulsion of positively charged arginine residues in the S4 segment (Larsson et al., 1996; Jiang et al., 2003; Long et al., 2005a, b). This conformational change is coupled to the opening of the intracellular cytoplasmic gate, permitting K^+ ions to flow down their electrochemical gradient, resulting in cellular repolarization.

Q1 monomers only assemble with other Q1 monomers to form homotetrameric ion conducting channels, unlike other family members such as KCNQ2 and KCNQ3 that co-assemble to form a Q2/Q3 heteromeric channel (Wang et. al., 1998). In addition, Q1 channel activation kinetics is slow compared to their neuronal Q2/Q3 and *Shaker*

counterparts. Presumably this is because the S4 helix of Q1 channels has less positive charge than neuronal counterparts, which manifests itself in slower channel opening (Panaghie and Abbott, 2007). Figure I-2 show depolarization families, as the channels are depolarized to greater potential the channels conducted greater amounts of current. Not all channels and channel complexes open and conduct equally at a respective voltages, hence individual channels have differing current-voltage relationships. A detailed inspection of tail currents recorded in high external K+ concentrations reveals Q1 channels inactivate and thus exist in at least 3 states: closed ↔ open ↔ inactive. Although the transition from open to inactive is hard to observe in Q1 channels, inactivated to closed is readily observed as a "hook" in the tail current, which is due to the channels passing from the inactive state to the open state about 10 times faster than the channels pass from the open state to the closed state (Figure I-2) (Pusch et al., 1998). Interestingly, to date Q1 channel currents have not been physiologically observed, but instead Q1 is always partnered with a KCNE modulatory β-subunit. This subunit not only removes or conceals the channel's inactive state, but also has a tremendous influence over channel gating kinetics and voltage dependence.

Partnering KCNE β-subunits

KCNQ1 channels assemble with all 5 KCNE (E1-E5) peptides (McCrossan and Abbott, 2004), a promiscuous family of mostly α-helical (Rocheleau et al., 2006; Kang et al.,

2008) type I (extracellular N-terminus, intracellular C-terminus) transmembrane β-subunits that range between ~100-150 amino acids. Surprisingly, given their simple structure and topology, KCNE peptides modulate the electrical output and provide Q1 channels with the necessary current diversity to meet the various K^+ requirements of Q1-expressing tissues (McCrossan and Abbott, 2004). For example, the ability of E1 to modulate Q1 channels in the heart is strikingly different from the ability of E3 to create a Q1 K^+ leak channel in the colon. A family of voltage clamp recordings show Q1/E3 complexes appear to open instantaneously, and as evident by the tails, close very quickly too, pass significant amounts of inward current, and are devoid of inactivation (figure I-2). Q1/E1 channels open and close very slowly, pass absolutely no inward current under physiological K^+ concentrations, and are more responsive to change in depolarization voltages. Oddly, currents do not plateau, meaning the channels do not reach equilibrium between closed and open despite incredibly long depolarizing pulses (~ 90 s) (figure I-2). Partnering with E4 or E5 creates a non-conducting complex at physiological voltages (figure I-2), while Q1/E2 channels are kinetically similar to Q1/E3 channels (Tinel et al., 2000; Jespersen et al., 2005).

It has been proposed that a triplet of amino acids within the transmembrane domain of E1 and E3 confers modulation specificity to Q1 channels, because swapping these three residues essentially converts the recipient KCNE into the donor (Melman et al., 2002). However, these results are in contrast with earlier KCNE1 deletion studies, which demonstrated that a C-terminal region (highly conserved between E1 and E3) was

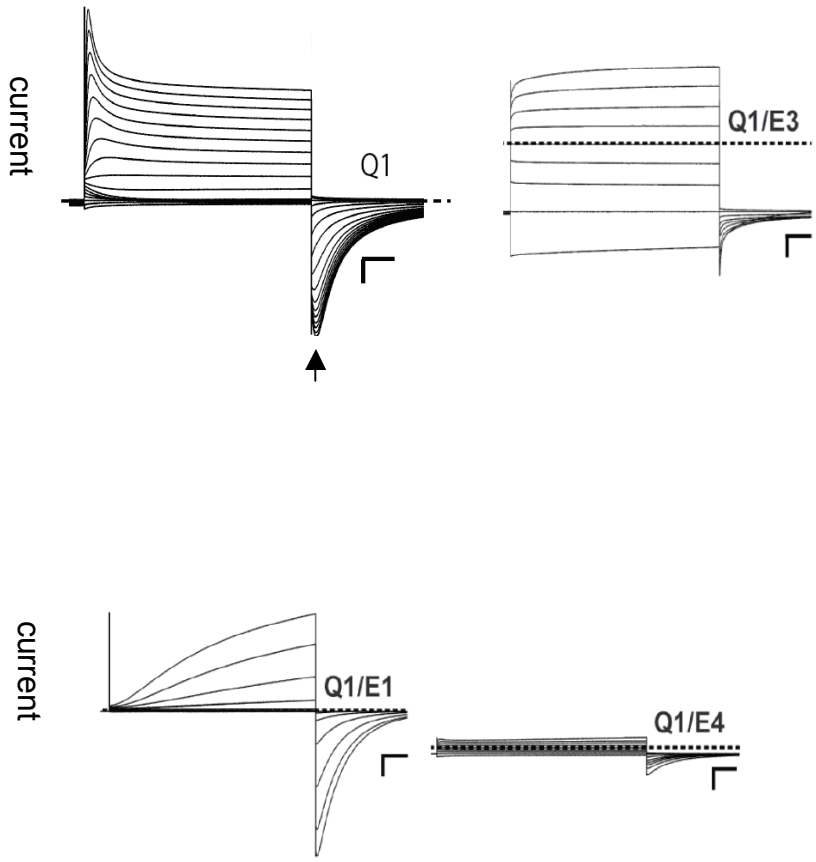

Figure I-2. TEVC recordings of Q1 and Q1/KCNE Channels

Two-electrode voltage clamp recordings for Q1 and homomeric Q1-KCNE complexes. Currents were elicited by a family of command voltages from –100 to 60 mV at 20-mV increments and recorded in KD50 solution. Arrow denotes the "hook tail" of Q1 channels, which is absent in Q1/KCNE complexes. Dashed line indicates zero current. Scale bars represent 1 μA (vertical axis) and 0.5 s (horizontal axis).

responsible for E1 modulation of Q1 (Takumi et al., 1991; Tapper and George, 2000). Work by Gage and Kobertz demonstrated that the E3 transmembrane domain is sufficient for assembly with and modulation of KCNQ1 channels and they suggested a bipartite model for Q1 modulation by E1 and E3 subunits. In this model, the E3 transmembrane domain is active in modulation and overrides the C-terminus' contribution to fast gating, whereas the E1 transmembrane domain is passive and reveals C-terminal modulation of Q1 channels (Takumi et al., 1991; Gage and Kobertz, 2004).

Two recent papers investigated whether KCNE peptides affect the voltage sensor equilibrium in Q1/KCNE complexes. Both used electrophysiological recordings and methanethiosulfonate (MTS) modification of state dependent cysteine residues to show E1 peptides do not slow the movement of S4 from the resting to active state. Therefore, slowed Q1/E1 activation may be due to a slowly opening intracellular gate (Nakajo and Kubo, 2007; Rocheleau and Kobertz, 2008). In addition, it was realized E3 shifts the voltage sensor equilibrium to favor the active state at hyperpolarizing potentials and thus uncouples S4 movement from the opening and closing of the cytoplasmic gate (Rocheleau and Kobertz, 2008).

Genetic mutations in β-subunits that lead to compromised complex function and disease (predominantly Long QT syndrome) underscore the physiological importance of properly assembled α/β-complexes (Splawski et al., 2000; Tyson et al., 2000). Long QT disease, which is literally a lengthening of the Q to T interval in an ECG recording, is characterized by a lengthening of the refractory period during the cardiac action potential, generally due to a delay in cellular repolarization. Despite the obvious requirement for

an α/β-subunit partnerships, basic structural questions surrounding these partnering peptides are still debated: (1) What is the location of KCNE peptides in Q1 complexes (Wang et al., 1996; Tai and Goldstein, 1998; Tapper and George, 2001), (2) What is the KCNE stoichiometry (Tzounopoulos et al., 1995; Wang and Goldstein, 1995; Salata et al., 1998; Wang et al., 1998; Chen et al., 2003), and (3) Can heteromeric complexes (i.e. a single Q1 channel with two different KCNE's) spontaneously assemble and function? (Wu et al., 2006, Manderfield, 2008).

The location of KCNE peptides relative to KCNQ1 channels has been debated. Some argue that it crosses the membrane at the channel periphery (Romey et al., 1997; Wang et al., 1996; Tapper and George, 2001) or traverses the S4 canal (Kurokawa et al., 2001). Others contend that KCNE residues gain exposure in the outer pore vestibule (Wang et al., 1996), reside close to the ion conduction pathway near the selectivity filter (Tai and Goldstein, 1998), and influence the structure of the internal pore vestibule from an unknown distance (Sesti et al., 2000). Studies in which Q1 was partnered E1 cysteine mutants found externally applied cadmium could induce pore blockage, suggesting KCNEs reside in or near the ion-conduction pathway (Tai and Goldstein, 1998).

The number of KCNE β-subunits in the K^+ channel complex has been a long-standing debate (Tzounopoulos et al., 1995; Wang and Goldstein, 1995; Salata et al., 1998; Wang et al., 1998; Chen et al., 2003). Using charybdotoxin binding experiments and chimeric complexes, Goldstein and co-workers have strongly argued that Q1 channels average 2 KCNE peptides per complex; however, they could not definitively rule out K^+ channel complexes containing a solitary KCNE peptide (Chen et al., 2003).

Q1 modulation is altered when greater and greater amounts of KCNE1 are expressed, leading to the notion that Q1/E1 channels form complexes with KCNE β-subunits with multiple stoichiometries (Salata et al., 1998; Wang et al., 1998) . The ensemble based approaches used in these studies measured the average number of KCNE peptides in the Q1 channel complex and therefore could not discern between fixed and mixed stoichiometries. This thesis presents a *chemical* method for discerning KCNE stoichiometry in functioning KCNQ1 K^+ complexes.

The realization that multiple KCNE peptides are expressed in the same tissue has raised the possibility that two different KCNE subunits could assemble with the same K^+ channel (Bendahhou et al., 2005; Lundquist et al., 2005; Lundquist et al., 2006). mRNAs of all 5 KCNE peptides and isoforms were found in multiple regions of the heart and in many different tissues and organs in the mouse. Equally surprising was that E4 was the most abundant KCNE transcript in the heart, a location where E1was assumed to far outnumber all others KCNE peptides to assure the physiologically required Q1/E1 complex is free to form unfettered. The notion that a heteromeric channels can form was strengthened with co-immunoprecipitation of one KCNE peptide (E4) by another KCNE peptide (E1) (Wu et al., 2006; Manderfield, 2008). However, these qualitative biochemical experiments were not definitive because it was unclear whether these precipitated complexes were functional. This thesis examines heteromeric channel formation and function using a chemical method.

Shaker K^+ Channels

Voltage-gated *Shaker* K^+ channels are also formed by the tetrameric assembly of α-subunits that form a K^+ selective aqueous pore (MacKinnon, 1991). Like Q1 channels, each monomer contains 6 transmembrane spanning segments; again S1-S4 forms a voltage sensor, while S5-S6 forms the pore domain. Unlike Q1, however, *Shaker* has not been shown to partner with a modulatory membrane embedded β-subunit and *is* glycosylated (Santacruz-Toloza et al., 1994; de Souza and Simon, 2002; Khanna et al., 2004).

Shaker channels, which are native to the hippocampal neurons of *Drosophila melanogastar* (Salkoff, 1990), have proved exceedingly useful as a model for the study of all voltage-gated K^+ channels. This is due to their ability to provide very robust and stable currents in a number of expression systems, amphibian to mammalian, and comply with a number of electrophysiological techniques, including two-electrode voltage clamp (TEVC) and single channel recordings.

Chapter IV of this thesis uses *Shaker*-inactivation removed (*Shaker*-IR) channels as a model to show that chemical tethering and labeling is not restricted to Q1 β-subunits (KCNE peptides). The Q1 α-subunits can also be modified using introduced cysteines or thiol containing extracellular glycans. *Shaker*-IR (herein referred to as simply *Shaker*) channels have a C-terminal domain removed that, when present, plugs the pore internally causing inactivation. These *Shaker*-IR channels are also mutated at position 425 (425G) to confer charybdotoxin sensitivity.

Peptide Toxins to Probe Channels

Studying channel complexes provides a unique set of challenges due to their membranous lipid environment. Fortunately, nature has provided a wide range of toxins (e.g. scorpion, spider, and snail) that selectively target subtypes of K^+ ion channels. Using various toxins it has been possible to determine α-subunit stoichiometry of K^+ channels (MacKinnon, 1991), map the outer channel vestibule (MacKinnon et al., 1998), improve our understanding of the roles played by individual channel types (Inglis et. al., 2003; Yoshida and Matsumoto, 2005) and aid in the synthesis of therapeutic compounds to target particular classes of potassium channels (Talley et. al**,** 2006).

Determining residues advantageous or deleterious to toxin binding has allowed toxin sensitivity to be engineered into previously insensitive channels (Goldstein et al., 1994). This technique was used to confer charybdotoxin (CTX) sensitivity on Q1 channels after studying CTX's interaction with its native targets, the big conductance K^+ (BK) and *Shaker* family channels (Smith et al., 1986; Goldstein et al., 1994; Chen et al., 2003). Furthermore, mapping studies along with NMR structural data has allowed non-native cysteines to be engineered into these cysteine rich toxins providing a reactive handle onto which different chemical moieties may be attached (Shimony et al., 1994; Posson et al., 2005; Yu et al., 2005). CTX is a 39 amino acid extremely stable globular peptide, due to 3 internal disulfide bridges, and binds to modified Q1 channels slightly off center of the pore with a 1:1 stoichiometry. The work presented here takes advantage,

of Q1 channels with engineered charybdotoxin sensitivity (Q1*) and a cysteine modified charybdotoxin (R19C).

Tethered blockers

Tethered blockers are chemical reagents comprised of an ion channel inhibitor or pore blocker linked to a reactive functional group. These bifunctional molecules typically act as affinity labeling reagents—binding first to the ion channel and then reacting with the target protein residue. For example, a channel blocker linked to a thiol reactive moiety can accelerate the kinetics of thiol modification 1000-fold by increasing the local concentration of the reactive group near the free thiol (Blaustein et al., 2000).

Blaustein and colleagues used tethered blockers to measure the distances from the extracellular segments of the K^+ channel voltage sensor to the external tetraethylammonium blocking site at the entrance of the pore (Blaustein et al., 2000). By synthesizing a panel of quaternary ammoniums (QA) linked to maleimides with varying length polyglycine tethers (Figure I-3), they could systematically find a tether that was just long enough to block the channel. The KcsA crystal structure (Doyle et al., 1998) was then used to calibrate the distances measured with the different-length tethered blockers. These blockers in combination with electrophysiology revealed that the top of the S3 segment is the farthest away from the center of the *Shaker* K^+ channel followed closely by the S1 segment, and the extended S3-S4 loop is the closest (Blaustein, 2002).

In addition to the ability of tethered blockers to report on K^+ channel architecture, a K^+ channel tethered blocker with a light-activatable linker was used to control K^+ channel function in neurons. A photoswitchable reagent, composed of a maleimide linked to a quaternary amine through a spacer that adopts an extended *trans* configuration in visible light, or a condensed *cis* conformation under UV light, was used to turn modified *Shaker* channels "on" or "off" by blocking or unblocking channels (Banghart et al., 2004; Volgraf et al., 2006). The straightforward approach and modularity of the tethered blocker technology was utilized in this thesis.

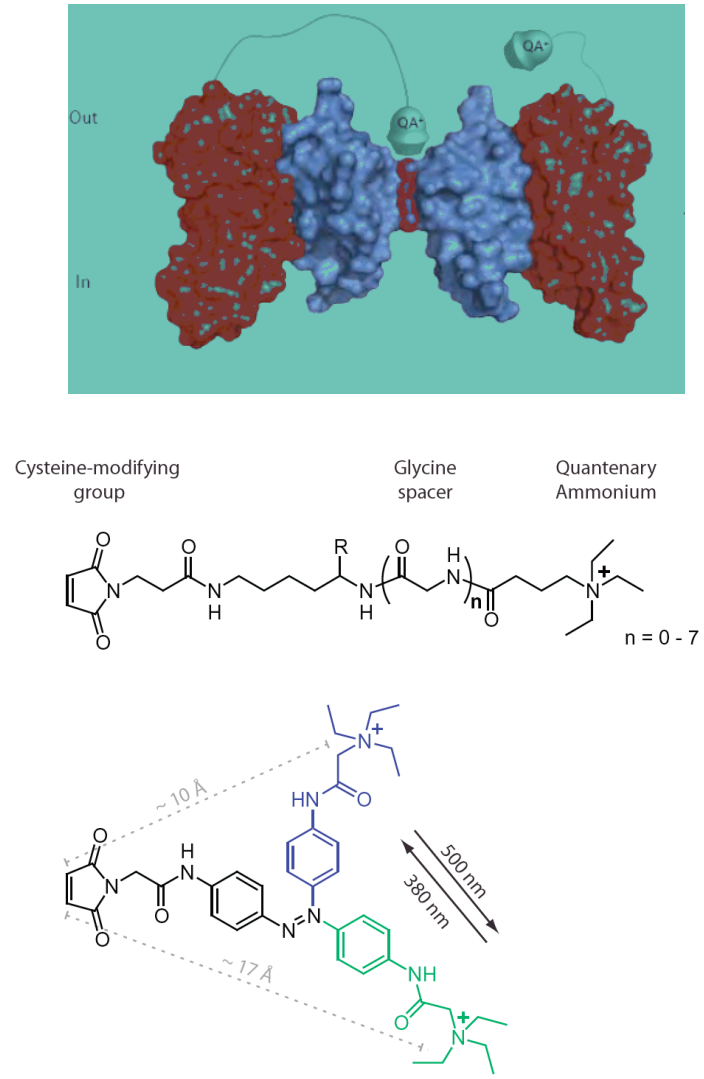

Figure I-3. **Tethered blockers and inhibitors of K^+ channel function**

(top) Kv channel modified with quaternary ammonium tethered blockers. The linker on the tethered blocker on the left voltage sensor is long enough to allow the QA to reach its binding site and block conduction whereas the tethered blocker on the right voltage sensor is too short and the conductance of the channel is unaffected. **(middle)** Chemical structures of tethered blockers. The effective tether length can be adjusted by incorporating glycine residues using standard solid phase peptide synthesis. Gly(0): 21 Å; Gly(7): 45 Å. (**bottom**) A photoisomerizable azobenzene linker that changes its effective length by ~ 7 Å upon exposure to different wavelengths of light.

Cellular Glycosylation

Many K^+ channels destined for the cell surface are initially N-linked glycoslylated in the rough endoplasmic reticulum (ER), a process involving the covalent attachment of a branched saccharide chain to the amide nitrogen of asparagine side chains while the peptide is being synthesized (co-translational) or after the entire protein is synthesized (post-translational).

N-linked glycosylation occurs at N/X/T or S sequence motifs (where N is an asparagine residue, X is any amino acid but proline and T or S is a threonine or serine) and is important for efficient folding and trafficking of proteins to the cell surface (Santacruz-Toloza et al., 1994; Khanna et al., 2001; de Souza and Simon, 2002). The glycosylation process starts with the enzymatic addition of a 14-sugar precursor made up of 3 glucose, 9 mannose, and 2 N-acetylglucosamine (ManNAc) molecules, after oligosaccharide attachment and proper protein folding, the three terminal glucose residues are removed from the chain and the protein is exported from the ER to the Golgi. In the Golgi, further mannose trimming, addition of N-acetylglucosamine and 3-5 terminal sialic acid sugars results in a mature oligosaccharide signaling the glycosylation process is complete, and the protein is trafficked to the cell surface or final intracellular destination (Helenius and Aebi, 2001).

It was realized that mammalian cells grown with media containing non-natural thiol-containing ManNAc (a sialic acid precursor) will take up the modified sugar and incorporate it into the mature form of a glycan as the terminal sugar (Yarema et al., 1998;

Dube and Bertozzi, 2003). This allows all sialic acid containing cell surface proteins to have an accessible extracellular reactive thiol that can be used for various types of tethering chemistries (figure I-4). In addition to reactive thiols, azides or nucleophiles can be incorporated into the non-natural sugar providing an even more diverse array of chemical handles on the cell surface, thus allowing tethering chemistries with alkynes or electrophiles to be used (Laughlin and Bertozzi, 2007). This thesis explored possible ways to label endogenous channels in native cells types or tissues using these modified sugar moieties.

Outline of Thesis

The objective of this thesis was to 1) determine the stoichiometry of KCNE1 β-subunits in a functioning KCNQ1/KCNE1 complex, 2) determine whether two different KCNE β-subunits can partner with and modulate a single KCNQ1 channel, and 3) develop new cell surface labeling technologies using N-linked glycosylated proteins.

Chapter II described the synthesis and utilization of a chemically reversible Q1 channel blocker that, in combination with two-electrode voltage-clamp (TEVC) recordings of *Xenopus* oocytes, allowed the β-subunit stoichiometry of functioning

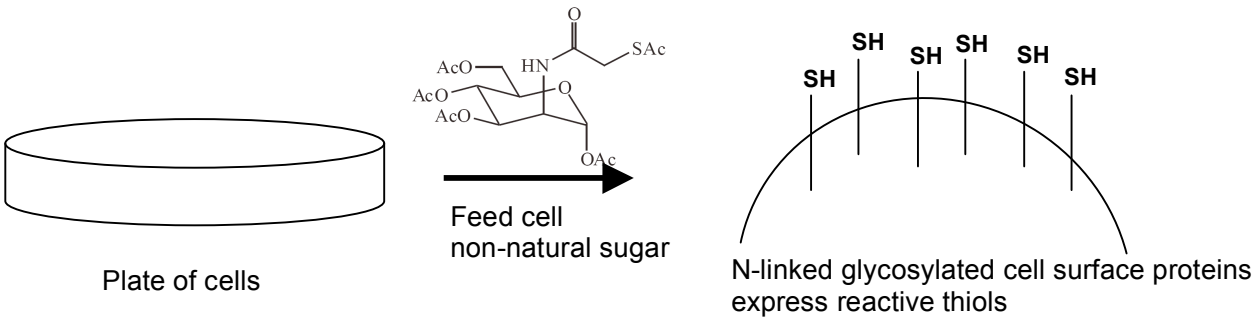

Figure I-4. Free thiol incorporation into glycosylated cell surface protein

Mammalian cells can be fed non-natural sugar precursors that contain aceylated thiols. Cellular machinery will remove the acetyl groups and incorporate the sugar into a glycan destined to be extracellular resulting in the cell surface expression of a reactive thiolate handle.

Q1/E1 complexes to be determined. It was found that the Q1/E1 ratio is fixed and there are two KCNE1 β-subunits in a fully assembled Q1/E1 channel complex.

Chapter III describes the experiments used to determine whether a single Q1 channel can partner with two different KCNE β-subunits and still pass current. This was accomplished by using TEVC recordings and a derivatized scorpion toxin that irreversibly inhibits Q1 K^+ channel complexes that contain a specific KCNE peptide. I found Q1/E1/E4, Q1/E1/E3, and Q1/E3/E4 complexes assemble and are functional. Furthermore, mathematical subtraction of currents allowed the visualization of currents generated from functioning heteromers and a hierarchy of KCNE peptide modulation of Q1 channels was proposed, E3>E1>>E4.

Chapter IV describes the synthesis and use of a reagent that is able to specifically label *Shaker* α-subunits or E1 β-subunits in functioning Q1 channels with biotin. TEVC recordings suggested biotin labeling present on the E1 peptide and *Shaker* channels. Repeating the experiments using cells grown with non-natural thiol-containing ManNAc sugars demonstrated a novel way to label native K^+ channel α- and β-subunits.

I collaborated with Zhengmao Hua, post-doctoral researcher in the Kobertz lab, to complete the work in Chapter IV. He synthesized the non-natural ManNAc sugar and a cleavable linker conjugated to biotin.

CHAPTER II: Counting Membrane-Embedded β-subunits in Functioning K^+ Channel Complexes

Abstract

Ion channels are multi-subunit proteins responsible for the generation and propagation of action potentials in nerve, muscle and heart as well as maintaining salt and water homeostasis in epithelium. The subunit composition and stoichiometry of these membrane protein complexes underlies their physiological function, as different cells pair up ion conducting α-subunits with specific regulatory β-subunits to produce complexes with diverse ion conducting and gating properties. However, determining the number of β-subunits in functioning ion channel complexes has been challenging and fraught with contradictory results.

This chapter describes the synthesis of a chemically-releasable, irreversible K^+ channel inhibitor and its iterative application to tally the number of β-subunits in a Q1/E1 K^+ channel complex where the stoichiometry of the complex is still debated. Using this inhibitor in TEVC electrical recordings, it was determined there are two KCNE subunits in a functioning tetrameric K^+ channel, breaking the apparent four-fold symmetry of the ion conducting pore. This digital determination rules out all other supra, sub and multiple stoichiometries, providing a uniform structural picture to interpret KCNE β-subunit

modulation of voltage-gated K^+ channels and the inherited mutations that cause dysfunction. Moreover, the architectural asymmetry of the K^+ channel complex affords a unique opportunity to therapeutically target ion channels that co-assemble with KCNE β-subunits. Given the wide assortment of specific ion channel inhibitors, this approach can be adapted to identify and enumerate the protein subunits in other multimeric ion channel complexes.

Introduction

Voltage-gated KCNQ1 K^+ channels are tetrameric integral membrane proteins that open and close in response to changes in membrane potential. To regulate cellular potassium flow in both excitable and non-excitable tissues, Q1 channels co-assemble with regulatory KCNE peptides, forming membrane-embedded K^+ channel complexes with different voltage-sensing and gating properties (McCrossan and Abbott, 2004).

Although the four-fold arrangement of the Q1 α-subunits along the ion conduction pathway is established and unquestioned, the number of KCNE β-subunits in the K^+ channel complex has not been definitively determined (Tzounopoulos et al., 1995; Wang and Goldstein, 1995; Wang et al., 1998; Chen et al., 2003). To determine the stoichiometry of a Q1-KCNE K^+ channel complex, an iterative cell surface modification scheme was devised where the labeling reagent specifically binds to the outer vestibule of the K^+ conduction pore while covalently modifying a cysteine-bearing KCNE peptide in the channel complex (Figure II-1). Once the reaction is complete, excess reagent is removed and the covalently bound toxin is chemically released, restoring K^+ channel complex function. However, the reactive cysteine in one KCNE peptide is irreversibly modified. Thus, the number of KCNE peptides in the K^+ channel complex is simply the number of complete modification cycles (reagent in, out, cleaved) required before the toxin binding becomes reversible.

For the outlined counting strategy to be operational, there are two absolute, but experimentally testable conditions: (1) the non-specific bimolecular reaction between

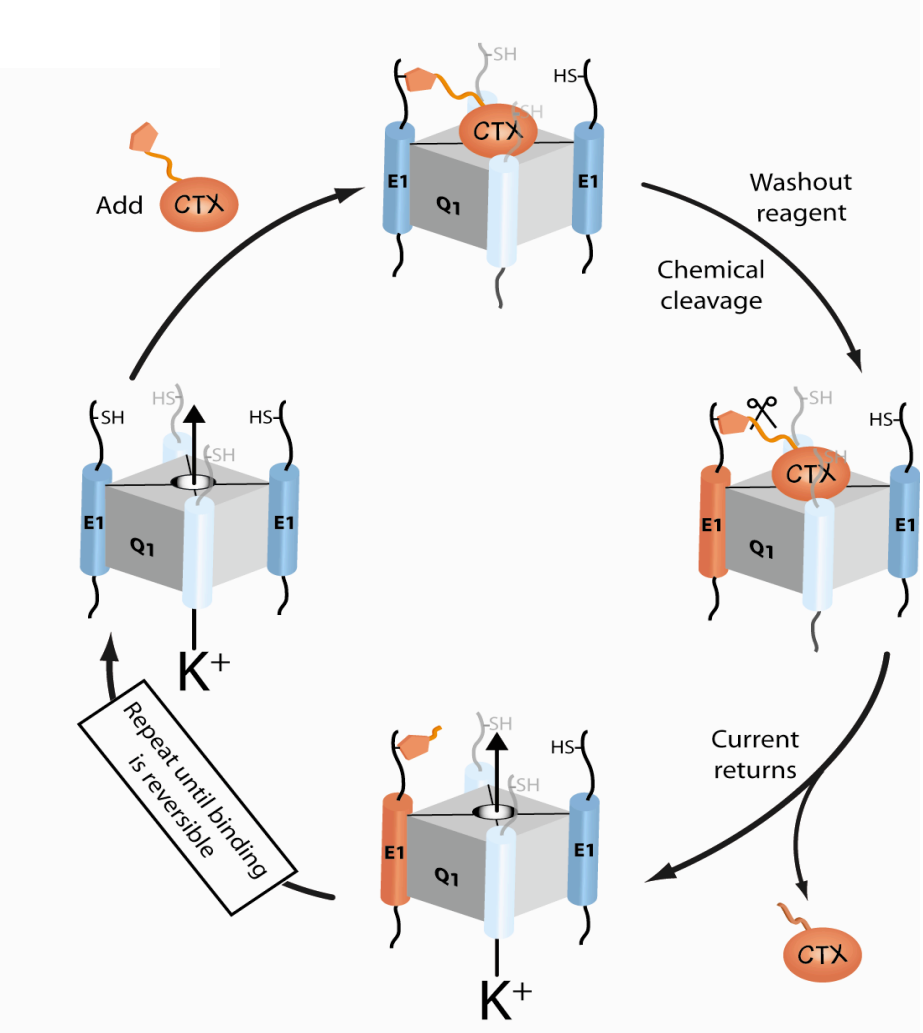

Figure II-1 A cartoon depiction of one modification cycle of the iterative counting strategy used to determine the number of KCNE1 subunits in a KCNQ1 K^+ channel complex using a derivatized charybdotoxin (CTX).

Starting with an unmodified channel complex (figure middle left) reagent is added (orange) and allowed to irreversibly block channels through maleimide-thiol tethering. After linker cleavage (middle right) the CTX blocking moiety is free to diffuse away, and E1 subunits are permanently modified (figure bottom middle). Each complete round of chemical treatment modifies one E1 subunit, allowing for the direct counting of KCNE subunits in the K^+ channel complex.

the reagent and the cysteine in the KCNE peptide must not occur. (2) Only one KCNE peptide in the K^+ channel complex may react during the exposure to the reagent.

Material and Methods

Mutagenesis and *In Vitro* Transcription:

For optimal CTX binding to the Q1/E1 complex, CTX sensitive Q1 and hemagglutinin-tagged E1 constructs between residues 11 and 12 were used and subcloned into a vector containing the 5' and 3' UTRs from the *Xenopus* β-globin gene for optimal expression in *Xenopus* oocytes. Site-directed mutagenesis was performed using Quickchange (Stratagene). mRNA *in vitro* transcription was performed by linearizing plasmid DNA with Mlu I (NEB) and run-off transcription with SP6 RNA polymerase (Promega) .

Oocyte preparation and cRNA injection:

Mature oocytes were surgically extracted from anesthetized *Xenopus laevis*. Isolated oocytes were mechanically separated and bathed in OR2 (mM): 82.5 NaCl, 2.5 KCl, 1 $MgCl_2$, 5 HEPES, pH 7.4 + 2 mg/ml collagenase (Worthington Biochemical Corp.) for 85-95 minutes to remove ovarian material and follicles. After rinsing, oocytes were incubated overnight at 18°C in ND96-bathing (ND96B) solution + gentamicin + glutathione (mM): 96 NaCl, 2 KCl, 1.8 $CaCl_2$, 1 $MgCl_2$, 5 HEPES, 50 μg/ml gentamicin (Sigma), 2 mM glutathione (Sigma), pH 7.4. For TEVC, oocytes were injected with a Q1:E1 mRNA ratio (15:5 ng) to ensure that E1 was in excess. Oocytes were incubated

for 3–5 days with 3 mM L-glutathione, pre-treated with 1 mM TCEP for 15 min before recording,

Electrophysiology

Currents were measured using two-electrode voltage clamp (OC-725-C, Warner Instrument Corp.) and data acquired with Digidata 1322A (Axon Instruments) running Clampex 8.2 (Axon Instruments) at RT. Electrodes were filled with 3M KCl, 5 mM EGTA, 10 mM HEPES, pH 7.6, and had resistance between 0.2 – 1.5 MΩ. A home-made gravity-fed perfusion chamber was used, in which complete solution exchange occurred within ~ 10 s. ND96 (mM): 96 NaCl, 2 KCl, 0.3 $CaCl_2$, 1 $MgCl_2$, 5 HEPES, pH 7.0. The current was measured by holding at – 80 mV and pulsing to +20 mV for 5 s every 30 s in ND96.

Cell Surface Chemistries:

Labeling reagents CTX-Clv and CTX-Mal (10 nM) were in ND96 solution with 50 µg mL^{-1} bovine serum albumin and were added to the bath by a gravity-fed perfusion system with a chamber clearing time of ~ 10 s. CTX-Clv cleavage was accomplished by 1 mM TCEP for ~180 s. To randomly label cell surface cysteines with Mal-ES (Lu et al., 2007), TCEP-pretreated oocytes were incubated with 10 µM Mal-ES in ND96 for 500 s.

Chemical Synthesis:

3-maleimido-N-[2-(phenylamino)ethyl]propanamide (2.1) was synthesized by dissolving 1.33 g (5 mmol) of 3-Maleimidopropionic acid N-hydroxysuccinimide ester (Aldrich) in 100 mL of methylene chloride. N-phenylethylenediamine (0.72 mL, 5.5 mmol) and triethylamine (0.78 mL, 5.5 mmol) were added and the solution turned yellow and a white precipitate formed. After 4 hours at room temperature, the precipitate was filtered and the solvents were removed in vacuo to afford a yellowish-orange oil. The crude material was purified by silica gel chromatography eluting with a gradient of 20:1 to 10:1 methylene chloride:ethyl acetate to yield 0.83 g (58%). ^{1}H NMR (400 MHz, $CDCl_3$) δ 2.53 (app t, 2 H, J = 7.0), 3.24–3.27 (m, 2 H), 3.47–3.51 (m, 2 H), 3.84 (app t, 2 H, J = 7.0), 6.61 (d, 2 H, J = 8.5), 6.62 (s, 2 H), 6.71 (t, 1 H, J = 7.3), 7.18 (t, 2 H, J = 8.5); ^{13}C NMR (100 MHz, $CDCl_3$) δ 34.26, 34.80, 39.00, 43.64, 112.7, 117.5, 129.3, 134.1, 147.9, 170.4, 170.6; HRMS (ESI) calculated for $C_{15}H_{17}O_3N_3$ $(M+H)^+$ equals 288.1348, experimentally found was 288.1.

Bis(chlorocarbonyl)disulfane (2.2) was synthesized via literature precedent (Barany et al., 1983; Martinez and Vega, 1986) with several modifications to simplify the procedure for small scale preparations. Ethoxythiocarbonyl chloride was synthesized as previously described (Martinez and Vega, 1986) and used without distillation. An equimolar (5 mmol) amount of chlorocarbonylsulfenyl chloride (Alfa Aesar) was added to neat ethoxythiocarbonyl chloride (5 mmol) and the reaction was allowed to stir overnight at

room temperature. The reaction was chilled to 0°C with an ice bath, a catalytic amount of $FeCl_3$ (~1 g) was added, and the reaction warmed slowly to room temperature overnight. The low boiling contaminants were removed by rotary evaporation at aspirator pressure and then the product was purified by distillation and characterized by NMR as previously described (Barany et al., 1983).

Cleavable bismaleimide (2.3). A solution of 0.83 g (2.9 mmol) of compound **2.1** in dry chloroform was chilled to – 20°C, and a solution of 175 μL (1.5 mmol) of bis(chlorocarbonyl)disulfane in 5 mL of chloroform was slowly added to this solution. The cooling bath was removed and the reaction was allowed to stir at room temperature for 1 hr. The reaction was diluted with chloroform, washed twice with 0.1 N HCl, and the organic layer was dried over Na_2SO_4. The solvents were removed *in vacuo* and the crude product was purified by silica gel chromatography eluting with a shallow gradient from $CHCl_3$ to 33:1 $CHCl_3$:methanol to afford 226 mg (23%). ^{1}H NMR (400 MHz, $CDCl_3$) δ 2.56 (app t, 4 H, J = 7.0), 3.44–3.48 (m, 4 H), 3.84–3.88 (m, 8 H), 6.62 (s, 4 H), 7.37–7.46 (m, 10H); ^{13}C NMR (100 MHz, methanol-d_4 with 10% $CDCl_3$) δ 33.26, 33.61, 36.56, 50.06, 128.9 (br. s), 129.1, 133.5, 138.6, 164.8, 170.0, 170.8; Different NMR solvents were needed because of differing solubility's of the compounds. HRMS (ESI) calculated for $C_{32}H_{32}O_8N_6S_2$ $(M+H)^+$ 693.1801, found 693.2.

Synthesis of CTX-Clv:

Recombinant CTX R19C was purified and the protected CTX-MTSET adduct was prepared according to Shimony and Miller (Shimony et al., 1994). CTX-Clv was synthesized as follows: 16 nmols of CTX-MTSET in 2 mL of low salt buffer: (mM) 10 NaCl, 10 KPi, pH 7.4 was reduced with 1 mM DTT for 45 mins. Reduced CTX was HPLC purified using a C18 column (4.6 mm x 250 mm) eluting with solvent A: 0.1% TFA; solvent B: acetonitrile; gradient 10 to 40% B over 30 min. The pH of the fraction containing reduced CTX was adjusted to pH 7.0 using 1 M KPi, pH 7.1, and a solution of 16 µmol of bismaleimide **2.3** in 90 µl neat acetonitrile was slowly added and allowed to react for 30 min at room temperature. The reaction was placed on ice for 10 min to precipitate excess unreacted bismaleimide **2.3**, which was removed by filtration (GHP Acrodisc 0.45 um, Pall Gelman Laboratory). CTX-Clv was desalted and HPLC purified using the column and solvents described above, using a 20 to 50% gradient B over 30 min. The concentration of purified CTX-Clv was determined by UV spectrometry (OD_{280} of 1.0 = 100 uM CTX) (Shimony et al., 1994) and labeling efficiency of CTX-R19C was determined to be 30% ± 8% (n = 7). The purified product was confirmed by ESI mass spectrometry (Figure II-2) and was aliquoted, lyophilized, and stored at – 20°C. Immediately prior to use, individual aliquots were resuspended in ND96 recording containing 30% acetonitrile to ensure CTX-Clv went into solution. This solution was then diluted such that the final acetonitrile concentration was 0.3% and the final CTX-Clv concentration was 10 nM.

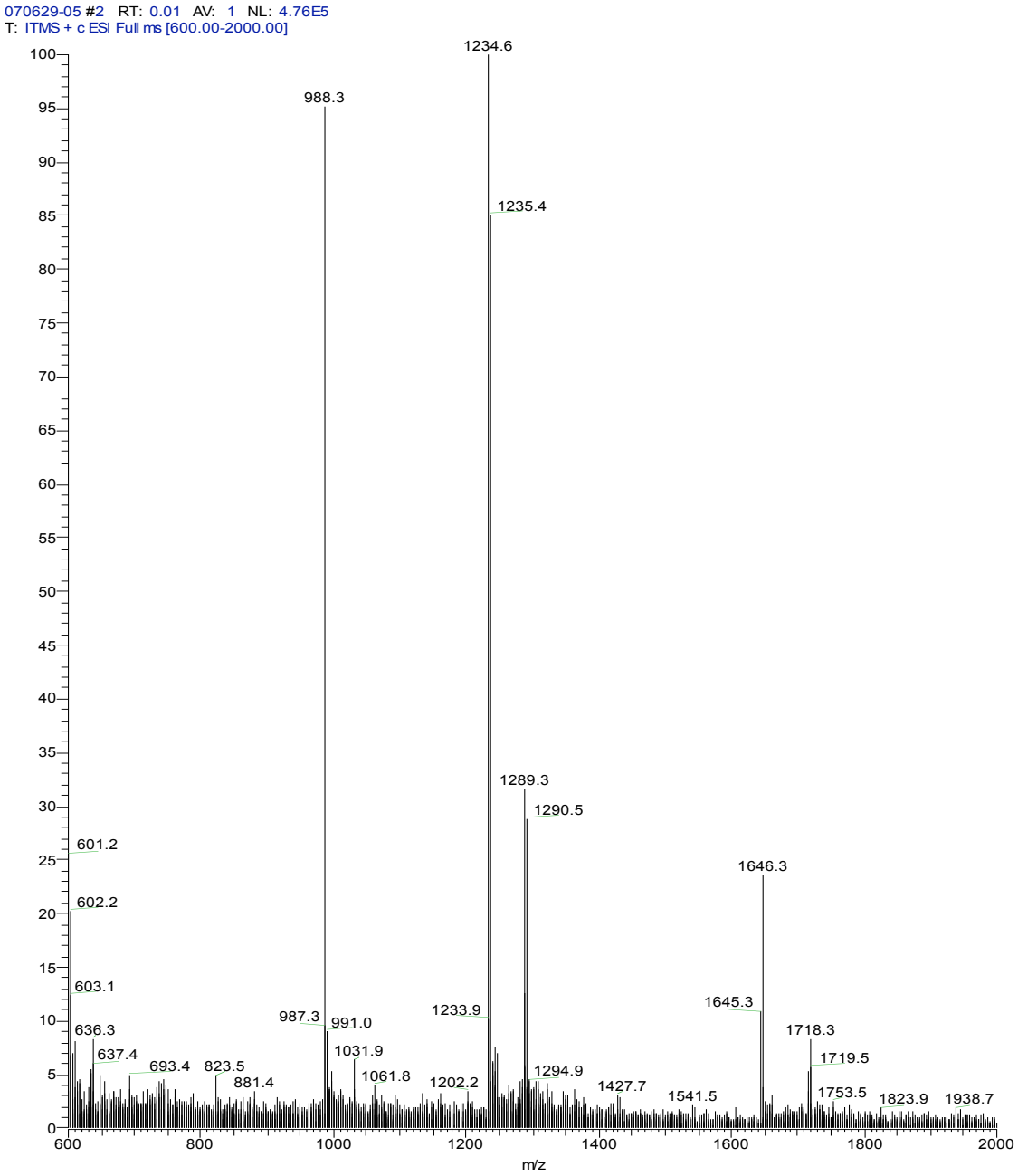

Figure II-2. CTX-Clv electrospray mass spectrum (positive mode).

Expected MW for CTX-Clv: 4933.0 (methionine oxidized); +3, 1646.0; +4, 1234; +5, 988. CTX-Clv: 5157 (methionine oxidized, 2 x TFA); +3, 1718.0; +4, 1289.5.

Binomial Analysis of MAL-ES Modification

The distribution of modified KCNE–K^+ channel complexes generated by a partial treatment of MAL-ES can be defined by the probability mass function if each modification occurs independently:

$$F(k;n,p) = \binom{n}{k} p^k (1-p)^{n-k},$$

where n is the number of KCNE peptides, k is the number of modified KCNE peptides, p is the probablility, and F is the fraction of K^+ channel complexes with all KCNE peptides modified when k = n. If one KCNE is modified per CTX-Clv treatment cycle, then Figure II-9 demands that there are two KCNE peptides in the complex. Therefore, p = 0.44 when k = 2, n = 2 and F = 0.19, which was experimentally determined after CTX-Clv washout (Figure II-10). The complementary cumulative distribution function predicts the reversibility in the second CTX-Clv washout.

$$R(x;n,p) = 1 - \sum_{k=0}^{x} \binom{n}{k} p^k (1-p)^{n-k},$$

where x is equal to the maximum number of MAL-ES modifications a K^+ channel complex can have such that there is at least one modifiable cysteine remaining in the

second cycle. For n = 2, x = 0 since all K^+ channel complexes will have one CTX-Clv modification, which occurred during the measuring of F. Thus, the expected reversibility for one CTX-Clv modification per cycle with two KCNE peptides in a K^+ channel complex (x = 0; n = 2 and p =0.44) is R = 0.69. Conversely, if two KCNE modifications occur per exposure to CTX-Clv, then each complex must have four KCNE peptides (Figure 4b) and p = 0.66 when k = 4, n = 4 and F = 0.19. In this scenario, x = 1 for the cumulative distribution function since only complexes with less than two MAL-ES modifications will have a modifiable cysteine in the second round of treatment. Thus, the expected reversibility for two CTX-Clv modifications per cycle with a 4 KCNE peptide–K^+ channel complex (x = 1; n = 4 and p =0.66) is R = 0.88. Non-integer KCNE modifications per CTX-Clv exposure are not considered since we did not observe any partial modifications or irreversibility in any of the rounds of the treatment. Integer modifications greater than two KCNE peptides are possible, however, these would result in R > 0.95 when F = 0.19.

Results

Central to the counting strategy is the chemically-releasable irreversible K^+ channel inhibitor. This reagent, CTX-Clv, is composed of three functional groups: (1) a high affinity K^+ channel inhibitor tethered to (2) a cysteine-specific modifying agent via (3) a cleavable linker (Figure II-3 top). For the K^+ channel inhibitor, charybdotoxin (CTX) was chosen, a peptide scorpion toxin that tightly binds to the tetrameric ion conduction pore with 1:1 stoichiometry (Smith et al., 1986). A maleimide was used for the cysteine-modifying agent since it forms an irreversible thioether bond with cysteines that is stable to reducing agents. For the cleavable linker, we synthesized a homo-bifunctional linker, which when cleaved with reductant does not reintroduce a thiol group. This is critical; reintroduction of a thiol would be detrimental because a complexed E1 peptide would be capable of participating in more than one round of tethered block, thus influencing the counting results. The linker was based on the cyclic dithiasuccinyl (Dts) amino protecting group (Barany and Merrifield, 1977). The linear linker, bis(N-phenylcarbamoyl)disulfane (figure II-3 top), is rapidly cleaved (< 2 min) with cell-compatible reductants (dithiolthreitol, β-mercaptoethanol, and Tris(2-carboxyethyl)phosphine (TCEP)) at biological pH, leaving behind secondary aryl amines with the concomitant release of two equivalents of carbonylsulfide gas (Figure II-3 middle and bottom).

To tether the maleimide to CTX, a cleavable bismaleimide **2.3** was synthesized. Commercially available 3-Maleimidopropionic acid N-hydroxysuccinimide ester was

reacted with N-phenylethyldiamine to afford 3-maleimido-N-[2-(phenylamino)ethyl] propanamide (**2.1**). Compound **2.2** was synthesized via literature precedent (Barany et al., 1983; Martinez and Vega, 1986). Addition of bis(chlorocarbonyl)disulfane **2.2** to 2 equivalents of maleimide **2.1** afforded the bismaleimide linker **2.3** in 25% yield after silica gel purification.

CTX-Clv was then synthesized by adding excess **2.3** to purified CTX R19C (figure II-5 and Methods). CTX mutant R19C, which upon derivatization with cysteine-modifying reagents has been shown to maintain its high affinity for the ion conduction pore of K^+ channels (Shimony et al., 1994). Briefly, the R19C mutated charybdotoxin was purified as a fusion protein with bacterial protein gene 9. After one round of purification using anion exchange, the negatively charged gene 9 was trypsinized allowing HPLC purified positively charged CTX-R19C to be labeled with MTSET and further purified using cation exchange. The mixed disulfide CTX-MTSET adduct was reduced, HPLC purified, and labeled with 500-fold molar excess **2.3** for 10 min. Excess bismaleimide was precipitated, and the labeled toxin was HPLC purified. Final CTX-Clv product was confirmed using ESI-MS (figure II-2).

CTX-Clv was first subjected to a battery of experimental tests to assess whether it could meet the two requirements of the repetitive labeling strategy. Since CTX does not bind to wild-type Q1 channels, we utilized a variant of Q1 (Q1*) that binds CTX with nanomolar affinity (Chen et al., 2003). $Q1/E1_{T14C}$ complexes were expressed in *Xenopus*

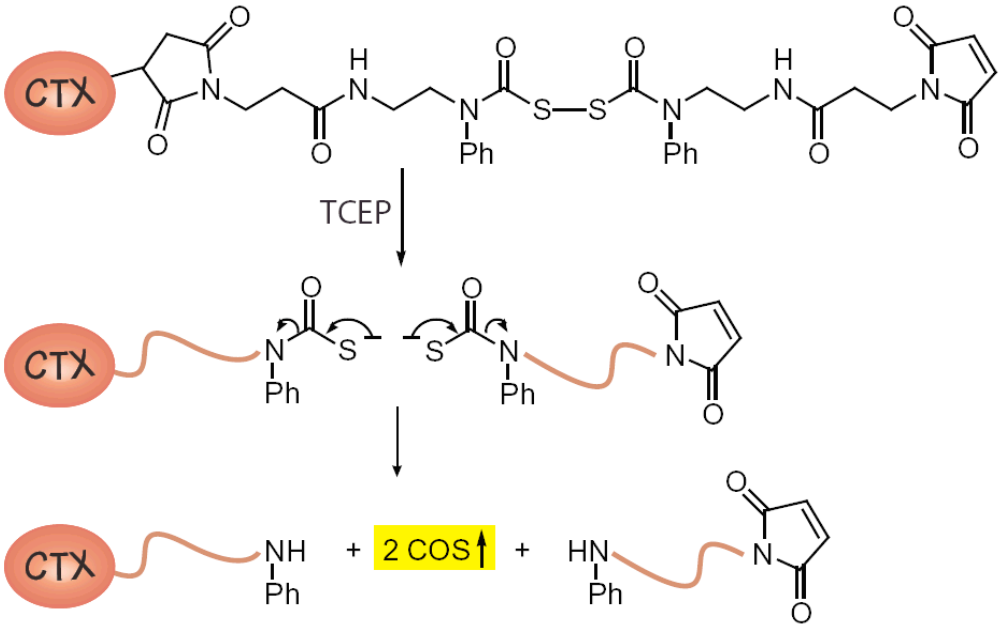

Figure II-3 Structures of the CTX-Clv reagent and TCEP cleavage of bis(N-phenylcarbamoyl)disulfane linkers and the resultant products.

The three essential components of CTX-Clv are Q1* channel inhibiting CTX, cleavable disulfide linker and reactive maleimide **(Top)**. 1 mM TCEP treatment cleaves CTX-Clv via disulfide reduction as shown **(middle)**. The 3 resulting products are modified CTX, a modified thiol reactive maleimide, and two carbonyl sulfide molecules released as a gas **(Bottom)**.

oocytes and the CTX-sensitive current was monitored since background endogenous oocyte currents are not inhibited by CTX (Kobertz and Miller, 1999; Morin and Kobertz, 2007). In all experiments, only ~85% of the total current could be inhibited (reversibly or irreversibly); even in the presence of 250 nM wild-type CTX (figure II-6), which based on the calculated dissociation constant for CTX-sensitive Q1/E1 complexes should afford 99.9% inhibition (Chen et al., 2003). We did not expect 100% block because Xenopus oocytes possess low levels of endogenous, CTX-insensitive Q1 channels that migrate to the cell surface with the injection of KCNE mRNAs (Figure II-7). Figure II-6 shows the normalized CTX-sensitive current elicited by a 20 mV pulse from an oocyte expressing $Q1/E1_{T14C}$ complexes. Treatment with 10 nM CTX-Clv followed by washout resulted in complete, irreversible inhibition of the K^+ channel complex in 3 min (Figure II-6a). The rapid irreversible inhibition observed with CTX-Clv was expected based on previous affinity-driven modifying agents, which increase the reagent's effective molarity thereby accelerating the chemical reaction (Blaustein et al., 2000). Subsequent treatment with 1 mM TCEP for 2 min relieves the irreversible inhibition and restores the current to pre-treated levels. Irreversible inhibition requires the cysteine in E1 since CTX-Clv is an entirely reversible inhibitor with wild type Q1/E1 complexes (Figure II-6b). These results demonstrate that each step in the modification cycle occurs quantitatively within minutes.

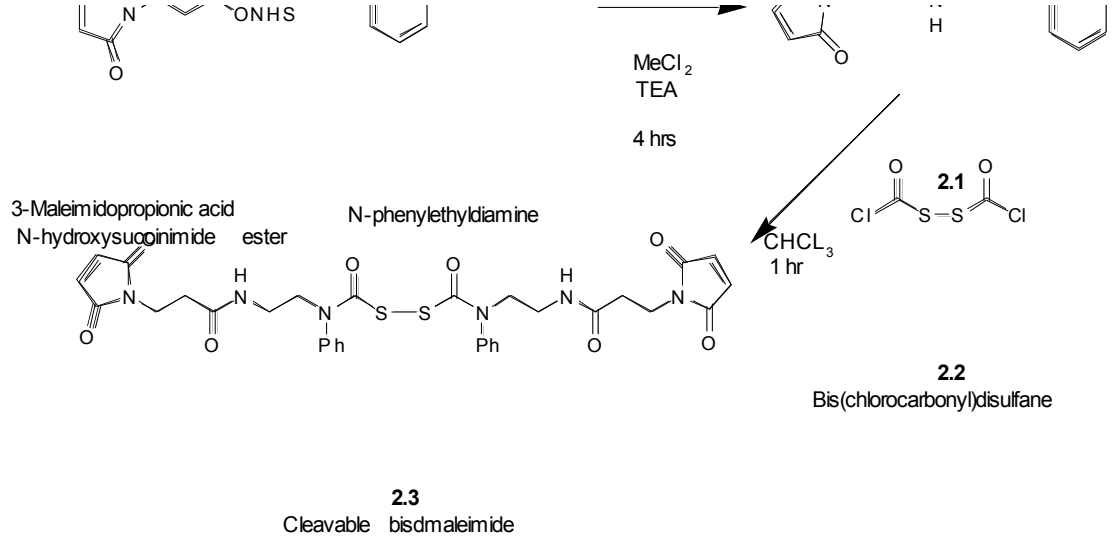

Figure II-4. Synthesis of cleavable bismaleimide (2.3)

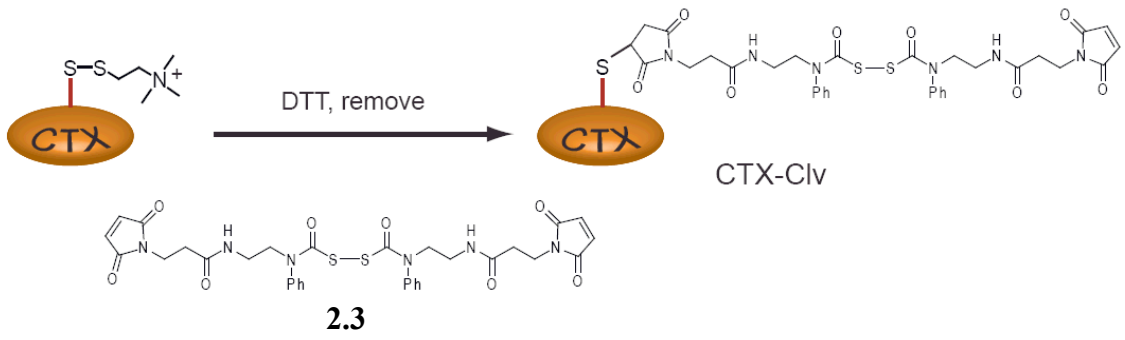

Figure II-5. Synthesis of CTX-Clv

The mixed disulfide CTX-MTSET adduct was reduced with DTT, HPLC purified, and labeled with 500-fold excess **2.3** for 10 min., HPLC purified, aliquoted and stored dry. Final CTX-Clv product was confirmed using ESI-MS (figure II-2).

To directly demonstrate the non-specific bimolecular reaction between CTX-Clv and $E1_{T14C}$ does not measurably occur, a competition experiment was performed in which $Q1/E1_{T14C}$ complexes were treated with 10 nM CTX-Clv and 500 nM of unlabeled CTX for an extended duration. CTX-Clv did not modify the $Q1/E1_{T14C}$ complex in the presence of excess competitor (unlabeled CTX), as evidenced by complete washout (Figure II-6c).

To determine whether a covalently tethered CTX-Clv prevents further toxin-accelerated modifications of the other KCNE peptides in the channel complex, a second competition experiment was performed, this time using CTX-Mal (detailed synthesis in Chapter III) (Figure II-6d), a non-cleavable version of CTX-Clv. CTX-Mal irreversibly inhibits $Q1/E1_{T14C}$ with a similar modification rate to CTX-Clv (Morin and Kobertz, 2007), yet the irreversible inhibition by CTX-Mal is completely resistant to TCEP treatment (Figure II-8b). $Q1/E1_{T14C}$ complexes were first irreversibly inhibited by CTX-Clv, as observed after washout (figure II-6d). The inhibited complexes were then treated with CTX-Mal for the same duration and the reagent was washed out. A final treatment with TCEP resulted in complete restoration of the current that was measured before the toxin treatment sequence began. This sequence of treatments shows a covalently tethered CTX-Clv prevents further toxin-accelerated modifications of the other KCNE peptides in the channel complex.

Figure II-6. Characterization of CTX-Clv

II-6 a-d (Left) Overlays of the total current elicited by a 20 mV pulse from oocytes expressing Q1/E1 and Q1/$E1_{T14C}$ complexes. Scale bars are 0.5 μA and 0.5 s. **(Right)** Normalized CTX-sensitive current (I/Imax). Oocytes were depolarized every 30 s and the data points were obtained at the end of a 5 s pulse. Gray and red data points correspond to the raw traces on the left.

a) One cycle of treatment. Q1/$E1_{T14C}$ complexes were treated with 10 nM CTX-Clv, followed by washout and 1 mM TCEP treatment, demonstrating one complete modification cycle.

b) Reversible inhibition of Q1/E1WT channels. Irreversible inhibition of Q1/E1 complexes requires an extracellular cysteine in E1 since wild type Q1/E1 complexes are only reversibly inhibited by 10 nM CTX-Clv.

c) Irreversible inhibition of Q1/$E1_{T14C}$ by 10 nM CTX-Clv is completely prevented in the presence of excess CTX (unlabeled). CTX-Clv did not modify the Q1/ $E1_{T14C}$ complex in the presence of 500 nM competitor (unlabeled CTX), as evidenced by complete washout demonstrating the non-specific bimolecular reaction between CTX-Clv and $E1_{T14C}$ does not measurably occur.

d) A tethered CTX-Clv prevents modification of the unmodified E1 peptides in Q1/E1T14C complexes by CTX-Mal. Q1/$E1_{T14C}$ complexes were irreversibly inhibited by CTX-Clv, inhibited complexes were then treated with CTX-Mal and the reagent was washed out. Treatment with TCEP restored current showing a covalently tethered CTX-Clv prevents further toxin-accelerated modifications of the other KCNE peptides in the channel complex.

a)

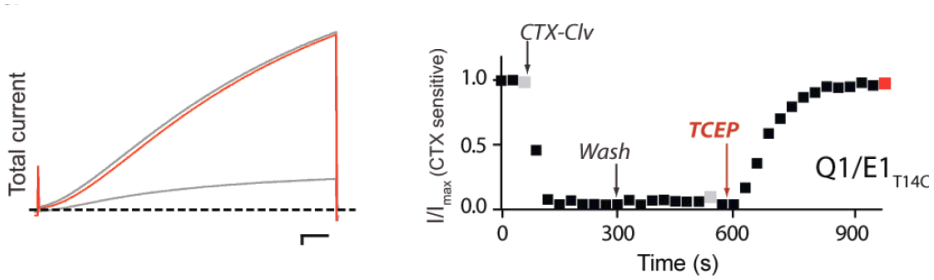
Total current
CTX-Clv
Wash
TCEP
Q1/E1T14C
I/Imax (CTX sensitive)
1.0
0.5
0.0
0
300
600
900
Time (s)

b)

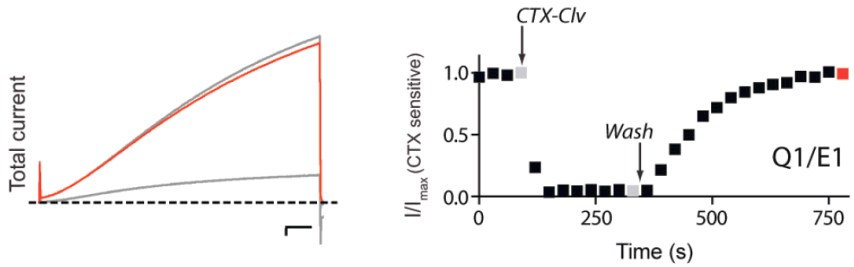
Total current
CTX-Clv
Wash
Q1/E1
I/Imax (CTX sensitive)
1.0
0.5
0.0
0
250
500
750
Time (s)

c)

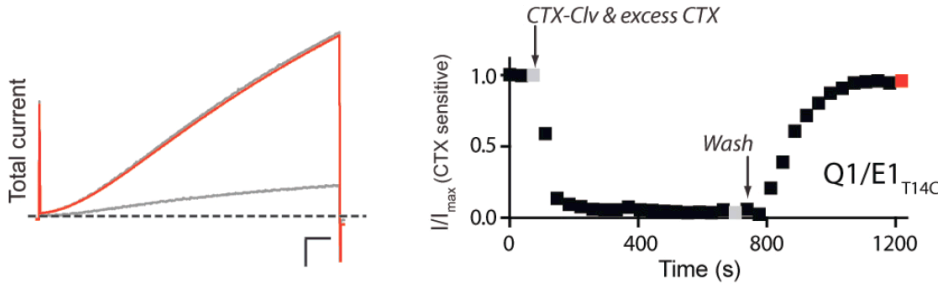
Total current
CTX-Clv & excess CTX
Wash
Q1/E1T14C
I/Imax (CTX sensitive)
1.0
0.5
0.0
0
400
800
1200
Time (s)

d)

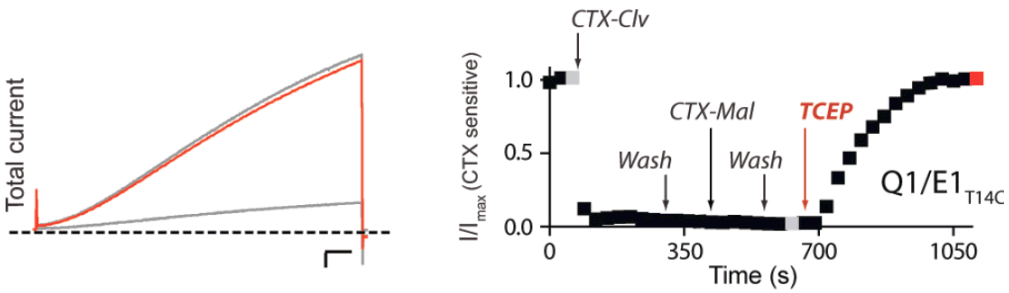
Total current
CTX-Clv
CTX-Mal
TCEP
Wash
Wash
Q1/E1T14C
I/Imax (CTX sensitive)
1.0
0.5
0.0
0
350
700
1050
Time (s)

Figure II-7. Expression of exogenous KCNE peptides in Xenopus oocytes results in assembly with endogenous Q1 channels and measurable cell surface expression.

Two-electrode voltage clamp recordings are in KD50 solution. Currents were elicited by a family of command voltages from – 100 to 60 mV at 20-mV increments. Dashed line indicates zero current. Scale bars represent 1 μA and 0.5 s.

With this now battle-tested reagent, CTX-Clv was used to count the number of KCNE peptides in the Q1 K^+ channel complex. $Q1/E1_{T14C}$ complexes were repetitively subjected to the modification cycle: CTX-Clv treatment, washout, and TCEP reductive cleavage (Figure II-9). The first two rounds required TCEP treatment to release CTX-Clv from the K^+ channel complex. The second round of CTX-Clv treatment proceeded as smoothly as the first, demonstrating that the molecular remnants left on the KCNE peptide after TCEP cleavage do not interfere with a subsequent round of binding and modification. In the third round, CTX-Clv once again inhibited the K^+ channel complex; however, inhibition was completely reversible with a simple washout, showing that it only takes two modification cycles to react with all of the KCNE peptides in a K^+ channel complex.

Although Figure II-6d demonstrated that a CTX-Clv bound and tethered to a K^+ channel complex prevents subsequent KCNE modifications by CTX-Mal, it was not directly shown that one, and only one, KCNE peptide reacts per CTX-Clv treatment. To do this, the difference in the probability mass function when n = 2, 4, or any even number of KCNE subunits (see Binomial Analysis of Modification) was used. $Q1/E1_{T14C}$ complexes were pre-treated with a membrane-impermeant maleimide (MAL-ES) (Lu et al., 2007) to randomly and independently react with a fraction of the cysteines in the N-terminus of the E1 peptide. Then the percentage of $Q1/E1_{T14C}$ complexes that were fully modified by this pre-treatment was determined by measuring the reversibility of CTX-Clv after one round of treatment and washout (Figure II-10). Based on the 19%

a)

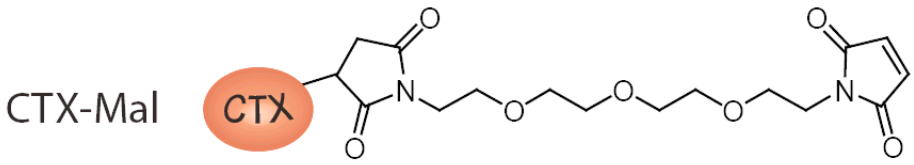

b)

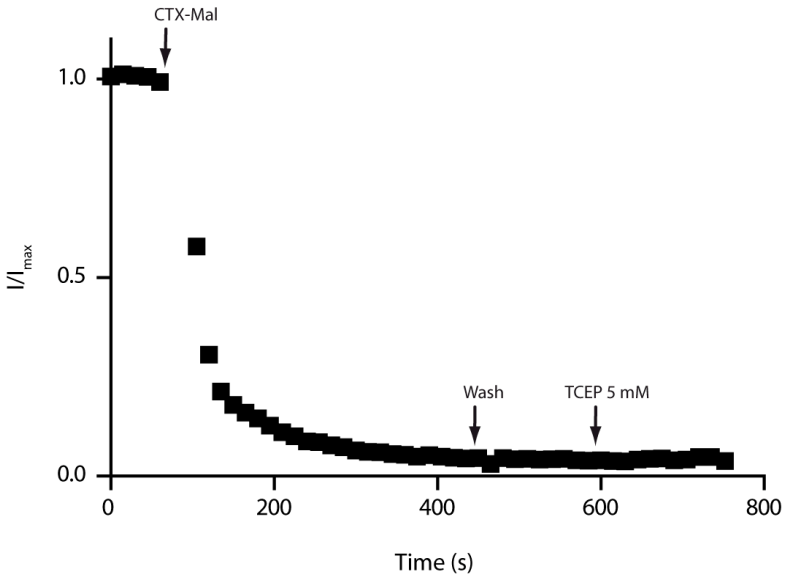

Figure II-8. CTX-Mal reagent is resistant to TCEP cleavage

(a) structure of CTX-Mal (detailed synthesis in chapter III), a non-cleavable version of CTX-Clv. **(b)** TCEP does not cleave CTX-Mal. KCNQ1-KCNE1$_{T14C}$ channels are irreversibly inhibited by 10 nM CTX-Mal treatment, and remain inhibited upon treatment with 5 mM TCEP. Current was monitored at +20 mV every 15 s.

reversible inhibition that was observed, the binomial distribution predicts that a second round of treatment with CTX-Clv would result in 69% reversibility if only one KCNE is modified per CTX-Clv treatment; 88%, if two KCNE peptides react per treatment. Cleavage of the previously tethered CTX-Clv, followed by another bolus of CTX-Clv, and washout resulted in 65 ± 4% (s.e.m.) reversibility (n = 3). We conclude that a tethered CTX-Clv protects unreacted E1 peptides from modification during the same round of treatment, that one and only one E1 peptide is modified per round of treatment, and therefore Q1 channels partner with 2 E1 β-subunits and this ratio remains fixed.

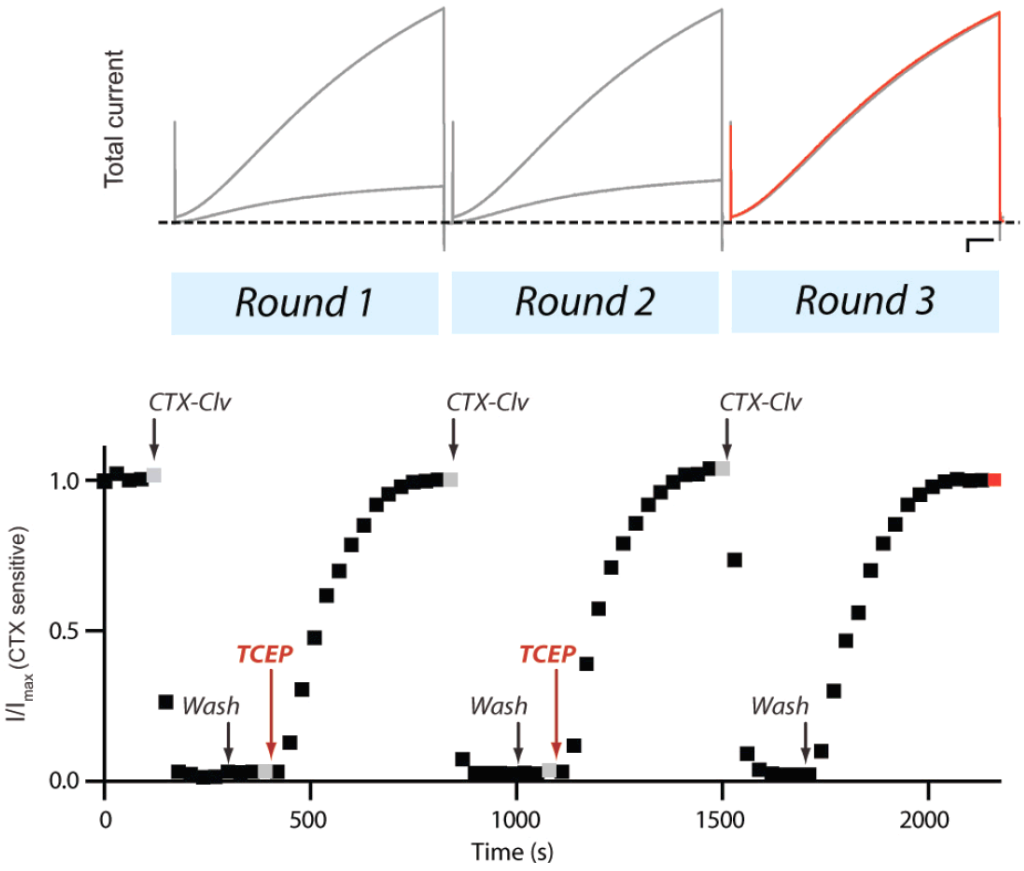

Figure II-9 KCNQ1 K^+ channel complexes contain 2 KCNE1 peptides.

Iterative counting of $E1_{T14C}$ subunits in a Q1 K^+ channel complex. (Above) Raw data showing the total current for each round. Scale bar is 0.5 µA and 0.5 s. (Below) $Q1/E1_{T14C}$ complexes were treated with two rounds (10 nM CTX-Clv, washout, 1 mM TCEP) of treatment before CTX-Clv binding became reversible. Oocytes were depolarized every 30 s and the data points were obtained at the end of a 5 s pulse. Gray and red data points correspond to the raw traces above.

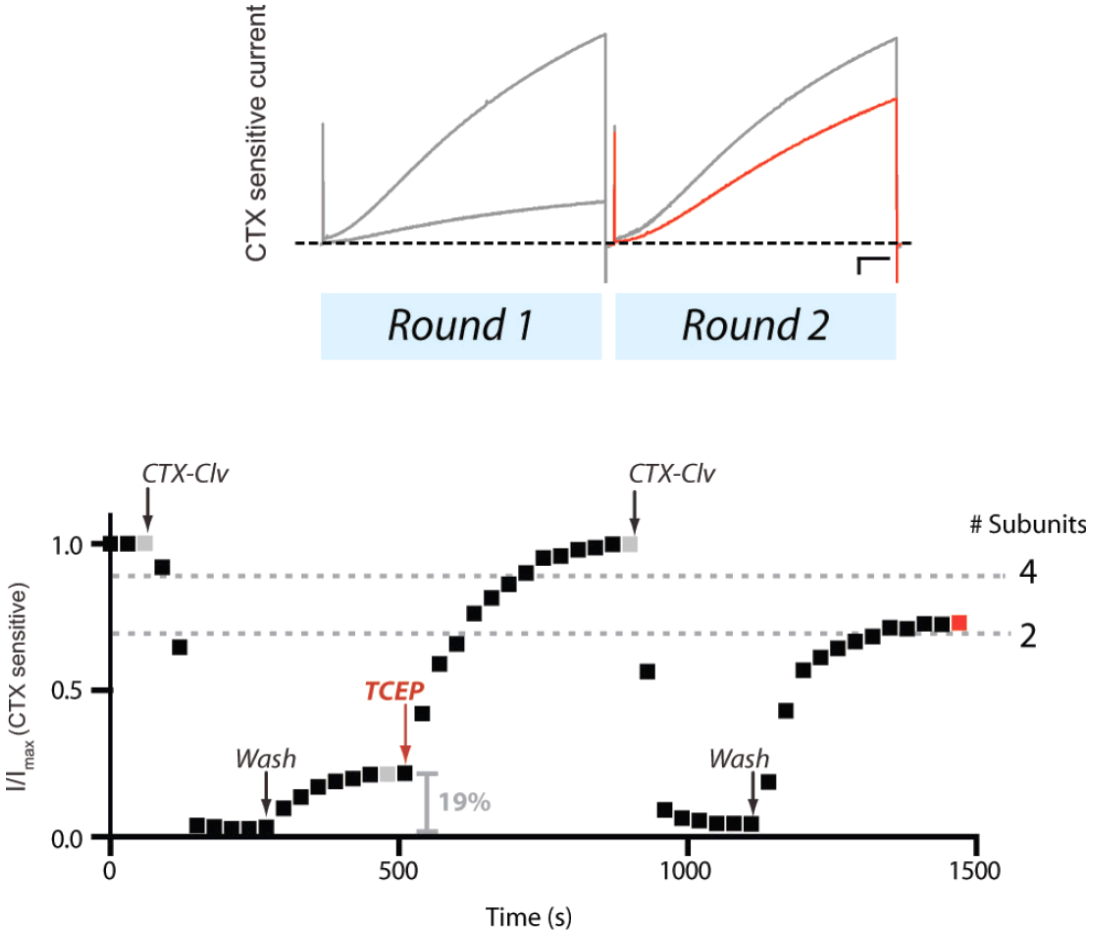

Figure II-10 Only one KCNE peptide reacts per CTX-Clv treatment.

(Above) CTX-sensitive current for each round. Scale bar is 0.5 μA and 0.5 s. (Below) Chemical modification of 19% of the cell surface Q1/ $E1_{T14C}$ complexes with 10 μM Mal-ES predicts that the reversibility of CTX-Clv in the second round will be 69% if one KCNE peptide reacts per round; 88% if two KCNE are modified per round (dotted lines, which correspond to two or four KCNE subunits in the K^+ channel complex). Washout of CTX-Clv after the second round of treatment results in 65 ± 4% (s.e.m.) reversibility (n = 3). I/I_{max} is the CTX-sensitive current that was normalized before chemical treatment. Gray and red data points correspond to the CTX-sensitive currents above.

Discussion

A tethered blocker approach was used to count KCNE β-peptides in a functioning Q1/E1 complex. It was reasoned that toxin binding is required for E1 modification and the non-specific bimolecular reaction between CTX-Clv and $E1_{T14C}$ does not measurably occur. This was based on model reactions between positively charged maleimides and thiols, which suggested the modification of $E1_{T14C}$ by CTX-Clv is ~ 1000-fold faster than the unaided bimolecular reaction (Lu et al., 2007). The observed accelerated modification rate indicated that toxin binding was required for modification and suggests that the non-specific bimolecular reaction between CTX-Clv and $E1_{T14C}$ does not measurably occur. Figure II-6c directly shows binding is required before modification since CTX-Clv did not modify the Q1/ $E1_{T14C}$ complex in the presence of excess competitor (unlabeled CTX).

In all experiments, only ~85% of the total current could be inhibited (reversibly or irreversibly); even in the presence of 250 nM wild-type CTX (figure II-6c), which based on the calculated dissociation constant for CTX-sensitive Q1/E1 complexes should afford 99.9% inhibition (Chen et al., 2003). We did not expect 100% block because Xenopus oocytes possess low levels of endogenous, CTX-insensitive Q1 channels that migrate to the cell surface with the injection of KCNE mRNAs (FigureII-7). Moreover, the near quantitative reactions observed in each round indicate that Q1/E1 complexes at the cell surface are essentially devoid of endogenous Xenopus KCNE peptides (Gordon et al., 2006) since their incorporation would result in incomplete modification cycles and

reversibility with CTX-Clv. The kinetics of CTX-Clv unbinding and the percent recovery did not vary from round to round (Table II-1).

The second competition experiment using CTX-Mal showed that a covalently tethered CTX-Clv acts as a highly concentrated competitive inhibitor and prevents further toxin-accelerated modifications of the other KCNE peptides in the channel complex. The results showed channels treated first with CTX-Clv and second with CTX-Mal were irreversibly blocked as expected. Upon TCEP treatment current fully returned indicating K^+ channel complexes with a tethered CTX-Clv are protected from subsequent modifications. Had CTX-Mal slipped past CTX-Clv and reacted with an E1 peptide, it would have been revealed as remaining block even after TCEP treatment. This was not the case as all current returned (Figure II-6d).

The results from the counting experiment (figure II-9) that show complete irreversible block during the first two cycles of CTX-Clv treatment and the results from the competition experiment with CTX-Mal (figure II-6d) indicate that mixed stoichiometries do not exist. If mixed stoichiometries were possible, partial return of current would be observed during the washout step (prior to cleavage) (figure II-9) and complete return of block would not have been observed due to non-cleavable CTX-Mal tethering (figure 6d), neither of these scenarios were observed. Our results clearly show that the channels have an even number of E1 peptides, but do not rule out the possibility that we were modifying two E1 peptides per treatment.

We directly showed that one, and only one, KCNE peptide reacts per CTX-Clv treatment by utilizing the difference in the probability mass function when n = 2, 4, or

any even number of KCNE subunits (figure II-10). Oocytes expressing Q1/E1$_{T14C}$ were treated with Mal-ES to non-specifically label cell surface cysteines; we did not know which or how many cysteines were reacted with during our treatment. One cycle of treatment with CTX-Clv reveals this however, and using the probability of mass function we predicted how much return of current (without cleaving) we would see during a second cycle of treatment, if there are two, three, four or more E1subunits. Fortunately, the numerical difference between each scenario is within our experimental measure. We performed the experiment and saw our results matched (within error) the predicted value observed if channels posses just two subunits. In fact, this experiment shows there are just two E1 subunits per channel; we did not want to draw our conclusions on this data alone, however, since we were matching our data to a predetermined outcome. Our supporting counting experiment (figure II-9) allows us to conclude that there are two KCNE peptides in a Q1 K^+ channel complex, resulting in a complex that is not four-fold symmetric.

The 4:2 (α:β) stoichiometry of the Q1/E1 complex has several broad implications on KCNE modulation of voltage-gated K^+ channels. If modulation is due to a direct KCNE–K^+ channel protein-protein interaction, then KCNE peptides either interact with only two of the α-subunits in a K^+ channel complex or they bifurcate adjacent α-subunits, making two unique sets of protein contacts with all four ion conducting subunits (Chen et al., 2003; Liu et al., 2007; Kang et al., 2008). Alternatively, KCNE modulation of K^+ channels could be allosteric in nature; the two subunits cooperate to influence protein conformation, thereby influencing modulation. Likewise, mutant KCNE peptides that

produce diseased K^+ channel complexes (Splawski et al., 1997; Sesti and Goldstein, 1998; Splawski et al., 2000; Ma et al., 2003) will impart their deleterious effects on ion conduction and channel gating due to their bifurcation of subunits or allosteric regulation.

Interpreting the effects of KCNE peptides on K^+ channel function is made even more complex with the discovery that a single Q1 channel can assemble with two different KCNE peptides to form a functional heteromeric complex (Morin and Kobertz, 2007). However, since each K^+ channel complex contains only two KCNE peptides, this allows for a simplified means of controlling K^+ conduction by greatly reducing the number of potential heteromeric complexes that can form.

Table II-1. Recovery parameters after CTX-Clv application[1]

Construct	Treatment	$\tau_{recovery}$ (s)	% recovery	n
Q1/E1	CTX-Clv	98 ± 1	95 ± 2	5
$Q1/E1_{T14C}$	CTX-Clv, TCEP	97 ± 1	96 ± 2	4
$Q1/E1_{T14C}$	CTX-Clv + excess CTX	155 ± 4	96 ± 1	3
$Q1/E1_{T14C}$	CTX-Clv, CTX-Mal, TCEP	94 ± 3	94 ± 1	3
$Q1/E1_{T14C}$	Round 1, TCEP	96 ±2	96 ± 2	3
$Q1/E1_{T14C}$	Round 2, TCEP	98 ± 3	98 ± 4	3
$Q1/E1_{T14C}$	Round 3	97 ± 1	94 ± 3	3

[1]Data are from individual experiments obtained from 3–5 oocytes. Treatment describes the sequential application of chemical reagents to the indicated construct. Round 1, Round 2, Round 3 indicates the 1st, 2nd, and 3rd rounds of subunit counting (Figure II-10), respectively. Time constants of recovery were fit to a single exponential as described in Material and Methods. Percent recovery is a comparison between the amount of current remaining after CTX-Clv release to the amount of current before CTX-Clv application. Values are mean ± SEM.

CHAPTER III: A Derivatized Scorpion Toxin Reveals the Functional Output of Heteromeric KCNQ1–KCNE K^+ Channel Complexes

Abstract

KCNE transmembrane peptides allow Q1 channels to produce the diversity of potassium currents needed for proper function in a variety of cells. Although all five KCNE transcripts have been found in cardiac and other tissues, it is unclear whether two different KCNE peptides can assemble with the same K^+ channel to form a functional complex. To test this hypothesis, I utilized a derivatized scorpion toxin that irreversibly inhibits Q1 channel complexes that contain a specific KCNE peptide. Using this KCNE sensor, it was shown that heteromeric complexes form, and the functional output from these complexes reveals a hierarchy in KCNE modulation of Q1 channels: E3 > E1 >> E4. Furthermore, the results demonstrate that Q1/E1/E4 complexes also generate a slowly activating current that has been previously attributed to homomeric Q1/E1 complexes, providing a potential functional role for KCNE4 peptides in the heart.

Introduction

To meet the potassium conduction requirements for a wide variety of tissues, Q1 K^+ channels co-assemble with different KCNE β-subunits to afford membrane-embedded complexes with distinctive gating properties. In the heart, the Q1/E1 K^+ channel complex has long been thought to generate the slowly activating cardiac I_{Ks} current (Barhanin et al., 1996; Sanguinetti et al., 1996). In contrast, E2 and E3 subunits have been shown to assemble with Q1 channel subunits in epithelial cells where they maintain salt and water homeostasis (Schroeder et al., 2000; Roepke et al., 2006). The biological roles of Q1/E4 and Q1/E5 complexes have yet to be defined.

Since current kinetics and amplitude of Q1 channels is controlled by KCNE peptides, their tissue distribution has been assumed to underlie Q1–KCNE complex modulation *in vivo*. Recently, all five KCNE transcripts have been detected in cardiac (Bendahhou et al., 2005; Lundquist et al., 2005) and other tissues (Lundquist et al., 2006), raising the possibility that two different KCNE peptides can assemble with the same Q1 channel to form a heteromeric complex. Determining the functional output of heteromeric Q1–KCNE complexes has been hampered by the fact that macroscopic electrical recordings measure the total current from a cell, making it difficult to deconvolute the contribution of heteromeric complexes (e.g., Q1/E1/E4) from two populations of homomeric complexes (e.g., Q1/E1 and Q1/E4) functioning at the cell surface. Co-immunoprecipitation of one KCNE peptide by another KCNE peptide has indirectly hinted at heteromeric complex formation (Wu et al., 2006; Manderfield and

George, 2008). However, these qualitative biochemical experiments are unsatisfying given that it is unclear whether these precipitated complexes are functional. To determine whether heteromeric complexes function at the cell surface, a tethered blocker approach in combination with electrophysiological recordings was used.

Materials and Methods

Mutagenesis and in Vitro Transcription

The CTX sensitive Q1 construct (Chen et al., 2003), E1, E3, and E4 were subcloned into a vector containing the 5' and 3' untranslated regions from the Xenopus β-globin gene for optimal expression in Xenopus oocytes. Single point mutations in KCNE peptides were introduced using QuikChange site-directed mutagenesis (Stratagene). Mutated sequences were confirmed by DNA sequencing of the entire gene. E1 and E3 constructs possessed the hemagglutinin (HA) tag, YPYDVPDYA, in the N-terminus between residues 22 and 23 and 11 and 12, respectively, which has been shown to increase CTX toxin affinity (Chen et al., 2003). The complementary DNA plasmids were linearized with Mlu I, and complementary RNA was synthesized by run-off transcription using SP6 (E1) or T7 (E3 and E4) RNA polymerase (Promega).

Electrophysiology

Standard techniques were used for preparation of and recording from Xenopus oocytes by two-electrode voltage clamp 2–4 d (5–6 d for E4) after cRNA injection (methods chapter II Oocyte preparation). Oocytes expressing KCNE extracellular cysteine residues were stored in ND96 bathing solution (96 mM NaCl, 2 mM KCl, 1.8 mM CaCl2, 5 mM HEPES, pH 7.4), 50 μg mL^{-1} gentamicin containing 2 mM L-glutathione (Sigma) and incubated in ND96 recording (96 mM NaCl, 2 mM KCl, 0.3 mM

CaCl2, 1 mM MgCl2, 5 mM HEPES, pH 7.4, containing 1 mM TCEP (CalBioChem)) for 10 min prior to recording. cRNA injection ratios were as follows: Q1/E1, Q1/$E1_{T14C}$, Q1/E3, Q1/$E3_{C31S}$, and Q1/$E4_{L2C}$, 3:1; Q1/$E1_{T14C}$/$E3_{C31S}$, Q1/E1/E3, and Q1/$E4_{L2C}$/$E3_{C31S}$, 4:1:0.2; Q1/E1/$E4_{L2C}$, 4:1:1.

To generate activation curves (**Activation Curve Analysis**), current–voltage relationships were measured in ND96 or KD50 (50 mM KCl, 48 mM NaCl, 0.3 mM, CaCl2, 1 mM MgCl2, 5 mM HEPES, pH 7.4) by holding at -80 mV and pulsing for 2 or 4 s to potentials between -100 and +60 mV in 10-mV increments for 4 s, after which oocytes were returned to – 80 mV. The interpulse interval was 15 s.

For CTX experiments, bath solutions also contained 50 μg mL^{-1} bovine serum albumin. Solution exchanges were performed by gravity-fed perfusion system with a chamber clearing time of ~10 s. Families of currents before and after CTX-Mal block were recorded in the appropriate bath solution by holding at -80 mV and pulsing from -100 to +60 mV in 20 mV increments. Currents from heteromeric Q1–KCNE complexes (Q1/E1/E4, Q1/E3/E4, Q1E3/E1) were revealed by subtracting block after CTX-Mal washout families from pre-block family traces (Clampfit 9.0 Axon Instruments).

Activation Curve Analysis

The amplitude of the tail currents were measured 3 ms after return to – 80 mV and plotted versus the depolarized potential. The resultant activation curves were initially fit to a Boltzmann function, $y = A2 + (A1-A2)/(1+e^{(V-V_{½})*(-zF/RT)})$, where $V_{½}$ is the midpoint

of activation and z is the maximum slope. The upper and lower asymptotes, A1 and A2, respectively, were left to vary, allowing data to be fit in cases where channels did not fully close or were not fully activated in the voltage ranges that can be used with oocytes (-100 to +60 mV). After the initial fit, the tail current amplitudes were normalized such that the upper asymptote (A1) was equal to 1. These data were refit to the Boltzmann function, and the lower asymptote (A2) of the second fit was used to compare basal activation of the wild type Q1-E3 complexes.

CTX Derivatization.

Recombinant CTX R19C was purified and the protected CTX-MTSET adduct was prepared according to Shimony et al. (Shimony et al., 1994). CTX-Mal was synthesized as follows: 16 nmol of CTX-MTSET in 2 mL of Buffer C (10 mM NaCl, 10 mM KPi, pH 7.4) was reduced with 1 mM DTT for 30 min and bound to a SP Sephedex (Sigma) cation exchange column. DTT was washed from the column using 150 mL of Buffer C, and the resin bound CTX was labeled with 3 mL of 5 mM $BM[PEO]_3$ (Pierce) in Buffer C. After 10 min, the column was washed with Buffer C to remove excess label, and CTX-Mal was eluted with 1 M NaCl in 10 mM KPi, pH 7.4. CTX-Mal was desalted and HPLC purified using a C18 column (4.6 mm 250 mm) eluting with solvent A (0.1% TFA)/solvent B (acetonitrile) gradient 10% to 40% B over 30 min. The concentration of purified CTX-Mal was determined by UV spectrometry (OD280 of 1.0 100 μM CTX (Shimony et al., 1994) and labeling efficiency of CTX-R19C was determined to be 35% ± 5% (n = 10).

The purified product was confirmed by electrospray ionization mass spectrometry (Figure III-1) and was aliquoted, lyophilized, and stored at -20 °C. Individual aliquots were resuspended in recording solutions immediately prior to use.

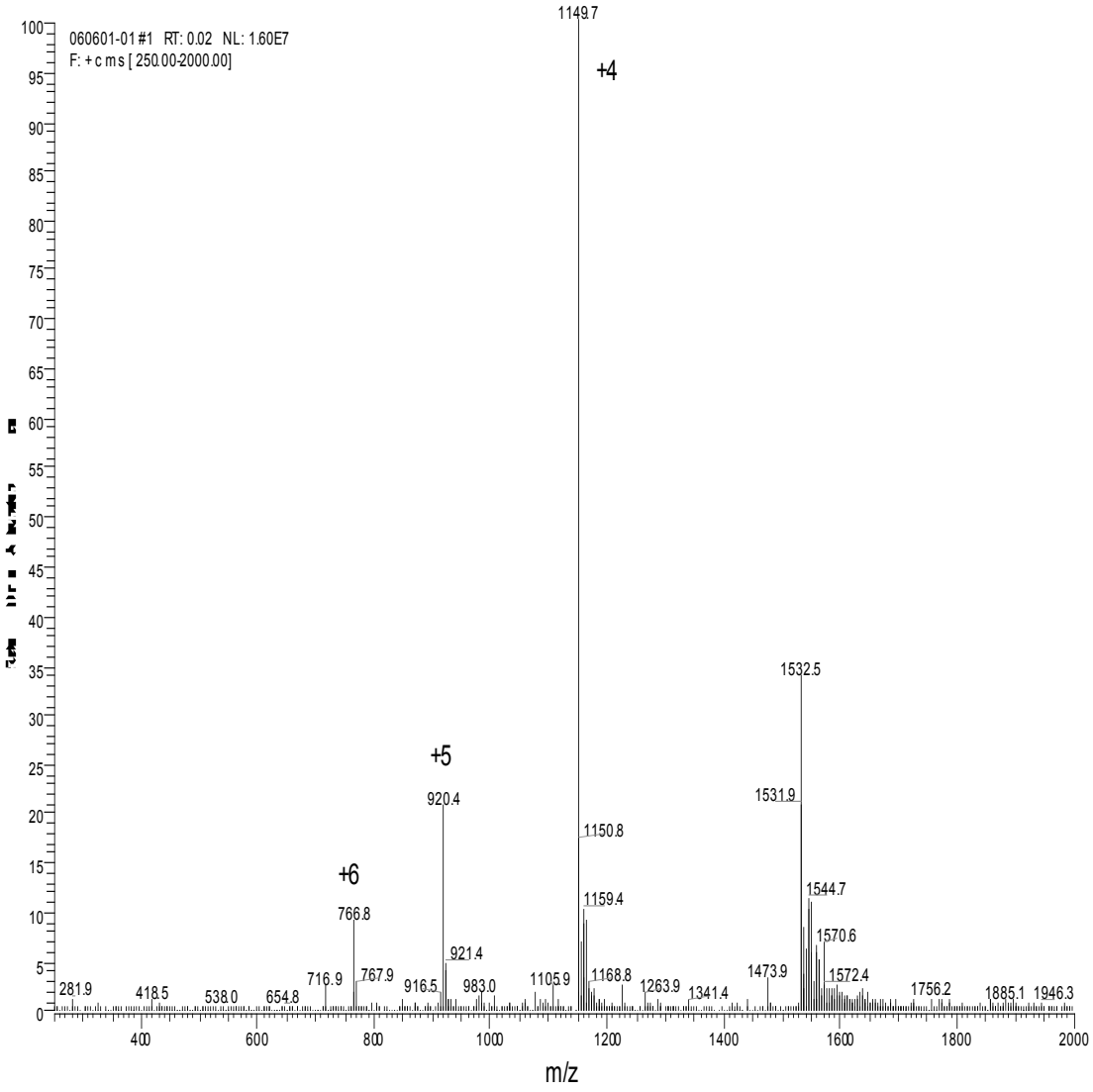

Figure III-1 CTX-Mal electrospray mass spectrum (positive mode).

Expected MW for CTX-Mal: 4593.0 (methionine oxidized); +**3**, 1532.0; +**4**, 1149.3; +**5**, 919.6; +**6**, 766.5.

Results

KCNE peptides have a striking effect on the opening and closing of Q1 channels, and these gating differences have been traditionally used to identify the composition of homomeric Q1–KCNE complexes (Figure III-2). Q1/E1 complexes are strongly voltage-dependent and upon depolarization give rise to a slowly activating K^+ current (Barhanin et al., 1996; Sanguinetti et al., 1996) whereas Q1/E3 complexes are open at both negative and positive voltages and have nearly instantaneous gating kinetics (Figure III-2) (Schroeder et al., 2000). In contrast, when Q1 assembles with E4, the complexes are essentially non-conducting at the plasma membrane (Figure III-2) (Grunnet et al., 2002). Coexpression of Q1 and E1 with E3 or E4 results in an amalgam of currents (Figure III-2), and visual inspection or activation curve analysis (Figure III-2) does not reveal whether there are heteromeric Q1–KCNE complexes functioning at the plasma membrane.

To detect KCNE peptides in functioning Q1 channel complexes, a synthetically modified charybdotoxin (CTX) was generated to specifically react with cysteine residues within the N-termini of KCNE peptides (Figure III-3a). As discussed in Chapter 2, an arginine on the backside of the toxin can be mutated to cysteine (R19C) for derivatization without affecting its affinity for K^+ channels (Shimony et al., 1994; Posson et al., 2005). To convert CTX into a cysteine reactive inhibitor (CTX-Mal), R19C mutated charybdotoxin was purified as a fusion protein from E. coli and subsequently purified as the mixed disulfide CTX-MTSET adduct. CTX-MTSET was reduced with DTT, bound

to a cation exchange column, labeled with 100-fold excess bismaleimide (BM-PEO_3) (Pierce) (figure III-3b) and HPLC purified after elution with high salt (see Methods section for details).

As mentioned in Chapter II, CTX does not inhibit native Q1/E1 complexes; therefore, we utilized a variant of Q1 (Q1*) that is blocked by nanomolar concentrations of toxin (Chen et al., 2003). CTX-sensitive Q1/E1 complexes do not possess any extracellular cysteines and thus CTX-Mal should reversibly bind to these complexes. When cells expressing CTX-sensitive Q1/E1 complexes were treated with 10 nM CTX-Mal, the current was blocked, and then upon washout, it fully recovered to pretreated levels, demonstrating that inhibition was reversible (Figure III-4a). Q1/E3 complexes were also reversibly blocked by CTX-Mal when the lone cysteine in E3 (C31S) was removed by mutagenesis (Figure III-4b). These control experiments showed that chemical derivatization of CTX did not disrupt binding to the Q1 channel pore.

Next the N-terminus of E1 was cysteine-scanned to find residues that were covalently modifiable by CTX-Mal. The N-termini of KCNE peptides are ideal for cysteine mutagenesis because these regions in E1 and E3 are not required for assembly with or modulation of Q1 channels (Takumi et al., 1991; Gage and Kobertz, 2004). Mutation of three E1 residues (Thr14, Gln22, and Ser34) to cysteine resulted in Q1/E1 complexes with wild-type gating kinetics that were irreversibly blocked by CTX-Mal. $Q1/E1_{T14C}$ complexes were the most reactive, showing no relief of inhibition upon washout of CTX-Mal (Figure III-4c). Covalent tethering of CTX-Mal to $Q1/E1_{T14C}$

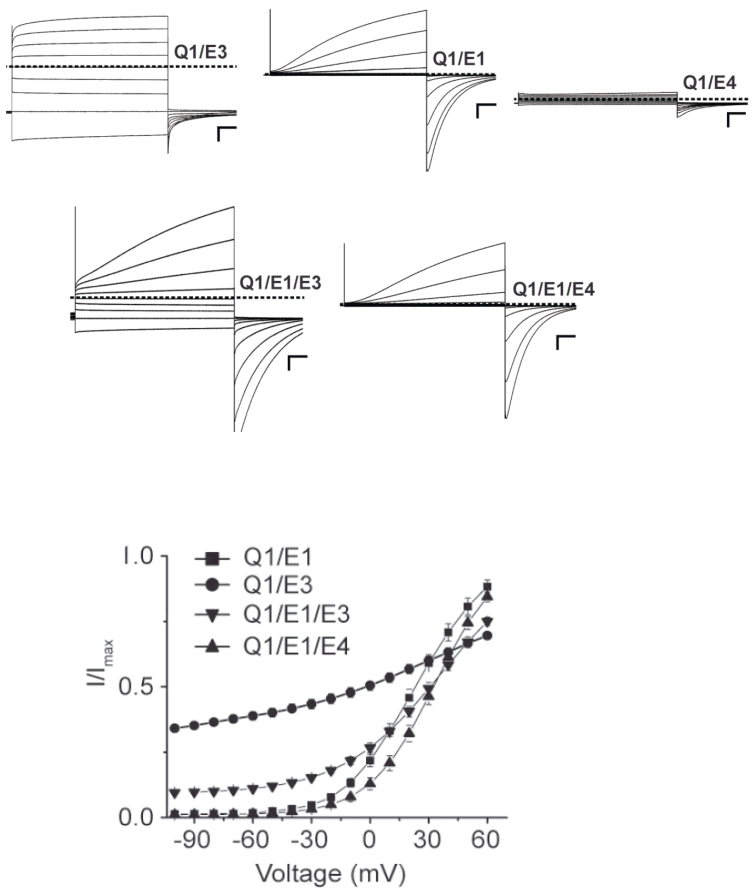

Figure III-2 Co-expression of KCNQ1 channels with two different KCNE peptides gives rise to an amalgam of voltage-dependent and -independent currents.

(**Top**) **Two-electrode voltage clamp recordings for homo- and heteromeric Q1-KCNE complexes**. Inspecting current traces alone does not reveal heteromeric complex formation as opposed to two homomeric populations giving visually hybrid macroscopic current. Currents were elicited by a family of command voltages from –100 to 60 mV at 20-mV increments and recorded in KD50 solution. Dashed line indicates zero current. Scale bars represent 1 μA and 0.5 s. (**bottom**) **Voltage-activation curves of homo- and heteromeric Q1-KCNE complexes.** The data were fit to a Boltzmann and normalized for channels that are open at negative potentials (Gage and Kobertz, 2004). Data were averaged from 3–5 oocytes each and error bars are ± SEM. Activation curve analysis does not reveal whether there are heteromeric Q1–KCNE complexes functioning at the plasma membrane.

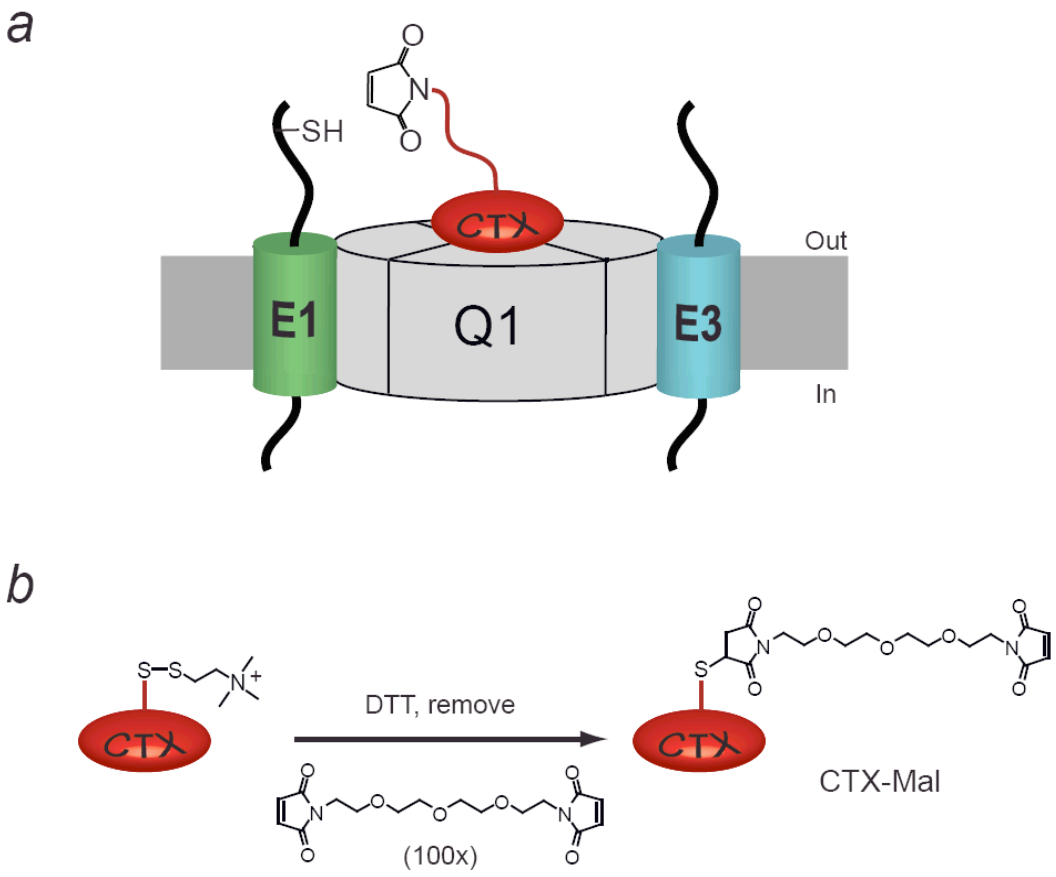

Figure III-3 Cartoon depiction of the toxin tethering reaction between CTX-Mal and a cysteine residue in E1 and CTX-Mal reagent synthesis.

a) To detect KCNE peptides, a synthetically modified charybdotoxin (CTX) was generated to specifically react with cysteine residues within the N-termini of KCNE peptides. Shown is the strategy to detect E1 peptides in Q1/E1/E3 heteromeric complexes. **b)** MTSET protected CTX was reduced and reacted with 100 fold excess BM[PEO]$_3$, the final product was HPLC purified and confirmed by ESI-MS.

required binding to the channel pore given that the reaction was completely prevented by competitive inhibition with 250 nM CTX (Figure III-4d). As was observed in Chapter 2, only ~ 85% of the total current could be inhibited (reversibly or irreversibly); even in the presence of 250 nM wild-type CTX, (Figure III-4d), which is presumably due to the low levels of endogenous, CTX-insensitive Q1 channels that migrate to the cell surface with the injection of KCNE mRNAs (figure II-7).

Armed with a reagent to detect KCNE peptides in K^+ channel complexes, we determined whether Q1/E1/E3 complexes assemble and are functional. We first placed the target cysteine in E1 (and removed the native cysteine in E3, C31S). Coexpression of $Q1/E1_{T14C}/E3_{C31S}$ resulted in both outward and inward currents in response to a family of depolarizations in a 50 mM external K^+ solution that allows for the visualization of the inward currents (shaded pink) (Figure III-5). Treatment of these cells with CTX-Mal covalently modifies and irreversibly blocks Q1 channel complexes that have assembled with $E1_{T14C}$ peptides. Upon washout, ~80% of the CTX-sensitive current generated by a -100 mV test potential was irreversibly inhibited (Figure III-5). The 80% reduction in current must be a result of blocking $Q1/E1_{T14C}/E3_{C31S}$ complexes since $Q1/E1_{T14C}$ complexes, even though irreversibly blocked in this assay, are closed and do not pass inward current at -100 mV (Figure I-2). The remaining 20% of inward current comes from $Q1/E3_{C31S}$, which lacks the cysteine and therefore cannot be irreversibly blocked (Figure III-5 after). Examination of the current–voltage traces after CTX-Mal washout (Figure III-5 after) shows an E1 component, which we postulate is due to endogenous CTX-insensitive Q1 channels partnering with $E1_{T14C}$ that cannot be blocked by CTX. To

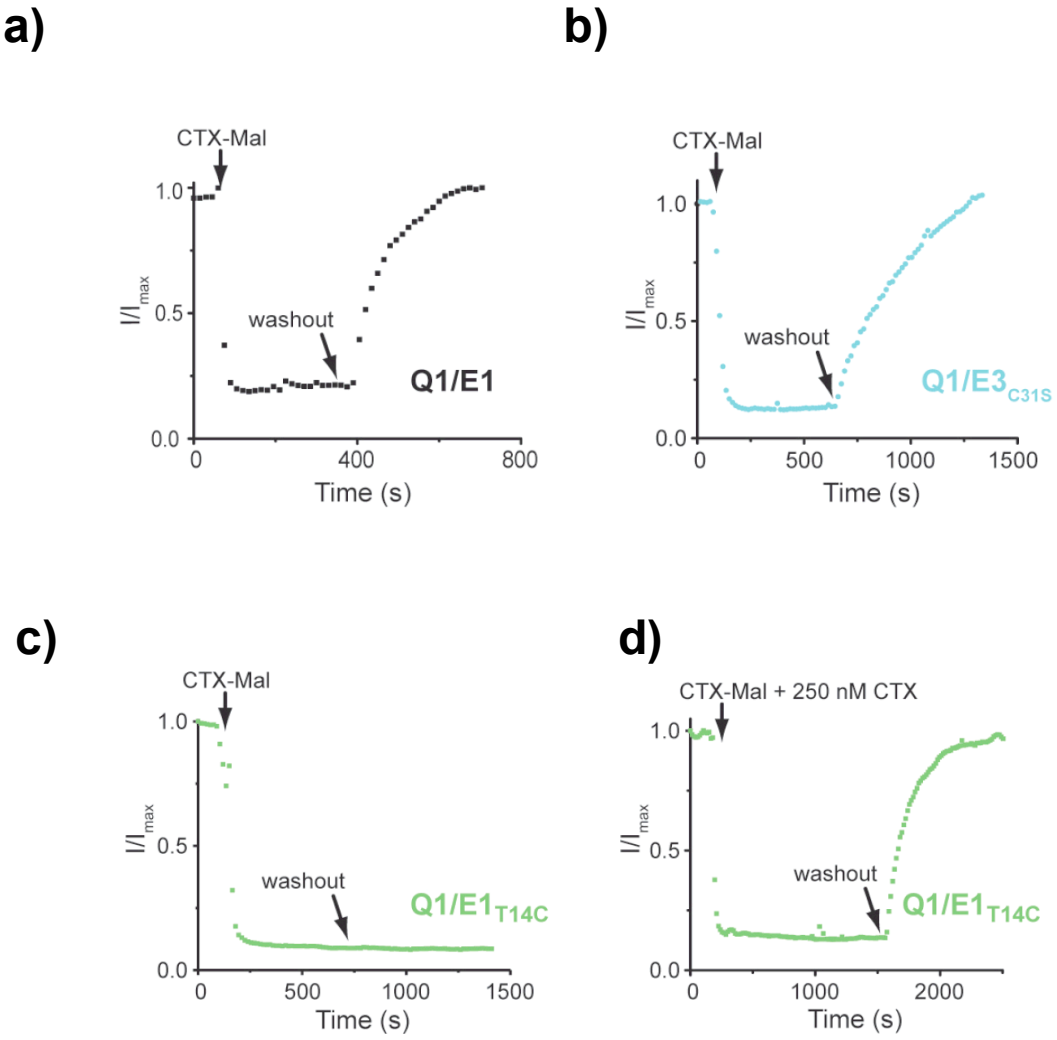

Figure III-4 Characterization of CTX-Mal on Q1/KCNE channels.

a and b) Reversible inhibition of Q1-KCNE complexes that lack extracellular cysteines. a) Q1/E1 and **b)** $Q1/E3_{C31S}$ complexes are not permanently inhibited with 10 nM CTX-Mal in ND96 solution. Current was monitored at 20 mV every 15 s.

c and d) Application of CTX-Mal to $Q1/E1_{T14C}$ complexes. c) Single cysteine containing $Q1/E1_{T14C}$ complexes were irreversibly inhibited as demonstrated by no current return after CTX-Mal washout. **d)** Inhibition was completely prevented in the presence of excess (250 nM) CTX showing CTX-Mal must bind to the channel to allow tethering between the reactive maleimide and thiol containing cysteine to occur.

visualize the currents that are irreversibly blocked by CTX-Mal, we mathematically subtracted the remaining current after block from the before block currents (Figure III-5 subtraction). This allowed visualization of the macroscopic current coming from a mixture of Q1/E1$_{T14C}$ and Q1/E1$_{T14C}$/E3$_{C31S}$ complexes at the cell surface.

To determine whether Q1/E1/E3 complexes possess any time-dependent activation at positive potentials, we utilized the native cysteine in E3 and looked at irreversible block of outward currents in wild-type Q1/E1/E3 complexes. In this assay Q1/E1/E3 and Q1/E3 channels were irreversibly blocked due to the native cysteine in E3, while Q1/E1 channels (lacking the cysteine) were reversibly inhibited. In this configuration, subtraction of the after traces from before reveals the macroscopic current of blocked Q1/E1/E3 and Q1/E3 complexes. After CTX-Mal treatment and subsequent washout of cells expressing Q1/E1/E3, we saw a reduction of both inward and outward currents as before (Figure III-6). Mathematical subtraction revealed that heteromeric Q1/E1/E3 complexes slowly activate at positive voltages and slowly deactivate upon repolarization (Figure III-6 subtraction).

Next it was determined whether Q1/E1/E4 complexes were functional. E4 is the most abundant KCNE transcript in heart (Bendahhou et al., 2005; Lundquist et al., 2006), yet when the peptide assembles with Q1, it produces a non-conducting channel complex (Figure III-2) (Grunnet et al., 2002). Therefore, to detect functional Q1/E1/E4 complexes, the cysteine residue was placed in E4. When E4$_{L2C}$ was coexpressed with Q1/E1, the resultant CTX-sensitive currents in ND96 solution were irreversibly blocked (52% ± 3%) by CTX-Mal upon washout (Figure III-7). Irreversible blockade of any current indicates

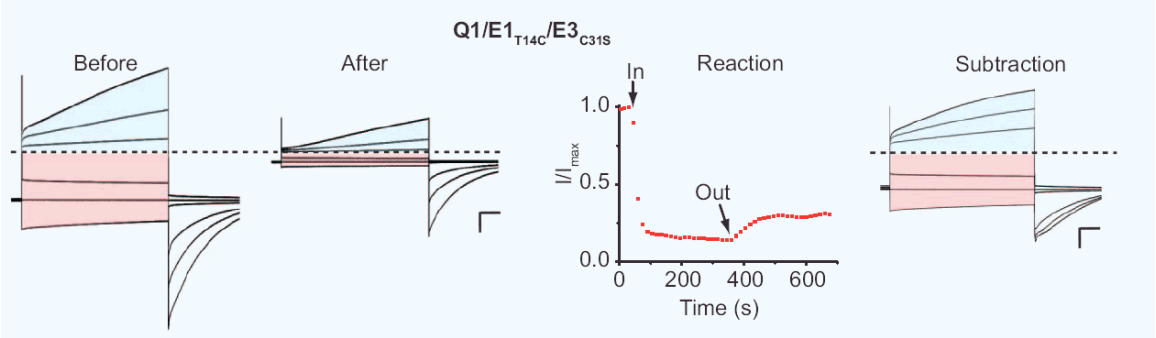

Figure III-5 Detection of heteromeric Q1/E1/E3 complexes with CTX-Mal.

Q1/E1$_{T14C}$/E3$_{C31S}$ current traces shown are pre-treatment (*Before*) and after washout (*After*) of 10 nM CTX-Mal. Currents were measured in KD50 solution and were from command voltages (– 100, – 80, – 60, 0, 20, and 40 mV). Outward currents are shaded blue; inward are shaded red. Dashed line indicates zero current. Scale bars represent 1 μA and 0.5 s.

Reaction profiles (*Reaction*) with 10 nM CTX-Mal were monitored at – 100 mV every 15 s in KD50 solution. For Q1/E1$_{T14C}$/E3$_{C31S}$, 78 ± 2% of the CTX-sensitive current was irreversibly inhibited after washout.

Mathematical subtraction reveals heteromeric Q1/E1$_{T14C}$/E3. Complexes show the inward current afforded by heteromeric Q1/E1/E3 complexes. *Subtraction* traces are a mathematical difference of the After and Before traces. Outward currents are shaded blue; inward are shaded red. Dashed line indicates zero current. Scale bars represent 1 μA and 0.5 s.

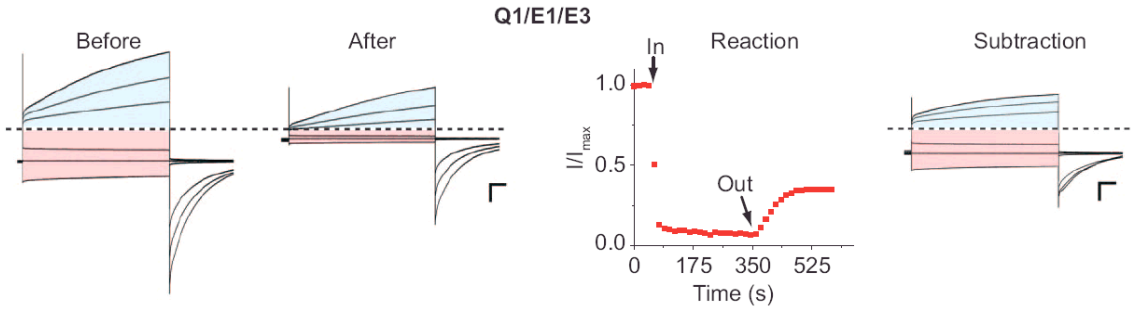

Figure III-6 Detection of heteromeric Q1/E1/E3 complexes with CTX-Mal assaying Q1/E1/E3 (using native cysteine (C31) in E3).

Current traces shown are pre-treatment (*Before*) and after washout (*After*) of 10 nM CTX-Mal. Currents were measured in KD50 solution and were from command voltages (– 100, – 80, – 60, 0, 20, and 40 mV). Outward currents are shaded blue; inward are shaded red. Dashed line indicates zero current. Scale bars represent 1 μA and 0.5 s.

Reaction profiles (***Reaction***) with 10 nM CTX-Mal were monitored at – 100 mV every 15 s in KD50 solution. 74 ± 4% of the CTX-sensitive current was irreversibly inhibited after washout. Data were averaged from 3–5 oocytes ± SEM.

Mathematical subtraction reveals that heteromeric Q1/E1/E3. Complexes slowly activate at positive voltages and slowly deactivate upon repolarization. *Subtraction* traces are a mathematical difference of the After and Before traces. Outward currents are shaded blue; inward are shaded red. Dashed line indicates zero current. Scale bars represent 1 μA and 0.5 s.

Q1/E1/E4 complex assembly given that homomeric Q1/$E4_{L2C}$ complexes are like wild-type Q1/E4 and non-conducting.

The amount of irreversible inhibition measured was predictably dependent on the ratio of E1/$E4_{L2C}$ expressed. Injection ratios that favored the formation of Q1/E1 homomers resulted in a reduction of irreversible block, whereas injection of more $E4_{L2C}$ mRNA resulted in an increase of irreversible block (Figure III-7 bottom). Subtraction of the after traces from the before traces revealed the gating kinetics of Q1/E1/E4 complexes (Figure III-7 top). Since the gating kinetics of Q1/E1/E4 complexes looked very similar to Q1/E1 currents, we were curious if E4 had any effect on channel activation. Recording Q1/E1/$E4_{L2C}$ families in KD50, treating with CTX-Mal and subtracting after currents from before allowed for the generation of activation curves for the heteromeric Q1/E1/E4 complex. Current-voltage analysis of tail current recordings in high K^+ shows virtually no change in the voltage dependence of activation (Figure III-8).

E4 also forms functional heteromeric Q1 complexes with E3. Q1/$E3_{C31S}$/$E4_{L2C}$ complexes were irreversibly inhibited by CTX-Mal in ND96 solution (Figure III-9), and again, subtraction of the after traces from the before traces revealed the gating kinetics of Q1/E3/E4 complexes (Figure III-9 subtraction). Although E4 is present in both heteromeric complexes studied, the peptide has little effect on the gating kinetics. Thus for Q1 channels, E3 and E1 dictate gating in heteromeric complexes with E4 peptides.

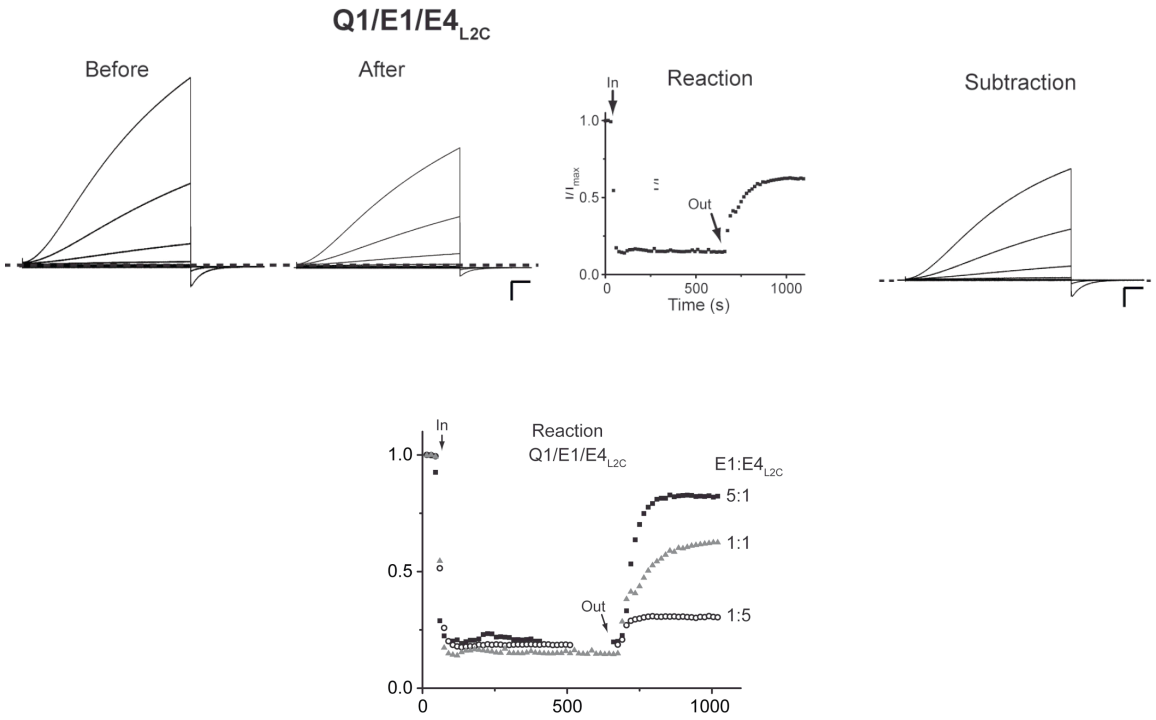

Figure III-7 E4 peptides form heteromeric complexes with Q1 and E1.

(Top) Q1/E1/E4$_{L2C}$ current traces shown are pre-treatment (*Before*) and after washout (*After*) of 10 nM CTX-Mal. Currents were measured in ND96 and elicited by a family of command voltages from – 100 to 40 mV with 20-mV steps. Dashed line indicates zero current. Scale bars represent 1 μA and 0.5 s. Reaction profiles (*Reaction*) with 10 nM CTX-Mal were monitored at 20 mV every 15 s in ND96 solution. For Q1/E1/E4$_{L2C}$, 52 ± 3% of the CTX-sensitive current was irreversibly inhibited after washout. Data were averaged from 2–5 oocytes ± SEM. Mathematical subtraction reveals gating kinetics of Q1/E1/E4 heteromeric complexes. *Subtraction* traces are a mathematical difference of the After and Before traces. Dashed line indicates zero current. Scale bars represent 1 μA and 0.5 s.

(Bottom) Irreversible block of Q1/E1/E4L2C complexes is dependent on the amount of E4$_{L2C}$. RNA injection rations were varied (E1:E4$_{L2C}$): 5:1, squares; 1:1 triangles; 1:5 open circles, which yielded 19 ± 3%, 52 ± 3%, and 86 ± 4 irreversible block of the CTX-sensitive current after washout. Data were averages from 2—5 oocytes.

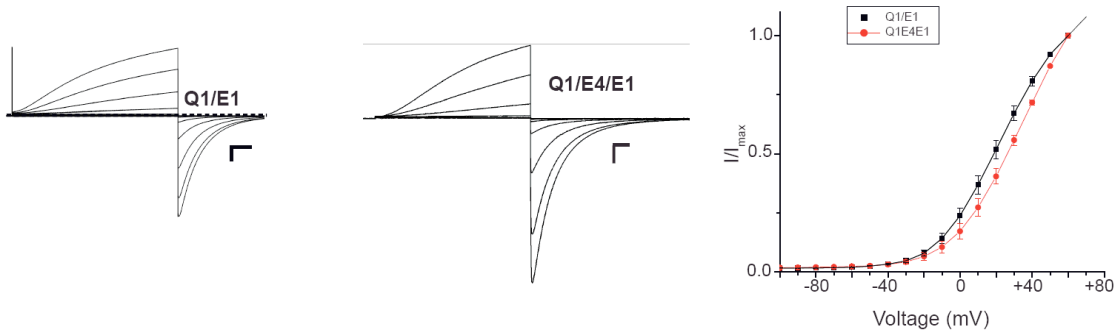

Figure III-8. Current voltage analysis of Q1/E1 currents v. Q1/E1/E4 complexes.

(Left and Middle) Currents were measured in KD50 and elicited by a family of command voltages from – 100 to 40 mV with 20-mV steps. Scale bars represent 1 μA and 0.5 s. **Voltage-activation curves of Q1/E1 and Q1/E1/E4 complexes.** The data were fit to a Boltzmann, data were averaged from 3–5 oocytes each and error bars are ± SEM.

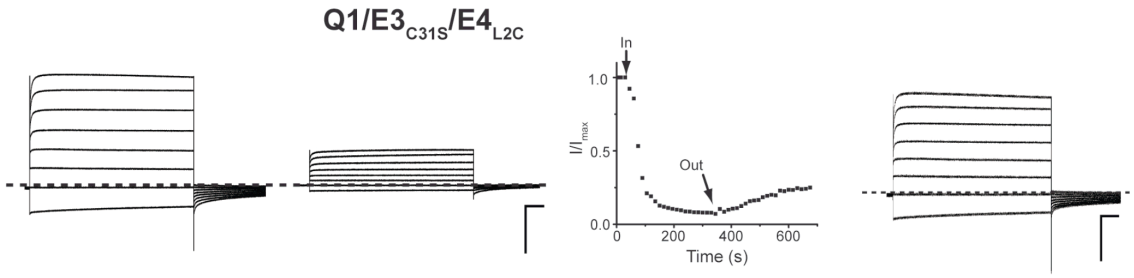

Figure III-9. KCNE4 peptides form heteromeric complexes with KCNQ1 and KCNE3.

Q1/E3$_{C31S}$/E4$_{L2C}$ current traces shown are pre-treatment (*Before*) and after washout (*After*) of 10 nM CTX-Mal. Currents were measured in ND96 and elicited by a family of command voltages from – 100 to 40 mV with 20-mV steps. Dashed line indicates zero current. Scale bars represent 1 μA and 0.5 s. **Reaction profiles** (*Reaction*) with 10 nM CTX-Mal were monitored at 20 mV every 15 s in ND96 solution. For Q1/E3/E4$_{L2C}$, 80 ± 1% of the CTX-sensitive current was irreversibly inhibited after washout. Data were averaged from 2 oocytes ± SEM. **Mathematical subtraction reveals gating kinetics and current voltage relationship of Q1/E3/E4 heteromeric complexes. *Subtraction*** traces are a mathematical difference of the After and Before traces. Dashed line indicates zero current. Scale bars represent 1 μA and 0.5 s.

Discussion

CTX-Mal was used to detect and visualize currents coming from heteromeric Q1/KCNE complexes. Using this reagent we were able to conclude Q1/E1/E3, Q1/E1/E4, and Q1/E3/E4 heteromers form and function, and by mathematical subtraction of current after block from currents before block we were able to visualize currents coming from these mixed complexes.

When the target cysteine was placed in E1 to examine Q1/E1/E3 complexes, the subtracted traces were a mixture of currents from Q1/E1 homomers and Q1/E1/E3 heteromers. However, since homomeric Q1/E1 complexes are closed and non-conducting with test potentials less than – 30 mV (Figure III-2), the inward currents in the subtracted traces in Figure III-6 are entirely from $Q1/E1_{T14C}/E3_{C31S}$ complexes. Unlike the inward currents, the outward currents (shaded blue) in the subtracted traces are contaminated with slowly activating homomeric $Q1/E1_{T14C}$ currents.

To visualize outward currents in Q1/E1/E3 and determine whether the complexes possess any time-dependent activation at positive potentials, we utilized the native cysteine in E3 and looked at irreversible block of outward currents in wild type Q1/E1/E3 complexes. The blocked outward currents in this configuration will still be a mixture of homo- and heteromeric complexes; however, the homomeric complexes are Q1/E3, which are devoid of slow gating (Figure III-2). Thus, any slow gating observed would be due to heteromeric Q1/E1/E3 complexes. Mathematical subtraction reveals that heteromeric Q1/E1/E3 complexes slowly activate at positive voltages and slowly

deactivate upon repolarization (Figure III-5 and III-6, Subtraction). In total, these results show that the Q1/E1/E3 complex generates current with the combined properties of homomeric Q1/E1 and Q1/E3 complexes: it is a heteromeric complex that closes slowly (E1-like), is partially open at negative potentials (E3-like), and slowly opens with positive depolarizations (E1-like).

To ascertain whether Q1/E1/E4 complexes were functional we placed the target cysteine in E4. Since Q1/E4 complexes are non-conducting any irreversible block we observe must be due to heteromeric Q1/E1/E4 complexes. When $E4_{L2C}$ was co-expressed with Q1/E1, the resultant CTX-sensitive currents in ND96 solution were irreversibly blocked (52 ± 3%) by CTX-Mal upon washout (Figure III-7). Furthermore, injection ratios that favored the formation of Q1/E1 homomers resulted in a reduction of irreversible block whereas injection of more $E4_{L2C}$ mRNA resulted in an increase of irreversible block (Figure III-7 bottom). The difference between the after and the before traces revealed the gating kinetics of Q1/E1/E4 complexes (Figure III-7, Subtraction), which resemble the cardiac I_{Ks} current that has been attributed to Q1/E1 complexes.

E4 also forms functional heteromeric Q1-complexes with E3. Figure III-9 shows that $Q1/E3_{C31S}/E4_{L2C}$ complexes were irreversibly blocked by CTX-Mal in ND96 solution. Although E4 is present in both heteromeric complexes studied, the peptide has little effect on the gating kinetics. Thus for Q1 channels, E3 and E1 dictate gating in heteromeric complexes with E4 peptides.

The results using CTX-Mal demonstrate that a tetrameric Q1 channel can simultaneously assemble with two different KCNE peptides. In addition, we determined

that, when channels do pass current, certain KCNE peptides govern Q1 modulation in heteromeric complexes: E3>E1>>E4, where the dominant peptide has substantial control over the opening and closing of the channel. Although it was shown that heteromeric Q1–KCNE complexes form, we cannot determine the assembly preference for KCNE peptides with Q1 subunits because an endpoint (current expression) was examined and not the biogenesis and stability of the protein subunits. Assembly preference could be determined by assaying protein expression of each subunit. The results also indicate that the N-termini of KCNE peptides are near the Q1 channel outer vestibule since the linker connecting CTX to the maleimide is too short to reach beyond the S3–S4 loop of the voltage sensor (Blaustein et al., 2000). On the basis of a NMR structure of CTX bound to a bacterial K^+ channel (Yu et al., 2005), the position the KCNE N-terminus is within 20 Å of the ion conduction pathway.

This hierarchy of KCNE modulation of Q1 channels has several implications for KCNE physiology. In the heart, it has been assumed that homomeric Q1/E1 complexes produce the unmistakably slowly activating/deactivating I_{Ks} current involved in repolarization (Barhanin et al., 1996; Sanguinetti et al., 1996). E4 may also generate the cardiac I_{Ks} current because Q1/E1/E4 and Q1/E1 complexes have similar gating kinetics. Likewise, in most epithelial cells where the resting membrane potential is negative, the assembly of E1, E4, or E5 with Q1 has been questioned given that these complexes would be essentially closed. However, E1 and E4 peptides can act as structural surrogates in Q1/E3 heteromeric complexes to produce channels that are open at negative potentials and thus may partake in salt and water homeostasis (Schroeder et. al., 2000). In either

case, these heteromeric complexes can substitute for homomeric complexes; however, they require the presence of the dominant KCNE peptide, consistent with KCNE knockout mice studies (Vetter et al., 1996; Roepke et al., 2006).

In contrast, over expression of constitutively conducting Q1/E1/E3 complexes could be detrimental in maintaining the cardiac action and resting potentials, suggesting that cells regulate Q1–KCNE assembly. Simple binary transcriptional regulation of functionally opposed KCNE peptides could be used to control the potassium efflux of a cell. Alternatively, KCNE assembly with Q1 channel subunits may be regulated at the protein folding level. If Q1–KCNE assembly is chaperone mediated, these proteins must reside in either the ER or cis-Golgi since KCNE peptides assemble with Q1 channels early in the secretory pathway (Chandrasekhar et al., 2006).

The discovery that heteromeric Q1–KCNE complexes are functionally expressed at the cell surface implies that other voltage-gated K^+ channels will be amenable to co-assembly with two (or more) different KCNE peptides. Given the cadre of scorpion and spider toxins available to specifically inhibit a wide range of ion channels, our approach can be readily applied to study other membrane-embedded β-subunits in functioning ion channel complexes.

CHAPTER IV: Toxin-directed labeling of K^+ channel α- and β-subunits in native cells

Abstract

A major limitation of the tethered blocker technology we have utilized in our studies in chapters II and III is that it requires an extracellular cysteine in the protein under study to provide a reactive handle and therefore is not compatible with most native proteins *in vivo*. This limitation may be overcome by allowing native proteins to incorporate a non-native thiol into their overall structure through cellular post-translational modifications. This would provide the necessary chemical handle to allow toxin-directed chemical labeling of endogenous ion channels in native cell types and tissues.

Chapter IV shows that *Xenopus* oocytes incubated in media containing the non-natural sugar aceylated-thiol MaNAc (a sialic acid precursor) will take-up, de-acetylate and incorporate this thiolate-sugar into its extracellularly displayed N-linked glycans. KCNE β-subunits and *Shaker* channel α-subunits decorated with these thiol-glycans can be irreversibly blocked using CTX-Lclv-biotin, a derivatized charybdotoxin that upon linker cleavage labels channels with biotin. Here, covalent tethering is through the exogenous thiol in the sugar, as opposed to a mutated cysteine residue as in Chapters II

and III. This technique of tethered block through thiol-modified sugars provides a means for probing endogenous channels in native tissues.

Introduction

Expression systems are excellent tools for the structure-function characterization of voltage-gated ion channels and have proved instrumental in countless biophysical studies. However, it is imperative that channels also be studied in their native cells under endogenous expression levels to fully understand their physiological roles. This challenging task would be aided by the ability to selectively label a specific ion channel of interest in its native environment with experimentally useful probes, such as biotin and fluorophores. Labeled endogenous channels would be valuable in identifying native partners, investigating trafficking pathways and cellular architecture, along with recycling and degradation rates, and localization studies. Major hurdles to labeling a particular population of channels on the cell surface include: 1) the channel under study lacks a useful handle that would permit chemical modification, and/or 2) the labeling reagent is not specific for the channel under study. For example, many available biotin and fluorescent labeling reagents non-specifically label all proteins on the cell surface that express a particular reactive group, commonly thiols or primary amines on extracellularly exposed amino acid side chains.

The experiments discussed in previous sections of this thesis utilized channels that had mutant cysteines introduced into their extracellular loops. We would like to

probe these channels in their native tissues without the need to transfect in the modified channel or subunit under study. Based on previous work (Yarema et al., 1998; Dube and Bertozzi, 2003), it was reasoned that cells grown on unnatural sialic acid precursors that contain a thiol group (Figure IV-1a) would take-up and incorporate the modified sugar into N-linked glycans on glycoproteins trafficking through the Golgi to the plasma membrane. This metabolic labeling approach would provide the necessary chemical handle to label native *Shaker* channels and KCNE β-subunits with channel specific toxin derivatives.

To demonstrate the feasibility of this idea, CTX-Lclv-Biotin was developed. This reagent is similar to those already discussed, which block and tether to channels through a covalent maleimide-thiol linkage; however, upon linker cleavage, current is restored and α- or β-subunits are permanently labeled with biotin (Figure IV-Ib). The idea of using biotin as a label was two-fold; first, it would allow us to perform Western blot analysis for our labeled protein when showing proof of principle experiments, as there are many commercially available antibodies specific to biotin and directly conjugated to HRP. Second, biotin-tagged molecules are useful in pull-down experiments to assay protein-protein interactions by fishing out the biotinylated protein with avidin beads.

Before metabolically labeling cells with non-natural sugars, we first confirmed that the CTX-Clv-Biotin reagent irreversibly blocks thiol-containing Q1/E1 complexes and *Shaker* channels expressed in *Xenopus* oocytes, and that current is restored upon linker cleavage. We then performed a similar experiment with *Xenopus* oocytes expressing CTX-sensitive, "wild-type" Q1/E1 or *Shaker* channels that were incubated

with a thiol-modified N-acetylmannosamine derivative. These channels were irreversibly blocked, suggesting that the modified sugars were taken-up, incorporated into the extracellular glycans of the proteins, and provided a reactive handle to which the reagent could tether. In all, these results show promising preliminary experiments that the tetherered blocker technology discussed in Chapters II and III can be used to label channels in native cells.

A)

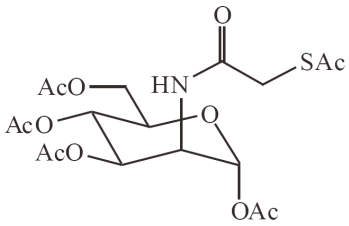

4.1

B)

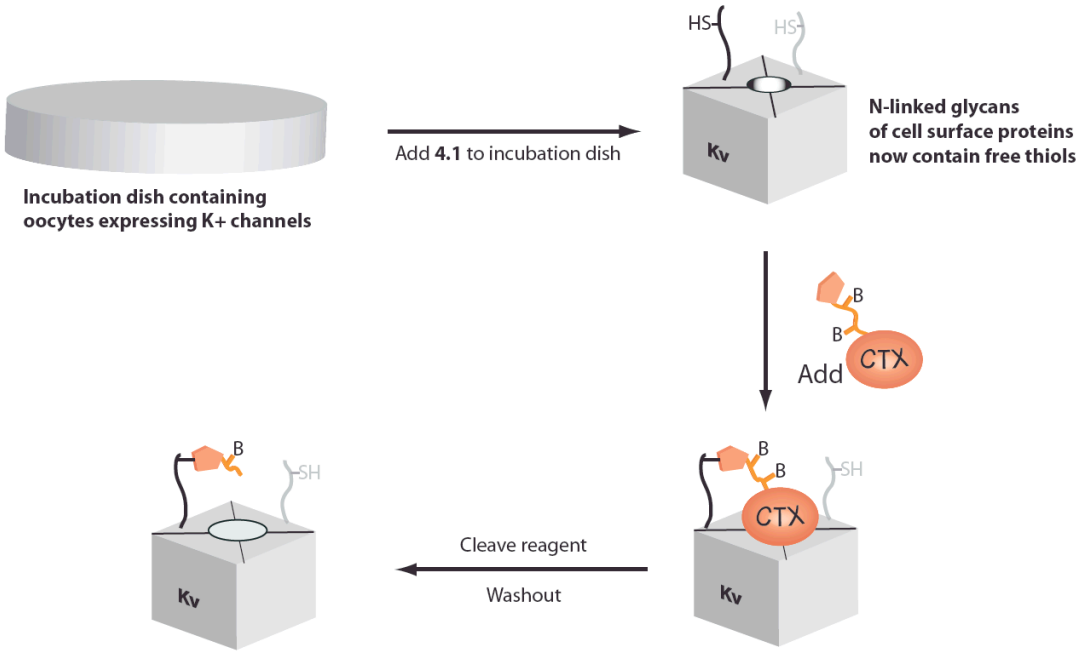

Figure IV-1 Structure of 1,3,4,6-tetra-O-acetyl-2-acetylthioacetamido-2-deoxy-a-D-mannopyranose 4.1 (Ac5ManNTGc) and metabolic labeling of N-glycosylated cell surface proteins.

(**A**) The thiol containing ManNAc non-natural sugar analog is a thiol containing aceylated sialic acid precursor. (**B**) Oocytes fed this sugar will deacylate and incorporate it into glycans containing terminal sialic acids, resulting in the expression of reactive extracellular thiols (SH), which can be labeled with biotin (B) using CTX-Clv-Biotin.

Material and Methods

Mutagenesis and *In Vitro* Transcription:

For optimal CTX binding to the Q1/E1 complex, CTX sensitive Q1 (Q1*) and hemagglutinin-tagged E1 constructs were used (Chen et al., 2003) and subcloned into a pCDNA3.1+ plasmid containing the 5' and 3' UTRs from the *Xenopus* β-globin gene and mammalian gene for optimal expression in both *Xenopus* oocytes and mammalian CHO cells. *Shaker* constructs were subcloned into a modified pBluescript SK+ vector (Statagene) with the 5' and 3' UTR from the *Xenopus* β-globin and mammalian gene for optimal expression in oocytes or CHO cells. Site-directed mutagenesis was performed by Quickchange Mutagenesis (Stratagene) using E1 primers described in Chapter II and mRNA *in vitro* run-off transcription was performed by linearizing with MluI (NEB) and synthesizing with T7 RNA polymerase (Promega).

Electrophysiology:

Standard techniques and solutions were used for the preparation of and recording from *Xenopus* oocytes by two-electrode voltage clamp (Rudy and Iverson, 1992) 2–4 d after cRNA injection (methods chapter III). Oocytes expressing KCNE extracellular cysteine residues were stored in ND96 bathing solution (96 mM NaCl, 2 mM KCl, 1.8 mM CaCl2, 5 mM HEPES, pH 7.4, 50 μg mL^{-1} gentamicin containing 2 mM L-glutathione (Sigma)) and incubated in ND96 recording (96 mM NaCl, 2 mM KCl, 0.3

mM $CaCl_2$, 1 mM $MgCl_2$, 5 mM HEPES, pH 7.4, containing 1 mM TCEP (CalBioChem)) for 10 min prior to recording. Oocytes were injected with a Q1:E1 mRNA ratio (15:5 ng) to ensure that E1 was in excess or 5 ng Shaker-IR. Oocytes were incubated for 3–5 days with 3 mM L-glutathione, pre-treated with 1 mM TCEP for 15 min before recording, and the current was measured by holding at – 80 mV and pulsing to +20 mV for 5 s every 30 s.

Cell Surface Chemistries:

Oocyte labeling: Labeling reagent CTX-Clv-Biotin (10 nM) was in ND96 solution with 50 μg mL^{-1} bovine serum albumin and was added to the bath by a gravity-fed perfusion system with a chamber clearing time of ~ 10 s. CTX-Clv-Biotin cleavage was accomplished by 1 mM TCEP for ~180 s.

Metabolic Labeling with Non-natural Sugars:

Metabolic labeling of oocytes was performed by evaporating 100 μl of a 10 mM solution of Ac_5ManNTGc in ethanol onto a 30 mm x 7 mm incubation dish. Approximately 30 oocytes in 2 ml ND96 solution (methods chapter II) were added to each dish. The solution in the incubation dish was changed every 24 hr. with freshly evaporated Ac_5ManNTGc until recordings were performed.

Chemical Synthesis:

Non-natural ManNAc synthesis:

1,3,4,6-tetra-O-acetyl-2-acetylthioacetamido-2-deoxy-a-D-mannopyranose (Ac$_5$ManNTGc) **4.1**: Thiol containing non-natural ManNAc sugar synthesis was performed according to Yarema, Nature Protocols, Vo1, No. 5, 2006, 2377. The purified product was confirmed by electrospray ionization mass spectrometry (Figure IV-2) and was aliquoted, lyophilized, and stored at -20 °C. For oocytes uptake of Ac$_5$ManNTGc, 100 ul of a 10 mM solution in ethanol was evaporated onto oocyte incubation dishes.

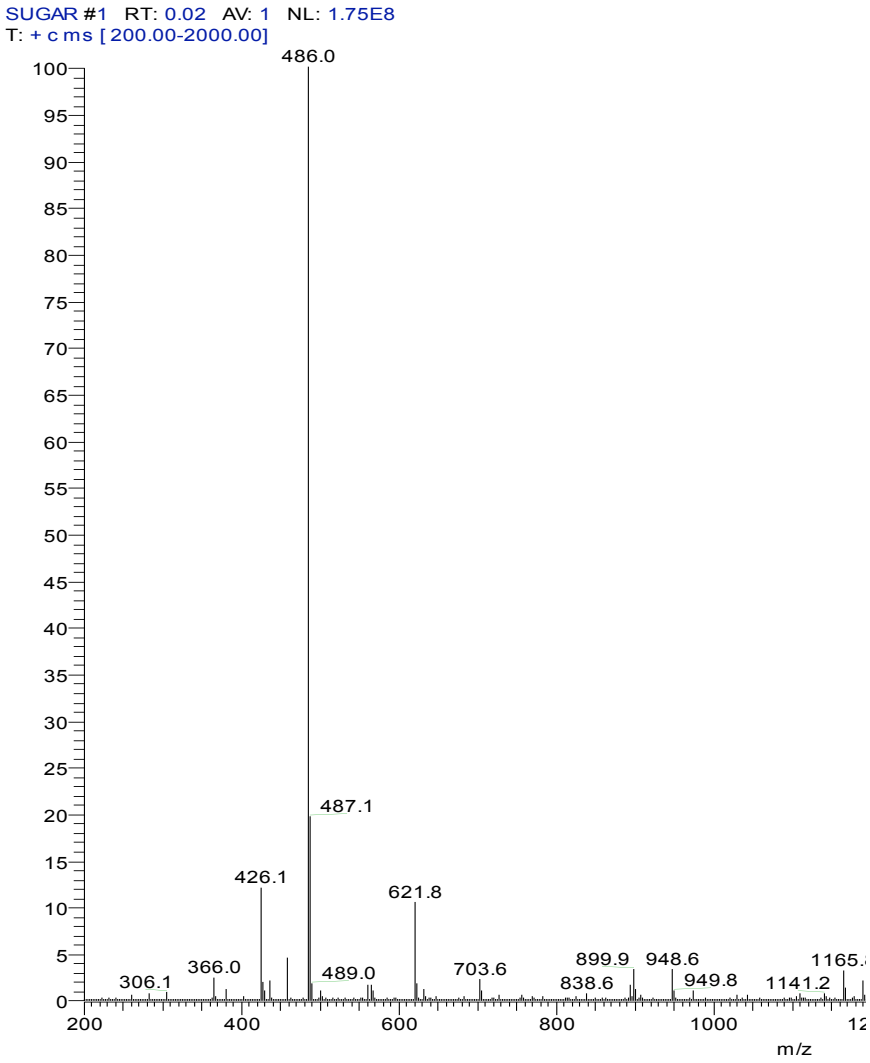

Figure IV-2 Ac_5ManNTGc electrospray mass spectrum (positive mode).

Expected MW for Ac5ManNTGc: +1 486.0

Synthesis of cleavable linker precursors and cleavable linker:

Bis(Fmoc-Lysine (Boc)) cystamide (**4.2**)**:** A solution of cystamine dihydrochloride 0.113 mg (0.5 mmol) in 15 mL methanol was added 204 mg (2.0 mmol) of triethylamine and Fmoc-Lys(Boc)-OPfp 0.635 g (1.0 mmol) at room temperature. The mixture was stirred at room temperature for 12 hours and a jelly-like solid was formed, and 15 mL of chloroform was added to make the reaction solution clear. The mixture was filtered through a short silica gel column (3.0 g of silica gel). The solvent was evaporated under vacuum to afford a crude product of compound **4.2** as a white solid. This crude product was used for next reaction without further purification.

Bis(Lysine-(Boc)) cystamide (**4.3**): The crude product of compound **4.2** in 20 mL methylene chloride and 1 mL of piperidine was added to the reaction solution. The reaction mixture was stirred at room temperature for 12 hours. The mixture was then evaporated to dryness to give a yellowish solid. This solid was added extracted with (50 mLx2) hexane and stirred vigrously by a magnetic stirrer. The supernatant hexanes layer was decanted. The solid residue was dissolved in 50 mL chloroform and washed with 15 mL water. The chloroform layer was dried with anhydrous sodium sulfate and evaporated under vacuum to give a white solid crude diamine compound **4.3** (~530 mg). This white solid was used for next reaction without further purification.

Bis(maleimido-Lysine-(Boc)) cystamide (**4.4):** The crude compound **4.3** was dissolved in 15 mL DMF and 460 mg (1.7 mmol) of maleimide NHS ester was added to the solution. The reaction was stirred for 2 days. Then the solvent was removed under vacuum to offer a white solid. The crude product was purified by silica gel chromatography eluting with 5:1 $CHCl_3$:MeOH to afford 100 mg compound **4.4** as confirmed by NRM (22% for 3 steps).

Bis(maleimido-lysine) cytamide (**4.5):** 100 mg of compound **4.4** (0.11 mmol) was added with a solution of 30 mL TFA, 30 mL $CHCl_3$ and 300 uL of water. This reaction mixture was stirred at room temperature for 5 hours and then the solvents were removed under vacuum to offer a white solid. The white solid was dissolved in 10 mL water and 10 mL $CHCl_3$ and stirred vigorously. The aqueous layer was separated and washed by 5 mL $CHCl_3$ again. The aqueous layer was then evaporated to give a white solid crude product **4.5**, as confirmed by NMR.

Bis(maleimido-lysine-biotin) cytamide (**4.6**): Crude product **4.5** was dissolved in 6 mL DMF and 81 mg of Biotin-NHS ester (0.24 mmol) and 29 mg Et_3N (0.29 mmol) were added. The reaction mixture was stirred at room temperature for 2 days. The solvent was removed under vacuum. The crude product was dissolved in 10 mL $CHCl_3$ and 10 mL water. The mixture was stirred vigrously for 20 min. Some solid did not go into either chloroform layer or aqueous layer. The solid was collected and dried under vacuum for 12 hours to give a solid 38 mg of cleavable bismaleimide **4.6** (0.036 mmol, 32% from

compound **4.4**). Product was confirmed by ESI-MS, ^{1}H NMR (400 MHz, $CDCl_3$) δ 1.10-1.70 (m, 4 H), 2.02 (m, 4 H), 2.38 (m, 4 H), 2.54 (m, 2 H), 2.60-2.80 (m, 8 H), 2.96 (m, 4 H), 3.09 (m, 2 H), 3.57 (m, 4 H), 4.10 (m, 4 H), 4.28 (m, 2 H), 6.35 (s, 2 H), 6.41 (s, 2 H), 6.98 (s, 4 H), 7.73 (m, 2H), 8.06 (m, 4 H).

CTX-Clv-Biotin Derivatization:

Recombinant CTX R19C was purified and the protected CTX-MTSET adduct was prepared according to Shimony et al. (Shimony et al., 1994). CTX-Lclv-Biotin was synthesized as follows: 16 nmol of CTX-MTSET in 2 mL of Buffer C (10 mM NaCl, 10 mM KPi, pH 7.4) was reduced with 1 mM DTT for 30 min and bound to a SP Sephedex (Sigma) cation exchange column. DTT was washed from the column using 150 mL of Buffer C, and the resin bound CTX was labeled with 3 mL of 5 mM Lclv-biotin in Buffer C with a final acetonitrile concentration of 5%. After 10 min, the column was washed with Buffer C to remove excess label, and CTX-Lclv-Biotin was eluted with 1 M NaCl in 10 mM KPi, pH 7.4. CTX-Lclv-Biotin (Figure IV-6) was desalted and HPLC purified using a C18 column (4.6 mm x 250 mm) eluting with solvent A (0.1% TFA)/solvent B (acetonitrile) gradient 10% to 40% B over 30 min. The concentration of purified CTX-Lclv-Biotin was determined by UV spectrometry (OD_{280} of 1.0 = 100 μM CTX (Shimony et al., 1994)) and labeling efficiency of CTX-R19C was determined to be 35% ± 5% (n = 10). The purified product was confirmed by electrospray ionization mass spectrometry

(Figure IV-3) and was aliquoted, lyophilized, and stored at -20 °C. Individual aliquots were resuspended in recording solutions immediately prior to use.

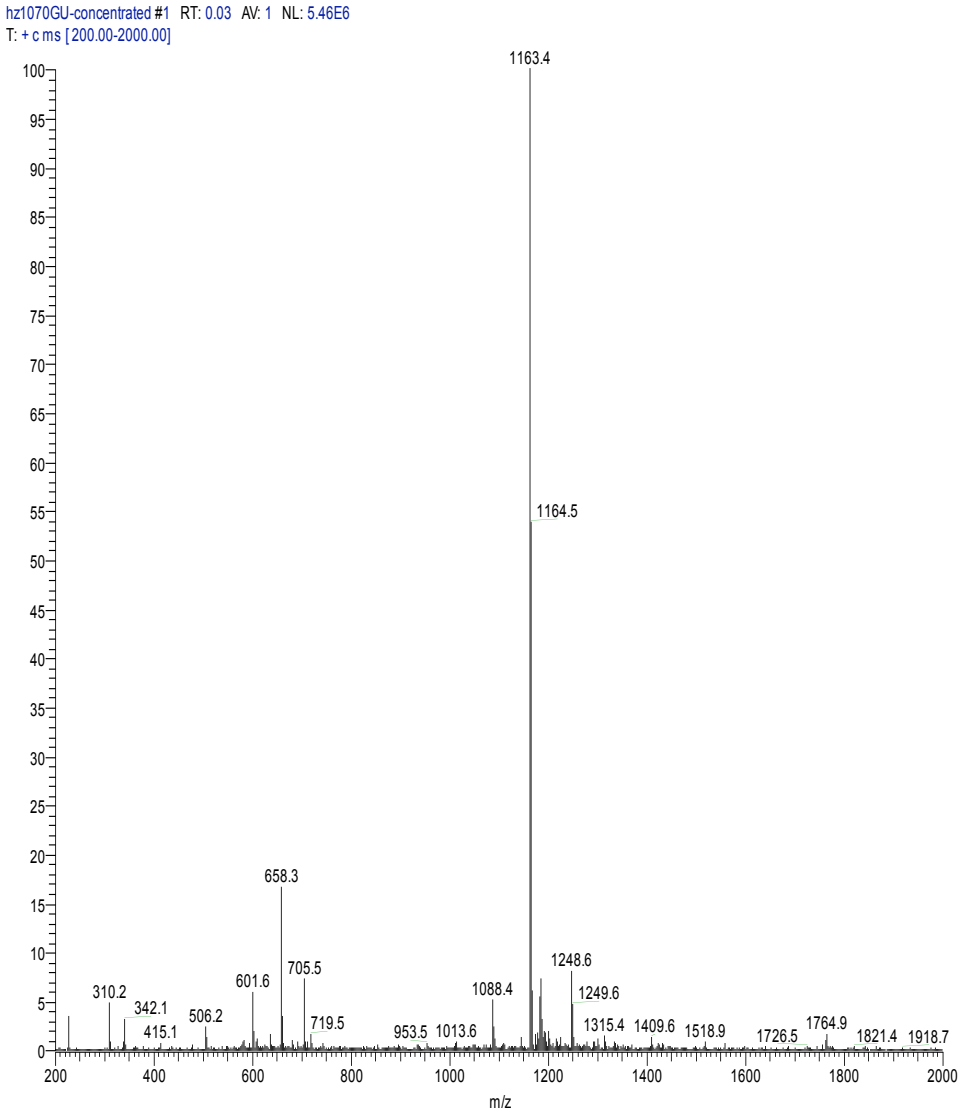

Figure IV-3 CTX-Clv-Biotin electrospray mass spectrum (positive mode).

Expected MW for CTX-Clv-Biotin: 4660.0 (methionine oxidized); +4, 1164.0; +7, 658.0.

Results

To label thiol-containing *Shaker* α- and E1 β-subunits with biotin the reagent CTX-Lclv-Biotin was created. This reagent consists of the K^+ channel blocking toxin charybdotoxin coupled to two molecules of biotin through a cleavable thiol reactive linker (Figure IV-6). The CTX portion of the reagent specifically delivers biotin to channels that bind CTX with high affinity, allowing the labeling reaction to be performed using nanomolar concentrations of the reagent. Considering the duration of the labeling reaction (mins.) using nanomolar concentrations of reagent, the non-toxin aided bimolecular reaction between the reagent and free thiol is inconsequential (less than 1%). Therefore, global labeling of all free thiols on the cell surface with biotin is prevented. As with the other previously described CTX-derivatives, once bound CTX-Clv-Biotin tethers to channels through a maleimide thiolate linkage resulting in irreversible channel block. Upon TCEP cleavage of the linker region, CTX and one molecule of biotin is washed out, while the other biotin molecule permanently labels the channel (Figure IV-1b). The CTX-Clv-Biotin reagent was created by reacting excess **4.7** with CTX-R19C. Compound **4.7** was synthesized by coupling 2 equivalents of commercially available Fmoc-Lys-(Boc)-OPfp with one equivalent of cystamine dihydrochloride in chloroform. The mixture was run over a silica column and solvents were evaporated in vacuo to afford compound **4.2.** The Fmoc protecting groups on compound **4.2** were selectively removed with piperidine to give diamine **4.3**. Two equivalents of maleimide NHS ester were coupled to one equivalent of diamine **4.3** using standard activated ester-amine

coupling chemistries. Solvents were removed under vacuum and the remaining white solid, compound **4.4**, was purified by silica gel chromatography (yield 22% for the three steps) (Figure IV-4).

The Boc protecting groups on compound **4.4** were removed using trifluoroacetic acid and water, and the solvents were removed under vacuum to give product **4.5** . Commercially available Biotin-NHS was dissolved in DMF and triethylamine and added to crude **4.5.** After two days, the solvents were removed and the product was extracted. A solid that did not dissolve in either layer was collected and dried under vacuum to give the biotin-bismaleimide, **4.6** (32% yield from last 2 steps) (Figure IV-5). CTX-Clv-Biotin was then synthesized by adding 100-fold molar excess of **4.6** to reduced CTX R19C, (Figure IV-6 bottom) and HPLC purified (see Methods section for details).

Before metabolically labeling with non-natural sugars, I first determined whether the CTX-Clv-Biotin reagent irreversibly blocks thiol-containing Q1/E1 complexes and *Shaker* channels, and upon linker cleavage current is restored. To do this we utilized the cysteine in $Q1/E1_{T14C}$, which was modifiable using linkers of similar length and structure (Morin and Kobertz, 2007, Morin and Kobertz, 2008). TEVC recordings show that $Q1/E1_{T14C}$ complexes are irreversibly blocked when exposed to this reagent, but upon treatment with 1 mM TCEP current is restored to original levels (Figure IV-7 top). This

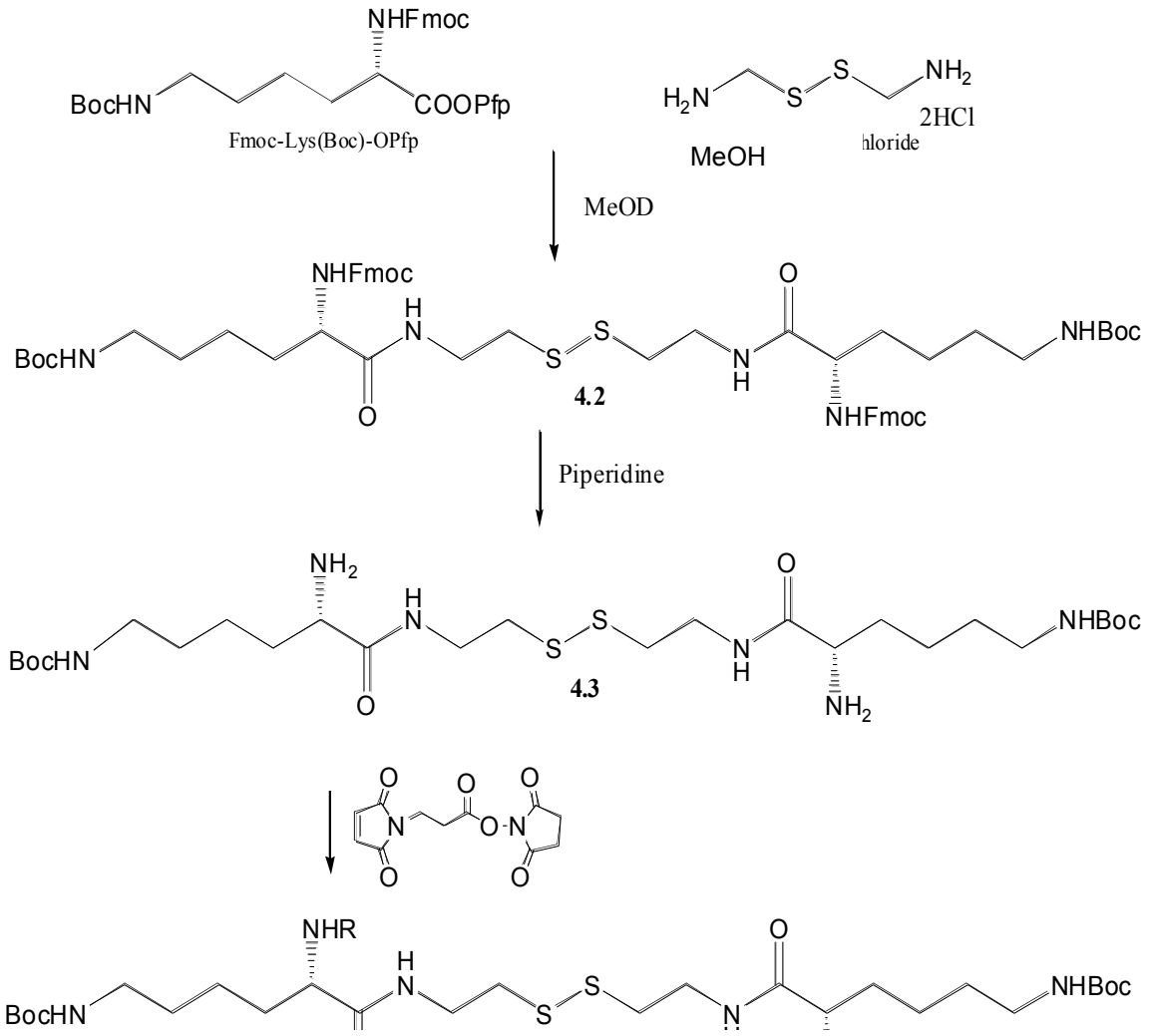

Figure IV-4. Synthesis of compound 4.4

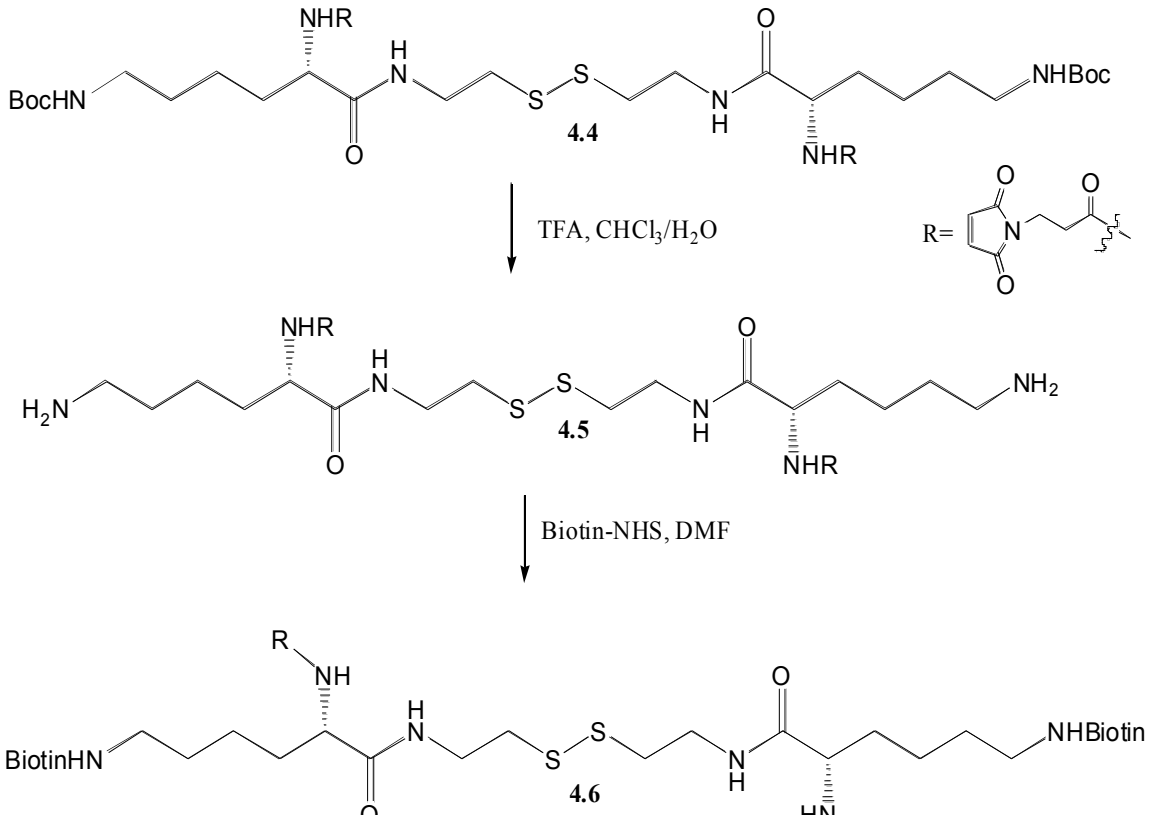

Figure IV-5. Chemical synthesis of compound 4.6.

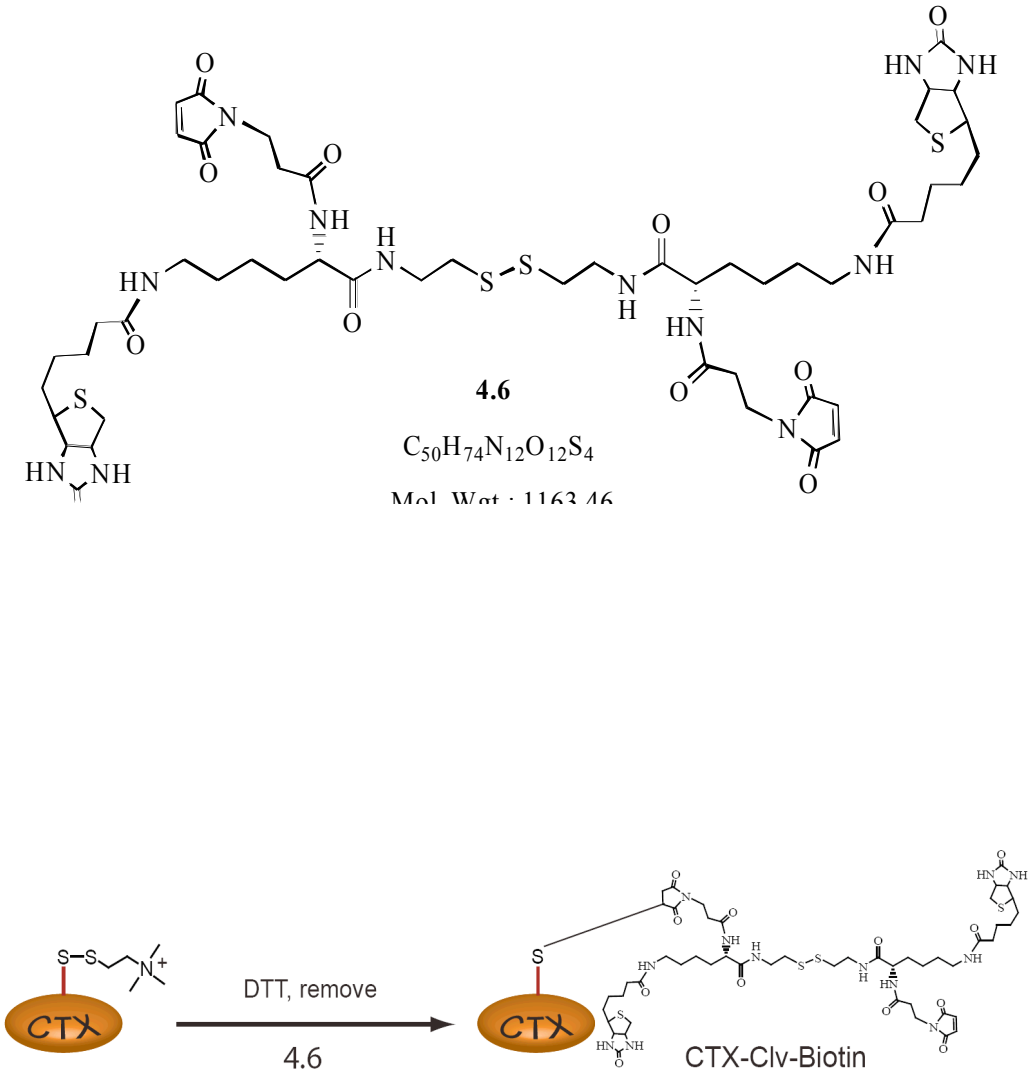

Figure IV-6. Structure of Clv-Biotin 4.6 and synthesis of CTX-Clv-Biotin

(Top) The Clv-Biotin reagent **4.6** consists of three main components, a cleavable disulfide bond, 2 biotin moieties and 2 thiol reactive maleimides. (**Bottom**) CTX-MTSET is reduced and reacted with excess **4.6** to create reagent CTX-Clv-Biotin.

indicates that the reagent is able to block and tether to channels, creating irreversible block, but upon chemical treatment the blocking moiety is liberated and presumably the channels are now labeled with biotin. Control experiments using E1 peptides lacking the exogenous cysteine showed CTX-Lclv-Biotin is unable to tether and therefore labeling is dependent on the cysteine introduced through mutagenesis (Figure IV-7 middle). Consistent with the other CTX derivatives, labeling was dependent on first binding to the channels, as labeling was prevented when CTX-Lclv-Biotin was competitively inhibited with excess CTX (Figure IV-7bottom).

Biotin labeling was not limited to the KCNE β-subunits, as *Shaker* channel α-subunits harboring a Q350C mutation, an extracellular position within *Shaker* that is less than 20 angstroms from the pore (Blaustein et al., 2000), were also irreversibly blocked by CTX-Lclv-Biotin. These channels were ~80% irreversibly blocked, as ~20% of the current returned upon reagent washout. Again, irreversible block could be reversed with mild reductant (Figure IV-8a). Control experiments using *Shaker* subunits lacking the exogenous cysteine showed CTX-Lclv-Biotin is unable to tether and therefore labeling is dependent on the cysteine introduced through mutagenesis (Figure IV-8b). Again labeling was dependent on first binding to the channels as irreversible block was prevented when CTX-Lclv-Biotin was competitively inhibited with excess CTX (Figure IV-8c).

Figure IV-7. Characterization of CTX-Clv-Biotin on KCNQ1/KCNE complexes.

Top-bottom) (Left) Overlays of the total current elicited by a 20 mV pulse from a -80 mV holding potential from oocytes expressing Q1/E1 complexes. Scale bars are 0.5 μA and 0.5 s. (Right) Normalized CTX-sensitive current (I/Imax). Oocytes were depolarized every 30 s and the data points were obtained at the end of a 5 s pulse. Gray and red data points correspond to the raw traces on the left.

Top) Q1/E1$_{T14C}$ complexes are irreversibly blocked by CTX-Clv-Biotin. Q1/E1$_{T14C}$ complexes were treated with 10 nM CTX-Clv, followed by washout and 1 mM TCEP treatment, demonstrating the ability of the reagent to label these complexes with biotin from delivered by CTX-Clv-Biotin.

Middle) Q1/E1 WT complexes are reversibly blocked by CTX-Clv-Biotin. Complexes were treated with 10 nM CTX-Clv, followed by washout, demonstrating the necessity of the cysteine residue for labeling to occur.

Bottom) Competitively inhibited Q1/E1$_{T14C}$ are reversibly blocked by CTX-Clv-Biotin. Complexes were treated with 500 nM CTX and 10 nM CTX-Clv, followed by washout, demonstrating the need to first bind to the channel for biotin labeling to occur.

Q1/E1$_{T14C}$

As discussed, the ultimate goal is to develop a technique to label native channels through the incorporation of non-native thiol containing sialic acids into the extracellular N-linked glycans of theses proteins. Aceylated thiol-containing ManNAc, a sialic acid precursor (Figure IV-1a) was synthesized (**Synthesis**) and Q1/E1 expressing oocytes were incubated with 10 μM thiol-sugar **4.1** for 3 days. To determine whether E1 β-subunits incorporated the unnatural glycans, the oocytes were treated with CTX-Mal, which irreversibly blocks Q1/E1 currents (Figure IV-9 top). Control experiments in which the modified sugar was absent from the media afforded the same amount of block, but was 100% reversible, showing the dependence of the labeling reaction on the sugar delivered thiol (Figure II-6b and Figure III-5a). A second control experiment showed irreversible block is dependent on an N-linked glycoslylated E1 peptide, because when assaying Q1 channels alone, which are not N-linked glycoslylated, only reversible block is seen with CTX-Mal (Figure IV-9 bottom).

The metabolically labeling experiment was repeated using oocytes expressing WT *Shaker* channels to demonstrate that tethering can occur through N-linked glycosylated α-subunits (Figure IV-10). WT *Shaker* channels incubated with the non-natural sialic acid precursor were irreversibly blocked by CTX-Mal whereas when the modified sugar was absent from the media the block was 100% reversible, showing the dependence of the labeling reaction on the sugar supplied thiol (Figure IV-8 bottom). Table IV-2 shows CTX-Clv-Biotin off rates are comparable to the other CTX-derivatives dissociating from Q1/KCNE complexes. *Shaker* channels have a greater affinity for charybdotoxin than Q1/KCNE complexes which slows the dissociation kinetics.

Figure IV-8. Characterization of CTX-Clv-Biotin on *Shaker* channels

(**Top-bottom**) Overlays of the total current elicited by a 20 mV pulse from oocytes expressing *Shaker* channels. Scale bars are 0.5 μA and 0.5 ms. (Right) Normalized CTX-sensitive current (I/Imax). Oocytes were depolarized every 10 s and the data points were obtained at the end of a 500 ms pulse. Gray and red data points correspond to the raw traces on the left.

(**Top**) ***Shaker* Q350C complexes are irreversible blocked by CTX-Clv-Biotin.** *Shaker* Q350C channels were treated with 10 nM CTX-Clv-biotin, followed by washout and 1 mM TCEP treatment, demonstrating the ability of the reagent to irreversibly block channel, and label these channles with biotin upon release.

(**Middle**) **Competitively inhibited *Shaker* channels are reversibly blocked by CTX-Clv-Biotin.** Complexes were treated with 500 nM CTX and 10 nM CTX-Clv-Biotin, followed by washout, demonstrating the need to bind to the channel to react with the free thiol and tether.

(**Bottom**) **Competitively inhibited *Shaker* 350C and *Shaker* (wild type) complexes are reversibly blocked by CTX-Clv-Biotin.** Complexes were treated with 10 nM CTX-Clv-Biotin, followed by washout, demonstrating the necessity of the cysteine residue for labeling to occur

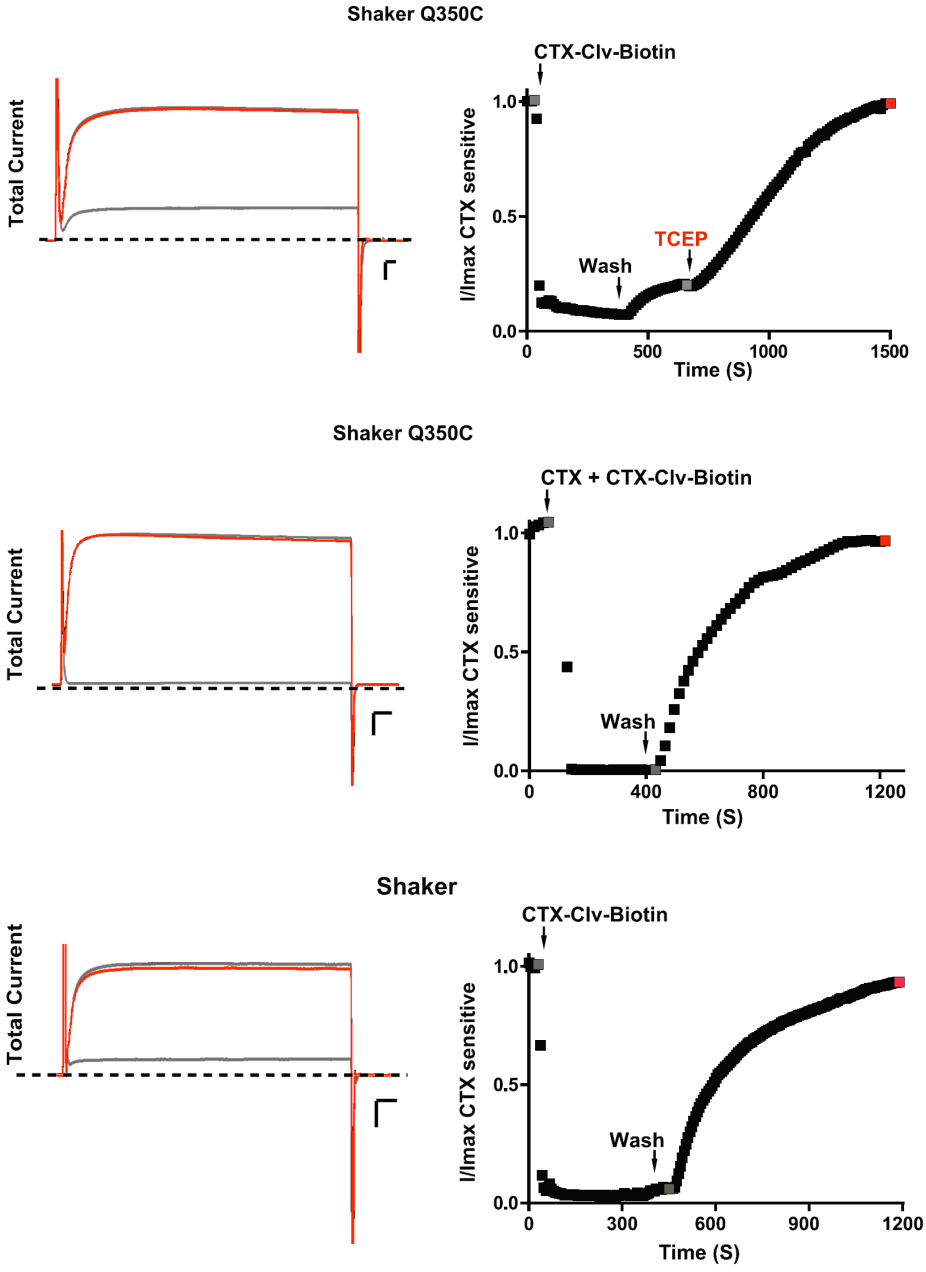
Shaker Q350C
Total Current
CTX-Clv-Biotin
I/Imax CTX sensitive
1.0
0.5
0.0
TCEP
Wash
0
500
1000
1500
Time (S)
Shaker Q350C
Total Current
CTX + CTX-Clv-Biotin
I/Imax CTX sensitive
1.0
0.5
0.0
Wash
0
400
800
1200
Time (S)
Shaker
Total Current
CTX-Clv-Biotin
I/Imax CTX sensitive
1.0
0.5
0.0
Wash
0
300
600
900
1200
Time (S)

Figure IV-9. Q1/E1WT complexes are irreversibly blocked by CTX-Mal when fed thiolated sialic acid, Q1 only channels are reversibly blocked.

(Left) Overlays of the total current elicited by a 20 mV pulse from oocytes expressing Q1/E1 WT (top) or Q1 only(bottom). Scale bars are 0.5 μA and 0.5 s. (Right) Normalized CTX-sensitive current (I/Imax). Oocytes were depolarized every 30 s and the data points were obtained at the end of a 5 s pulse. Gray and red data points correspond to the raw traces on the left. (**Top**) Acetylated thiol-MaNAc fed Q1/E1 complexes were treated with 10 nM CTX-Mal, followed by washout. Irreversible block demonstrates the non-natural sugar is displayed on the cell surface de-aceylated. (**Bottom**) Aceylated thiol-MaNAc fed Q1 only channels are irreversibly block by 10 nM CTX-Mal, demonstrating the requirement of E1 in this assay.

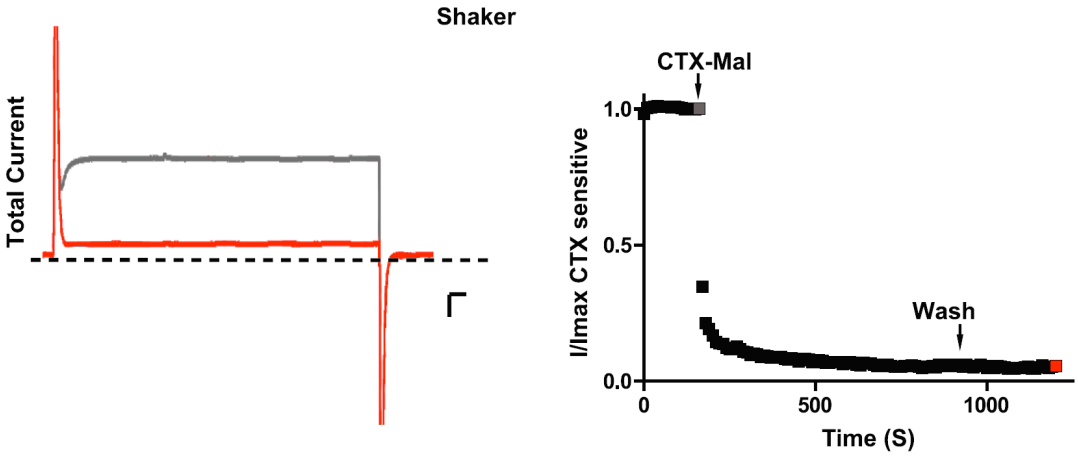

Figure IV-10. *Shaker* channels are irreversibly blocked by CTX-Mal when fed acetylated thiol-MaNAc.

(Left) Overlays of the total current elicited by a 20 mV pulse from oocytes expressing *Shaker* channels. Scale bars are 0.5 µA and 0.5 ms. (Right) Normalized CTX-sensitive current (I/Imax). Oocytes were depolarized every 10 s and the data points were obtained at the end of a 500 ms pulse. Gray and red data points correspond to the raw traces on the left. *Shaker* complexes were irreversibly blocked with 10 nM CTX-Mal demonstrating labeling can occur through thiol containing non-natural sugars.

Table IV-1. Recovery parameters after CTX-Clv application[1]

Construct	Treatment	$\tau_{recovery}$ (s)	% recovery	n
Q1/E1	CTX-Clv	98 ± 1	95 ± 2	5
$Q1/E1_{T14C}$	CTX-Clv, TCEP	97 ± 1	96 ± 2	4
$Q1/E1_{T14C}$	CTX-Clv + excess CTX	155 ± 4	96 ± 1	3
$Q1/E1_{T14C}$	CTX-Clv, CTX-Mal, TCEP	94 ± 3	94 ± 1	3
$Q1/E1_{T14C}$	CTX-Clv-Biotin	125 ± 5	96 ± 2	3
Shaker (Q350C)	CTX-Clv-Biotin	540 ± 12	98 ± 4	3

[1]Data are from individual experiments obtained from 3–5 oocytes. Treatment describes the sequential application of chemical reagents to the indicated construct. Time constants of recovery were fit to a single exponential as described in Material and Methods. Percent recovery is a comparison between the amount of current remaining after CTX-Clv release to the amount of current before CTX-Clv application. Values are mean ± SEM.

Discussion

A cleavable tethered blocker reagent was developed to label K^+ channel subunits with biotin. $Q1/E1_{T14C}$ complexes were irreversibly blocked upon exposure to the CTX-Clv-Biotin reagent, and current fully returned after TCEP induced linker cleavage (Figure IV-7a). Control experiments show this reaction is dependent on the mutated cysteine in the E1 peptide and the reagent must bind to the channel for labeling to occur (Figure IV-7b and c). Based on the design of the reagent, the channels are now presumably labeled with biotin. Western blotting of total cell surface proteins for biotin will confirm that indeed E1 is modified with biotin and this was specific, i.e. CTX was able to deliver the label to E1 peptides only and other thiol containing cell surface protein were not labeled. This experiment is currently being performed, along with appropriate controls, using mammalian CHO K-1 cells expressing $Q1/E1_{T14C}$ complexes.

The ability to use this labeling strategy in native cells to probe endogenous channels was realized by using a thiol-containing non-natural ManNAc derivative. Oocytes expressing "wild-type" Q1/E1 complexes incubated with this sugar were irreversibly blocked when exposed to the non-cleavable CTX-Mal reagent. The control experiments showed that this block was "sugar fed" dependent and require the proteins to be N-glycosylated (figure IV-9). This shows that oocytes are able to take-up, deacetylate, and incorporate this sialic acid precursor into N-linked glycans as they would native sialic acid. The CTX-Mal reagent does not contain the biotin label, but these results along with those discussed above (Figure IV-7) indicate that exposure of "sugar-fed"

channels to CTX-Clv-Biotin would result in biotin labeled channels via the sugar moiety. Again, Western blot analysis probing for biotin would reveal specific labeling of E1 peptides.

Consistent with experiments using other CTX derivatives, CTX-Lclv-Biotin does not afford 100% block of Q1E1 channels, likely due to non-CTX sensitive endogenous Q1 channels native to the oocyte partnering with E1 peptides to afford non-blockable I_{Ks} like current.

Electrophysiological experiments demonstrated that not only β, but *Shaker* channel α-subunits can also be labeled with biotin. Like Q1/E1 complexes, cells expressing *Shaker* (Q350C) channels or wild-type *Shaker* channels fed thiol-containing MaNAc, were irreversibly blocked by the CTX-Clv-Biotin or CTX-Mal reagent (Figure IV-8 and IV-10). Control experiments showed that when *Shaker* lacked an exogenous cysteine or was not sugar-fed block was completely reversible, demonstrating a free thiol is required for tethering the reagent to the channel. As with Q1/E1 complexes, Western blot analysis will conclusively demonstrate biotin labeling and that it is specific, i.e. the bimolecular reaction between the reagent and thiol (sugar or cysteine) occurs more slowly than the duration of the labeling experiment.

When using *Shaker* Q350C we do see a small level of reversibility upon reagent washout, possibly because the target cycteine (Q350C) in *Shaker* is not in an ideal location for tethering. The cysteine might be sterically blocked by other channel residues or only within reach when the linker is at its most extended conformation. With enough site directed mutagenesis a residue location that affords 100% irreversible block maybe

found. However, for the scope of these labeling experiments, 100% irreversible block is not a necessity. All that is needed is a high percentage of labeling at the cell surface for biochemical studies.

Contrary to the tethering experiments using *Shaker* channels with exogenous cysteines, irreversible block of *Shaker* channels was 100% when tethering through thiol containing glycans. This may happen because N-linked glycans have 3-5 sialic acid terminal sugars, thereby increasing the number of reactive thiols in the outer vestibule 5 fold, from 4 to 20, and therefore enabling more efficient tethering. Of note is that CTX-Clv-Biotin does block 100 % of the current in the experiments using *Shaker* channels, which do not comingle with oocyte endogenous Q1, and therefore all *Shaker* complexes are blockable.

Taken together, these results show a novel approach to labeling specific cell surface proteins and not all of proteins at the cell surface capable of being modified, i.e. any cell surface expressed protein with reduced thiols. This chapter discussed labeling with biotin, useful in pull down experiments to, for example, quantify a cell surface population or investigate interacting protein partners. To expand the experimental repertoire, the biotin moiety can easily be replaced by other functional groups, e.g. fluorophores, which would prove useful in FRET or trafficking experiments. Additionally, this chapter provides evidence that by growing cells on modified sugars the tethered blocker technology is compatible with WT channels and can be used to study channels in native tissues. This will provide a powerful tool to overcome one of the greatest hurdles in the ion channel field: assaying channels in their natural environment.

Chapter V: Future Directions

The results presented in Chapter II, which show two KCNE subunits per Q1/E1 complex, produce a number of questions concerning channel assembly, complex structure, and drug development. First, two KCNE beta-subunits per complex lend credence to the notion that these complexes assemble in the ER (Chandrasekhar et al., 2006) as dimers of dimers (Tu and Deutsch, 1999; Lu et al., 2007). This idea suggests that a KCNE subunit may bifurcate two Q1 alpha-subunits, acting as protinaceous glue that holds them together until fully assembled tetramers are formed and trafficked to the cell surface. Pulse chase labeling experiments may be able to differentiate between a dimer of dimers assembly scenario from assembled Q1 tetramers incorporating E1 peptides, one at a time or two simultaneously. Imaging radioactive gels would show assembling complexes, if E1 peptides join already assembled tetramers, a Q1x4 + E1x1 complex would be evident. If assembly occurs through a dimer of dimers, Q1x2 + E1x1 complexes would be seen. Given that the length of the shortest tethering linker was 20 angstroms, it suggests that the KCNE peptides reside no more than ~20 angstroms from the pore, perhaps positioning KCNE subunits in the cleft formed between subunits. This would allow the KCNE peptide to essentially line the pore, as suggested (Sesti et al., 2000; Tai and Goldstein, 1998; Tai et al., 1997) . Recent work has shown that the N-terminus of E1 contains two alpha helicies separated by a flexible region (Congbao Kang et al., 2008). It is therefore possible that the transmembrane region of E1 is farther than 20 angstroms

from the pore, but the N-terminal cysteine is modifiable because the N-terminus kinks closer to the ion conduction pathway. Furthermore, the 4:2 α:β stoichiometry provides a unique architectural scaffold on which to base the design of pharmacological agents that would target these channels.

The results in Chapter III, heteromeric complexes, generate the possibility that the well studied and well-defined cardiac I_{Ks} current is not only generated by Q1/E1 complexes, but Q1/E1/E4 complexes as well. The results show virtually no change in opening and closing channel kinetics and a slight change in the voltage dependence when E4 is present in the complex, which would allow the macroscopic current through these channels to be fine-tuned quickly to deal with cardiac stresses. At the very least, E4 may act as a structural surrogate, allowing the expression of fully formed functional complexes even when E1 is limiting. This idea is not all that far fetched given E4 is the most abundant KCNE mRNA transcript in the heart. A most pressing question that requires further study is how cells prevent deleterious complex assembly, as E3 is also expressed in the heart, but would generate a detrimental leak channel if complexed with Q1 (or Q1/E1). Perhaps E3 mRNA transcripts are degraded before protein translation, E3 partners with a channel other than Q1, or yet unknown cellular mechanism prevent Q1/E3 channel assembly. The CTX-Mal reagent could also be used to disentangle the phenotypic effects of KCNE mutations on assembly from those on modulation by deconvolving the functional contributions of unpartnered Q1 channels and mutant Q1–KCNE complexes.

Chapter IV discusses labeling specific cell surface proteins with experimentally useful tags. Biotin was used to show proof of principle, but the modular design of the cleavable linker allows it to easily incorporate other molecular entities, such as fluorophores that would be useful in monitoring recycling rates, degradation, or measuring distances between β-subunits using FRET experiments.

The fact that cells take-up and incorporate non-natural sugar derivatives into their extracellular glycans allows endogenous channels to display useful reactive handles. The use of non-natural thiol-containing-sugars allows the technology to be used in native cells, not only with ion channels, but any cell surface protein that is N-linked glycosylated and capable of binding a molecule (protein or synthetic compound) with high affinity. This would include transporters, notoriously difficult to study due to their complex function and membrane embedded structure. The questions that were answered in Chapters II and III could be reexamined in native cells using metabolical thiol incorporation. Furthermore, investigating the ability of Long QT causing mutants to assemble into complexes in native cells would be of significant medical relevance.

Finally, all tethering displayed in this thesis involved maleimides reacting with free thiols. It has been shown that similar tethering strategies using other chemistries work equally as well, such as directing a nucleophile toward an electrophiles (Fortin et al., 2008), or “click” chemistry between an alkyne and azide (Laughlin and Bertozzi, 2007). Give the modularity of the reagents used in this thesis, these different chemistries should be equally compatible.

In conclusion, this thesis demonstrates the importance of combining the perspectives and technical attributes on two scientific disciplines, biology and chemistry, to answer physiologically relevant questions.

Bibliography

Baker, K., Salkoff, L., 1990. . The Drosophila Shaker gene codes for a distinctive K+ current in a subset of neurons. *Neuron*. 4: 129-40

Banghart, M., K. Borges, E. Isacoff, D. Trauner, and R.H. Kramer. 2004. Light-activated ion channels for remote control of neuronal firing. *Nat Neurosci*. 7:1381-1386.

Barany, G., and R.B. Merrifield. 1977. A new amino protecting group removable by reduction. Chemistry of the dithiasuccinoyl (Dts) function. *J Am Chem Soc*. 99:7363-7365.

Barany, G., A.L. Schroll, A.W. Mott, and D.A. Halsrud. 1983. A General Strategy for Elaboration of the Bithiocarbonyl Functionality, -(C==O)SS-: Application to the Synthesis of Bis(chlorocarbonyl)disulfane and Related Derivatives of Thiocarbonic Acids. *J. Org. Chem.* 48:4750-4761.

Barhanin, J., F. Lesage, E. Guillemare, M. Fink, M. Lazdunski, and G. Romey. 1996. K_VLQT1 and IsK (minK) proteins associate to form the I_{Ks} cardiac potassium current. *Nature*. 384:78-80.

Bendahhou, S., C. Marionneau, K. Haurogne, M.M. Larroque, R. Derand, V. Szuts, D. Escande, S. Demolombe, and J. Barhanin. 2005. In vitro molecular interactions and distribution of KCNE family with KCNQ1 in the human heart. *Cardiovasc Res*. 67:529-538.

Bezanilla, F. 2006. The action potential: from voltage-gated conductances to molecular structures. *Biol Res*. 39:425-435.

Blaustein, R.O. 2002. Kinetics of tethering quaternary ammonium compounds to K(+) channels. *J Gen Physiol*. 120:203-216.

Blaustein, R.O., P.A. Cole, C. Williams, and C. Miller. 2000. Tethered blockers as molecular 'tape measures' for a voltage-gated K^+ channel. *Nat Struct Biol*. 7:309-311.

Chandrasekhar, K.D., T. Bas, and W.R. Kobertz. 2006. KCNE1 subunits require co-assembly with K^+ channels for efficient trafficking and cell surface expression. *J. Biol. Chem.* 281:40015-40023.

Chen, H., L.A. Kim, S. Rajan, S. Xu, and S.A. Goldstein. 2003. Charybdotoxin binding in the I_{Ks} pore demonstrates two MinK subunits in each channel complex. *Neuron*. 40:15-23.

Congbao Kang, C.T., Frank D. So¨nnichsen, Jarrod A. Smith, Jens Meiler,, J. Alfred L. George, Carlos G. Vanoye, Hak Jun Kim, and Charles R. Sanders, 2008. Structure of KCNE1 and Implications for How It Modulates the KCNQ1 PotassiumChannel. *Biochemistry*. in press

Cordero-Morales, J., Cuello, L., and Perozo, E., 2006. KcsA is voltage gated according to Voltage-dependent gating at the KcsA selectivity filter, *Nature Structural & Molecular Biology* 13, 319 - 322

de Souza, N.F., and S.M. Simon. 2002. Glycosylation affects the rate of traffic of the Shaker potassium channel through the secretory pathway. *Biochemistry*. 41:11351-11361.

Doyle, D.A., J. Morais Cabral, R.A. Pfuetzner, A. Kuo, J.M. Gulbis, S.L. Cohen, B.T. Chait, and R. MacKinnon. 1998. The structure of the potassium channel: molecular basis of K+ conduction and selectivity. *Science*. 280:69-77.

Dube, D.H., and C.R. Bertozzi. 2003. Metabolic oligosaccharide engineering as a tool for glycobiology. *Curr Opin Chem Biol*. 7:616-625.

Fortin, D.L., M.R. Banghart, T.W. Dunn, K. Borges, D.A. Wagenaar, Q. Gaudry, M.H. Karakossian, T.S. Otis, W.B. Kristan, D. Trauner, and R.H. Kramer. 2008. Photochemical control of endogenous ion channels and cellular excitability. *Nat Methods*. 5:331-338.

Gage, S.D., and W.R. Kobertz. 2004. KCNE3 Truncation Mutants Reveal a Bipartite Modulation of KCNQ1 K^+ Channels. *J. Gen. Physiol.* 124:759-771.

Goldstein, S.A., D.J. Pheasant, and C. Miller. 1994. The charybdotoxin receptor of a Shaker K^+ channel: peptide and channel residues mediating molecular recognition. *Neuron*. 12:1377-1388.

Gordon, E., T.K. Roepke, and G.W. Abbott. 2006. Endogenous KCNE subunits govern Kv2.1 K+ channel activation kinetics in Xenopus oocyte studies. *Biophys J*. 90:1223-1231.

Grunnet, M., T. Jespersen, H.B. Rasmussen, T. Ljungstrom, N.K. Jorgensen, S.P. Olesen, and D.A. Klaerke. 2002. KCNE4 is an inhibitory subunit to the KCNQ1 channel. *J Physiol*. 542:119-130.

Helenius, A., and M. Aebi. 2001. Intracellular functions of N-linked glycans. *Science*. 291:2364-2369.

Inglis V, Karpinski E, Benishin C (2003). Gamma-dendrotoxin blocks large conductance Ca2+-activated K+ channels in neuroblastoma cells. Life Sciences 73, 2291-2305

Jespersen, T., M. Grunnet, and S.P. Olesen. 2005. The KCNQ1 potassium channel: from gene to physiological function. *Physiology (Bethesda)*. 20:408-416.

Jiang, Y., A. Lee, J. Chen, V. Ruta, M. Cadene, B.T. Chait, and R. MacKinnon. 2003. X-ray structure of a voltage-dependent K+ channel. *Nature*. 423:33-41.

Khanna, R., E.J. Lee, and D.M. Papazian. 2004. Transient calnexin interaction confers long-term stability on folded K+ channel protein in the ER. *J Cell Sci*. 117:2897-2908.

Khanna, R., M.P. Myers, M. Laine, and D.M. Papazian. 2001. Glycosylation increases potassium channel stability and surface expression in mammalian cells. *J Biol Chem*. 276:34028-34034.

Kobertz, W.R., and C. Miller. 1999. K^+ channels lacking the 'tetramerization' domain: implications for pore structure. *Nat. Struct. Biol.* 6:1122-1125.

Kurokawa, J., H.K. Motoike, and R.S. Kass. 2001. TEA(+)-sensitive KCNQ1 constructs reveal pore-independent access to KCNE1 in assembled I(Ks) channels. *J Gen Physiol*. 117:43-52.

Larsson, H.P., O.S. Baker, D.S. Dhillon, and E.Y. Isacoff. 1996. Transmembrane movement of the shaker K+ channel S4. *Neuron*. 16:387-397.

Laughlin, S.T., and C.R. Bertozzi. 2007. Metabolic labeling of glycans with azido sugars and subsequent glycan-profiling and visualization via Staudinger ligation. *Nat Protoc*. 2:2930-2944.

Liu, X.S., M. Zhang, M. Jiang, D.M. Wu, and G.N. Tseng. 2007. Probing the Interaction Between KCNE2 and KCNQ1 in Their Transmembrane Regions. *J Membr Biol*. 216:117-127.

Long, S.B., E.B. Campbell, and R. Mackinnon. 2005a. Crystal structure of a mammalian voltage-dependent Shaker family K+ channel. *Science*. 309:897-903.

Long, S.B., E.B. Campbell, and R. Mackinnon. 2005b. Voltage sensor of Kv1.2: structural basis of electromechanical coupling. *Science*. 309:903-908.

Lu, J., W.R. Kobertz, and C. Deutsch. 2007. Mapping the Electrostatic Potential within the Ribosomal Exit Tunnel. *J. Mol. Biol.* 371:1378-1391.

Lundquist, A.L., L.J. Manderfield, C.G. Vanoye, C.S. Rogers, B.S. Donahue, P.A. Chang, D.C. Drinkwater, K.T. Murray, and A.L. George, Jr. 2005. Expression of multiple KCNE genes in human heart may enable variable modulation of I_{Ks}. *J Mol Cell Cardiol*. 38:277-287.

Lundquist, A.L., C.L. Turner, L.Y. Ballester, and A.L. George, Jr. 2006. Expression and transcriptional control of human KCNE genes. *Genomics*. 87:119-128.

Ma, L., C. Lin, S. Teng, Y. Chai, R. Bahring, V. Vardanyan, L. Li, O. Pongs, and R. Hui. 2003. Characterization of a novel Long QT syndrome mutation G52R-KCNE1 in a Chinese family. *Cardiovasc Res*. 59:612-619.

MacKinnon, R. 1991. Determination of the subunit stoichiometry of a voltage-activated potassium channel. *Nature*. 350:232-235.

MacKinnon, R., S.L. Cohen, A. Kuo, A. Lee, and B.T. Chait. 1998. Structural conservation in prokaryotic and eukaryotic potassium channels. *Science*. 280:106-109.

Manderfield, L.J., and A.L. George, Jr. 2008. KCNE4 can co-associate with the I(Ks) (KCNQ1-KCNE1) channel complex. *Febs J*. 275:1336-1349.

Martinez, M.A., and J.C. Vega. 1986. Synthesis of *O*-Alkyl Carbonochloridothioates. *Synthesis*. 9:760-761.

McCrossan, Z.A., and G.W. Abbott. 2004. The MinK-related peptides. *Neuropharmacology*. 47:787-821.

Melman, Y.F., A. Krumerman, and T.V. McDonald. 2002. A single transmembrane site in the KCNE-encoded proteins controls the specificity of KvLQT1 channel gating. *J Biol Chem*. 277:25187-25194.

Morin, T.M., and W.R. Kobertz. 2007. A Derivatized Scorpion Toxin Reveals the Functional Output of Heteromeric KCNQ1-KCNE K^+ Channel Complexes. *ACS Chem. Biol.* 2:469-473.

Nakajo, K., and Y. Kubo. 2007. KCNE1 and KCNE3 Stabilize and/or Slow Voltage Sensing S4 Segment of KCNQ1 Channel. *J Gen Physiol*. 130:269-281.

Panaghie, G., and G.W. Abbott. 2007. The role of S4 charges in voltage-dependent and voltage-independent KCNQ1 potassium channel complexes. *J Gen Physiol*. 129:121-133.

Posson, D.J., P. Ge, C. Miller, F. Bezanilla, and P.R. Selvin. 2005. Small vertical movement of a K^+ channel voltage sensor measured with luminescence energy transfer. *Nature*. 436:848-851.

Pusch, M., R. Magrassi, B. Wollnik, and F. Conti. 1998. Activation and inactivation of homomeric KvLQT1 potassium channels. *Biophys J*. 75:785-792.

Robbins, J. 2001. KCNQ potassium channels: physiology, pathophysiology, and pharmacology. *Pharmacol Ther*. 90:1-19.

Rocheleau, J.M., S.D. Gage, and W.R. Kobertz. 2006. Secondary Structure of a KCNE Cytoplasmic Domain. *J. Gen. Physiol.* 128:721-729.

Rocheleau, J.M., and W.R. Kobertz. 2008. KCNE peptides differently affect voltage sensor equilibrium and equilibration rates in KCNQ1 K^+ channels. *J. Gen. Physiol.* 131:59-68.

Roepke, T.K., A. Anantharam, P. Kirchhoff, S.M. Busque, J.B. Young, J.P. Geibel, D.J. Lerner, and G.W. Abbott. 2006. The KCNE2 potassium channel ancillary subunit is essential for gastric acid secretion. *J Biol Chem*. 281:23740-23747.

Romey, G., B. Attali, C. Chouabe, I. Abitbol, E. Guillemare, J. Barhanin, and M. Lazdunski. 1997. Molecular mechanism and functional significance of the MinK control of the KvLQT1 channel activity. *J Biol Chem*. 272:16713-16716.

Rudy, B., and L.E. Iverson. 1992. General Oocyte Care. *In* Methods Enzymol. 225-345.

Salata, J.J., N.K. Jurkiewicz, J. Wang, B.E. Evans, H.T. Orme, and M.C. Sanguinetti. 1998. A novel benzodiazepine that activates cardiac slow delayed rectifier K+ currents. *Mol Pharmacol*. 54:220-230.

Sanguinetti, M.C., M.E. Curran, A. Zou, J. Shen, P.S. Spector, D.L. Atkinson, and M.T. Keating. 1996. Coassembly of K_VLQT1 and minK (IsK) proteins to form cardiac I_{Ks} potassium channel. *Nature*. 384:80-83.

Santacruz-Toloza, L., Y. Huang, S.A. John, and D.M. Papazian. 1994. Glycosylation of shaker potassium channel protein in insect cell culture and in Xenopus oocytes. *Biochemistry*. 33:5607-5613.

Schroeder, B.C., S. Waldegger, S. Fehr, M. Bleich, R. Warth, R. Greger, and T.J. Jentsch. 2000. A constitutively open potassium channel formed by KCNQ1 and KCNE3. *Nature*. 403:196-199.

Sesti, F., and S.A. Goldstein. 1998. Single-channel characteristics of wild-type IKs channels and channels formed with two minK mutants that cause long QT syndrome. *J Gen Physiol*. 112:651-663.

Sesti, F., K.K. Tai, and S.A. Goldstein. 2000. MinK endows the I(Ks) potassium channel pore with sensitivity to internal tetraethylammonium. *Biophys J*. 79:1369-1378.

Shimony, E., T. Sun, L. Kolmakova-Partensky, and C. Miller. 1994. Engineering a uniquely reactive thiol into a cysteine-rich peptide. *Protein Eng*. 7:503-507.

Smith, C., M. Phillips, and C. Miller. 1986. Purification of charybdotoxin, a specific inhibitor of the high-conductance Ca^{2+}-activated K^{+} channel. *J Biol Chem*. 261:14607-14613.

Splawski, I., J. Shen, K.W. Timothy, M.H. Lehmann, S. Priori, J.L. Robinson, A.J. Moss, P.J. Schwartz, J.A. Towbin, G.M. Vincent, and M.T. Keating. 2000. Spectrum of mutations in long-QT syndrome genes. KVLQT1, HERG, SCN5A, KCNE1, and KCNE2. *Circulation*. 102:1178-1185.

Splawski, I., M. Tristani-Firouzi, M.H. Lehmann, M.C. Sanguinetti, and M.T. Keating. 1997. Mutations in the hminK gene cause long QT syndrome and suppress IKs function. *Nat Genet*. 17:338-340.

Tai, K.K., and S.A. Goldstein. 1998. The conduction pore of a cardiac potassium channel. *Nature*. 391:605-608.

Tai, K.K., K.W. Wang, and S.A. Goldstein. 1997. MinK potassium channels are heteromultimeric complexes. *J Biol Chem*. 272:1654-1658.

Takumi, T., K. Moriyoshi, I. Aramori, T. Ishii, S. Oiki, Y. Okada, H. Ohkubo, and S. Nakanishi. 1991. Alteration of channel activities and gating by mutations of slow I_{SK} potassium channel. *J Biol Chem*. 266:22192-22198.

Tapper, A.R., and A.L. George, Jr. 2000. MinK subdomains that mediate modulation of and association with KvLQT1. *J Gen Physiol*. 116:379-390.

Tapper, A.R., and A.L. George, Jr. 2001. Location and orientation of minK within the I(Ks) potassium channel complex. *J Biol Chem*. 276:38249-38254.

Tinel, N., S. Diochot, M. Borsotto, M. Lazdunski, and J. Barhanin. 2000. KCNE2 confers background current characteristics to the cardiac KCNQ1 potassium channel. *Embo J*. 19:6326-6330.

Tu, L., and C. Deutsch. 1999. Evidence for dimerization of dimers in K+ channel assembly. *Biophys J*. 76:2004-2017.

Tyson, J., L. Tranebjaerg, M. McEntagart, L.A. Larsen, M. Christiansen, M.L. Whiteford, J. Bathen, B. Aslaksen, S.J. Sorland, O. Lund, M.E. Pembrey, S. Malcolm, and M. Bitner-Glindzicz. 2000. Mutational spectrum in the cardioauditory syndrome of Jervell and Lange-Nielsen. *Hum Genet*. 107:499-503.

Tzounopoulos, T., H.R. Guy, S. Durell, J.P. Adelman, and J. Maylie. 1995. min K channels form by assembly of at least 14 subunits. *Proc Natl Acad Sci U S A*. 92:9593-9597.

Vetter, D.E., J.R. Mann, P. Wangemann, J. Liu, K.J. McLaughlin, F. Lesage, D.C. Marcus, M. Lazdunski, S.F. Heinemann, and J. Barhanin. 1996. Inner ear defects induced by null mutation of the isk gene. *Neuron*. 17:1251-1264.

Volgraf, M., P. Gorostiza, R. Numano, R.H. Kramer, E.Y. Isacoff, and D. Trauner. 2006. Allosteric control of an ionotropic glutamate receptor with an optical switch. *Nat Chem Biol*. 2:47-52.

Wang, H., Pan, Z., Shi, W., Brown, B., Wymore, R., Cohen, I., Dixon, J., McKinnon, D. 1998. KCNQ2 and KCNQ3 Potassium Channel Subunits: Molecular Correlates of the M-Channel. *Science*. 282:5395:1890 - 189

Wang, K.W., and S.A. Goldstein. 1995. Subunit composition of minK potassium channels. *Neuron*. 14:1303-1309.

Wang, K.W., K.K. Tai, and S.A. Goldstein. 1996. MinK residues line a potassium channel pore. *Neuron*. 16:571-577.

Wang, W., J. Xia, and R.S. Kass. 1998. MinK-KvLQT1 fusion proteins, evidence for multiple stoichiometries of the assembled I_{sK} channel. *J Biol Chem*. 273:34069-34074.

Wu, D.M., M. Jiang, M. Zhang, X.S. Liu, Y.V. Korolkova, and G.N. Tseng. 2006. KCNE2 is colocalized with KCNQ1 and KCNE1 in cardiac myocytes and may function as a negative modulator of I_{Ks} current amplitude in the heart. *Heart Rhythm*. 3:1469-1480.

Yarema, K.J., L.K. Mahal, R.E. Bruehl, E.C. Rodriguez, and C.R. Bertozzi. 1998. Metabolic delivery of ketone groups to sialic acid residues. Application To cell surface glycoform engineering. *J Biol Chem*. 273:31168-31179.

Yoshida S and Matsumoto S (2005). Effects of alpha-dendrotoxin on K^+ currents and action potentials in tetrodotoxin-resistant adult rat trigeminal ganglion neurons. *J Pharmacol Exp Ther* 314:437-445

Yu, L., C. Sun, D. Song, J. Shen, N. Xu, A. Gunasekera, P.J. Hajduk, and E.T. Olejniczak. 2005. Nuclear magnetic resonance structural studies of a potassium channel-charybdotoxin complex. *Biochemistry*. 44:15834-15841.